2008

Incorporation of Cα,α-Disubstituted Amino Acids into Model Peptide Systems: Conformational Analysis and Possible Applications as Therapeutic Agents

Marcus A. Etienne
Louisiana State University and Agricultural and Mechanical College, metien2@lsu.edu

INCORPORATION OF $C^{\alpha,\alpha}$-DISUBSTITUTED AMINO ACIDS INTO MODEL PEPTIDE SYSTEMS: CONFORMATIONAL ANALYSIS AND APPLICATIONS AS POSSIBLE THERAPEUTIC AGENTS

A Dissertation
Submitted to the Graduate Faculty of the
Louisiana State University and
Agricultural and Mechanical College
in partial fulfillment of the
requirements for the degree of
Doctor of Philosophy

in

The Department of Chemistry

By
Marcus A. Etienne
B.S., Southern University, 2001
May 2008

ACKNOWLEDGMENTS

Dr. Robert P. Hammer
Hammer Laboratory
LSU Alzheimer's Group
LSU NMR Facility (Dale Treleaven, Thomas Weldeghiorghis, and Frank Zhou)
LSU Mass Spectrometry Facility (Tracy McCarley and Renee Simms)
LSU Department of Chemistry

Graduate Committee
Dr. Robin McCarley, Dr. Paul Russo, Dr. Graca Vicente,
and Dr. Subramaniam Sathivel

Collaborators
Dr. Timothy Keiderling (University of Illinois at Chicago), Rong Haung (University of Illinois at Chicago), Dr. George Barany (University of Minnesota), Larry Masterson (University of Minnesota), Dr. Guinluigi Veglia (University of Minnesota), and
Dr. David Morgan (University of South Florida)

Special Thanks
Martha Juban, Catherine Thomas, Cindy Henk, Dr. Jed Aucoin, Dr. Nadia Edwin, Dr. Julia Moses, Dr. Shunzi Li, Dr. Jia Wang, Dr. Yanwen Fu, Dr. Mariah McMasters, and Cyrus Bett

Funding
Louisiana Board of Regents Graduate Fellowship and the National Institute on Aging (AG17983)

Parts of this dissertation were collaborative and have been published in the listings below

1. Huang, Rong; Setnička, Vladimír; Etienne, Marcus A.; Kim, Joohyum; Kubelka, Jan ; Hammer, Robert P.; Keiderking, Timothy A. **Cross-strand Coupling of a β-Hairpin Peptide Stabilized with an Aib-Gly Turn using Isotope-Edited IR Spectroscopy**, *Journal of American Chemical Society*, (**2007**), 129(5), 13592-13603.
2. Masterson, Larry R.; Etienne, Marcus A.; Porcelli, Fernando.; Barany, George; Hammer, Robert P.; Gianluigi, V. **Non-Stereogenic α-Aminoisobutyryl-Glycyl (Aib-Gly) Dipeptidyl Unit Nucleates a Type I′ β-Turn in Linear Peptides in Aqueous Solutions**, *Biopolymers* (**2007**), 88(5), 746-753.
3. Etienne, Marcus A.; Aucoin, Jed P.; Fu, Yanwen.; McCarley, Robin L.; Hammer, Robert P. **Stiochiometric Inhibition of Amyloid β-Protein Aggregation with Peptides Containing $C^{\alpha,\alpha}$-Disubstituted Amino Acids,** *Journal of the American Chemical Society* (**2006**), *128*(11), 3522-3523.
4. Fu, Yanwen; Etienne, Marcus A.; Hammer, Robert P. **Facile Synthesis of α,α-Diisobutylglycine and Anchoring its Derivatives onto PAL-PEG-PS Resin.** *Journal of Organic Chemistry* (**2003**), *68*(25), 9854-9857.
5. Etienne, Marcus A.; Edwin, Nadia J.; Aucoin, Jed P.; Russo, Paul S.; McCarley, Robin L.; Hammer, Robert P. "**Amyloid β- Protein Aggregation**", Peptide Characterization and Application Protocols. *Methods in Molecular Biology* 386. NJ (2007).

TABLE OF CONTENTS

LIST OF TABLES

LIST OF FIGURES

LIST OF SCHEMES

LIST OF EQUATIONS

LIST OF ABBREVIATIONS

Amino acids and peptides are abbreviated and designated following the "Rules of the IUPAC-IUB Commission of Biochemical Nomenclature" (*J. Biol. Chem.* **1985,** 260, 14-42.). Amino acid symbol denote the L-configuration unless otherwise noted. The following additional abbreviations are used:

AAA	amino acid analysis
ααAA	$C^{\alpha,\alpha}$-disubstituted amino acid
Ac	acetyl
AD	Alzheimer's disease
Aβ	β-amyloid peptide
Abs	absorbance
AFM	atomic force microscopy
Aib	aminoisobutyric acid
APP	amyloid precursor protein
BACE	β-site APP cleaving enzyme
BBB	blood brain barrier
BOP-Cl	bis(2-oxo-3-oxazolidinyl)phosphinic chloride
Cα	alpha carbon
Cβ	beta carbon
CCA	α-cyano-4-hydroxycinnamic acid
CD	circular dichroism
cmc	critical micelle concentration
CSA	camphorsulfonic acid

d	doublet
DBU	1,8-diazobicyclo[4.5.0]undec-7-ene
Dbzg	$C^{\alpha,\alpha}$-dibenzylglycine
DCC	dicyclohexylcarbodiimide
Dibg	$C^{\alpha,\alpha}$-diisobutylglycine
DIEA	*N*,*N*-diisopropylethylamine
DLS	dynamic light scattering
Dpg	$C^{\alpha,\alpha}$-dipropylglycine
EM	electron microscopy
ESI	electrospray ionization
Fmoc	9-fluorenylmethoxycarbonyl
FTIR	Fourier-transform infared spectroscopy
Hα	alpha hydrogen
HATU	*N*-[(dimethyamino)-1H-1, 2, 3-triazolo[4, 5-b]pyridino-1-ylmethylene]-*N*-methylmethanaminium hexafluorophosphate *N*-oxide
HBTU	*O*-(1-benzotriazol-1-yl)-1,1,3,3-tetramethyluronium hexafluorophosphate
hIAPP	human islet amyloid precursor protein
HOAt	1-hydroxy-7-azabenzotriazole
HOBt	1-hydroxybenzotriazole
HPLC	high-performance liquid chromatography
IR	infrared spectroscopy
LWAβ	low molecular weight Aβ
M	molar

m	multiplet
MALDI	matrix-assisted laser desorption/ionization
Me	*N*-methylated
MHz	megahertz
min	minute
μm	micrometer (micron)
μM	micromolar
μL	microliter
mL	milliliter
mM	millimolar
mmol	millimole
mol	mole
MTT	3-(4,5-dimethylthiazol-2-yl)-2,5-diphenyltetrazolium bromide
nm	nanometer
NGF	neuronal growth factor
NMR	nuclear magnetic resonance
NOE	nuclear overhauser effect
PAL	5-(4-Fmoc-aminomethyl-3,5-dimethoxyphenoxy)valeric acid handle [peptide amide linker]
PBS	phosphate buffered saline
PEG	polyethylene glycol
PEG-PS	polyethylene glycol-polystyrene (graft resin support)
PDA	photodiode array
PICUP	photo-induced cross-linking unmodified peptide

Pip	piperidine
PS1	presenilin 1
PS2	presenilin 2
PyAOP	7-azabenzotriazolyoxytris(pyrrolidino)phosphonium hexafluorophosphate
RC	random coiled
RMSD	root mean square deviation
ROESY	rotational nuclear overhauser effect spectroscopy
ROS	reactive oxidative species
rpm	revolutions per minute
Ru	Ruthenium
s	singlet
SDS	sodium dodecyl sulfate
sec	second
SEC	size exclusion chromatography
SFM	scanning force microscopy
SPPS	solid-phase peptide synthesis
SPAM	senile plaque associated biological molecules
t	triplet
t_R	retention time
TBAB	tetrabutylammonium bromide
TBTU	*N*-(1H-benzotriazole-1-yl)-1,1,3,3-tetramethyluronium tetrafluoroborate
TEM	transmission electron microscopy

ThS	Thioflavin S
ThT	Thioflavin T
TIPS	triisopropylsilane
TOCSY	total correlation spectroscopy
US	United States
UV	ultraviolet spectroscopy

ABSTRACT

A diverse set of human diseases is associated with the misfolding of proteins into insoluble fibrillar structures that have predominantly β-sheet secondary structure. Thus it is imperative to elucidate the structural elements that contribute to β-sheet formation and stability. Peptides that autonomously form β-sheets are ideal models to study principles of protein folding and design. Gellman and coworkers first introduced an automonously folded β-hairpin (H-Arg-Tyr-Val-Glu-Val-**Yyy-Xxx**-Orn-Lys-Ile-Leu-Gln-NH_2) that remained monomeric up to ~1 mM. Circular dichroism (CD) and nuclear magnetic resonance (NMR) analyses revealed that incorporation of *non-stereogenic* Aib-Xxx dipeptidyl sequences into *i+1* and *i+2* positions of a model peptide nucleates a stable [2:4] *left-handed* type-I' β-turn in aqueous buffer. The Aib-Gly dipeptidyl sequence has a backbone conformation that is superimposable on corresponding hairpins containing the DPro-Gly (type-II') and Aib-DAla (type-I') sequences. The Aib-Gly turn sequence offers an attractive approach for preparing β-hairpin peptides because it eliminates cis-trans isomerization within the β-turn region.

Additionally, two peptides based on the hydrophobic core (Lys-Leu-Val-Phe-Phe) of amyloid β-protein (Aβ) that contain ααAAs at alternating positions, but differ in the positioning of the oligolysine chain (AMY-1, *C*-terminus; AMY-2, *N*-terminus) were prepared. The effects of AMY-1 and AMY-2 on the aggregation of Aβ were studied, and it was determined that at stoichiometric concentrations, both peptides completely stop Aβ fibrillogenesis. Equimolar mixtures of AMY-1 and Aβ form only globular aggregates as imaged by scanning force microscopy and transmission electron microscopy. These samples show no signs of protofibrillic or fibrillic material even after prolonged periods of time (4.5 months). Also, 10

mole percent of AMY-1 prevented Aβ self-assembly for long periods of time; aged samples (4.5 months) show only a few protofibrillic or fibrillic aggregates. AMY-2 interacts with Aβ differently in that equimolar mixtures form large (~ 1 μm) globular aggregates that do not progress to fibrils but precipitate out of solution. The differences in the aggregation mediated by the two peptides is discussed in terms of a model where the peptide mitigators interfere with the native ability of Aβ to self- assemble by hydrophobic interactions either at the *C*-terminus or *N*-terminus of the molecule.

CHAPTER 1.

INTRODUCTION

1.1 RESEARCH AIMS

The goal of this research project was to gain insight into structural elements that contribute to the stability of β-sheet secondary structures and design conformationally constrained peptides aimed to mitigate protein misfolding. The key structural element in the experimental design employed the use of $C^{\alpha,\alpha}$disubstituted amino acids (ααAAs) incorporated into peptide analogs. These amino acids are of particular interest because they have been shown to stabilize both helical and extended conformations.[1-5] The method of investigating ααAAs contribution to β-sheet stability relied on two experimental strategies: first, the use of β-hairpin peptide models for elucidation into the fundamental mechanism of β-sheet formation and stability and second, designing peptide analogs that have a high affinity for β-sheet assemblies and determining their efficacy in mitigating protein misfolding processes.

A specific aim of this research project was to determine the contribution of ααAAs as structural elements in both strand and turn portions of β-hairpin models. To meet this aim, β-hairpin peptides incorporating ααAAs in either the strand portion or in the *i+1* residue of a β-turn were synthesized. The ααAA contributions to β-sheet formation and stability were determined using circular dichroism spectroscopy (CD) and nuclear magnetic resonance (NMR) spectroscopy.

Peptide analogs were also designed to mitigate the misfolding of monomer proteins to misfolded states containing β-sheet secondary structures. In particular, this dissertation focuses on Aβ protein aggregates responsible for the formation of Aβ fibrils in Alzheimer's disease (AD). To this end, β-strand mimics were designed and synthesized. In vitro and in vivo characteristics of peptide analogs in the presence and absence of Aβ were also investigated.

1.2 PROTEIN FOLDING AND CONFORMATIONAL DISEASES

Proteins are macromolecules consisting of one or more polypeptide chains containing a few dozen to thousands of amino acids. The primary sequence of a protein or peptide, the amino acid sequence, is its most fundamental structural element.[6, 7] Folding of these linear sequences into intricate molecular structures, necessary for the activation of different biological and chemical processes, plays a vital role in sustaining living systems.[6, 8, 9]

Protein folding mechanisms are not completely understood.[8, 9] Scientists have speculated that the process by which proteins fold into their native conformational states is dependent upon the length of the peptide chain, a nucleation-condensation process where a peptide chain has a transition state ensemble of many conformations from high free energy states to the most thermodynamically stable lowest-free energy state, and the amino acid sequence.[7-11] At times, proteins form misfolded conformational states that compete with native protein folding pathways. Aggregation of proteins and peptides into misfolded states leads to debilitating and inactive cellular functions; therefore, a deeper understanding into the biological mechanism of protein folding/misfolding is paramount for understanding the etiology of "conformational diseases",[11-16] those characterized by protein misfolding, self association, aggregation, and protein deposition.

Among the protein conformational diseases is a specific class known as "amyloidosis". Approximately 20 different amyloidogenic precursor proteins have been implicated as a main component of the amyloidal aggregates many believe contribute to the pathogenesis associated with these diseases (Table 1.1).[14, 16-18] Amyloidogenic diseases affect many different tissues and organs such as the pancreas (amylin, type-II diabetes), liver (ATP7B, Wilson's disease), heart (light chain amyloidosis; systemic amyloidosis), and kidneys (β_2-microglobulin).[6, 11, 19-21] Those localized to the central nervous system and specific regions of the brain are more devastating because they cause cellular malfunctions that slowly deteriorate metacognition and mobility.

Table 1.1. Conformational diseases and their respective misfolded proteins.

PROTEIN	DISORDER
Amyloid β-peptide	Alzheimer's disease
Tau protein	Progressive supranuclear palsy, Pick's disease, dementia pugilistica
α-synuclein	Parkinson's disease
Prion proteins (Prp)	Creutzfeld-Jacob disease (CJD), fatal familial insomnia, sporadic insomnia, Gerstmann-Straussler-Scheinker disease (GSS)
β_2-microglobulin	Hemodialysis-associated amyloidosis
Amylin (IAPP)	Type II diabetes
Polyglutamine	Huntington's disease, Machado-Joseph atrophy
Transthyretin	Familial amyloid polyneuropathy, senile systemic amyloidosis
GFAP	Alexander's disease
ATP7B	Wilson's disease
Superoxide dismutase	Amylotropic lateral sclerosis
Haemoglobin	Sickle cell anemia
ABri/ADan	British/Danish dementia's
CTRF protein	Cystic fibrosis
Apolipoprotein A1 (ApoA1)	Familial amyloid polyneuropathy, endocrine disorders
AH and AL (immunoglobin heavy and light chain fragments)	Primary amyloidosis, immunity/inflammation disorders
ACys (cystatin C)	Hereditary cerebral amyloid angiopathy
ALys (lysozyme)	Hereditary systemic amyloidosis
Gelosin	Familial amyloid polyneuropathy (Finnish type)
AA (serum amyloid A)	Secondary amyloidosis
Prolactin	Prolactinoma of the pituitary
AFib (Fibrinogen A fragment)	Immunity/inflammation disorders
Calcitonin fragment	Endocrine disorders
Lactoferrin	Systemic disorders

These include Alzheimer's disease, Parkinson's disease, Huntington's disease, Creutzfeldt-Jakob disease, and amyotrophic lateral sclerosis (Lou Gehrig's disease) of which the amyloidogenic proteins, Aβ, α-synuclein, polyglutamine, prion proteins, and superoxide dismutase have been implicated.[17, 18, 20] An increased understanding of what factors induce or stabilize β-sheet secondary structures may offer a novel approach toward producing biologically active materials capable of combating protein conformational diseases.

1.3 THE STUDY OF β-SHEET SECONDARY STRUCTURE USING MODEL PEPTIDES

Model peptide systems have been the focus for understanding factors that contribute to β-sheet stability. Early attempts at investigating peptide secondary structure using peptide models were unsuccessful, and as a result, many investigators believed that short peptide fragments were largely unstructured in aqueous solution. With the development of more sophisticated instrumentation, peptides were found to be good models for studying secondary structure.

One of the simplest ways to study β-sheet structures is through β-sheet peptides known as β-hairpins;[22-24] structural motifs comprised of two antiparallel β-strands connected by a loop,[24-27] where the loop portion of the hairpin is known as the β-turn (Figure 1.1). A 16 amino acid residue peptide fragment of protein-G (B1 domain of immunoglobulin-G binding protein) was found to be monomeric upon dissolution and eventually adopted a β-hairpin structure suggesting the primacy of hairpins in the folding of protein-G.[28] Also, CD and NMR analyses revealed that a small peptide fragment derived from Platelet factor-4 (PF4) β-sheet domain maintained a well-ordered structure; thus, short peptides can be studied to elucidate factors that contribute to β-sheet stability.[29, 30]

β-Hairpin formation and stability has been studied extensively by accessing amino acid propensities in forming ordered secondary structures. Although side-chain interactions and

interstrand hydrogen bonding have been found to promote β-hairpin formation, they are not sufficient to sustain the hairpin.[25] Thus, introduction of stable turn motifs is critical for stabilizing β-hairpins, predicting folding kinetics, providing directional change in proteins, and serving as molecular recognition sites.[31, 32]

1.3.1 INTRODUCTION TO β-TURNS

Turns are the most common structure found in proteins and are necessary for predicting secondary structure. They contribute to protein stability and have been shown to possess therapeutic potential in peptide-based drug design strategies.[33] The term "β-turn" was first introduced in 1968 and was identified as being composed of four amino acid residues located in the *i* to *i+3* residues of a polypeptide chain (Figure 1.1). Much work has been devoted to

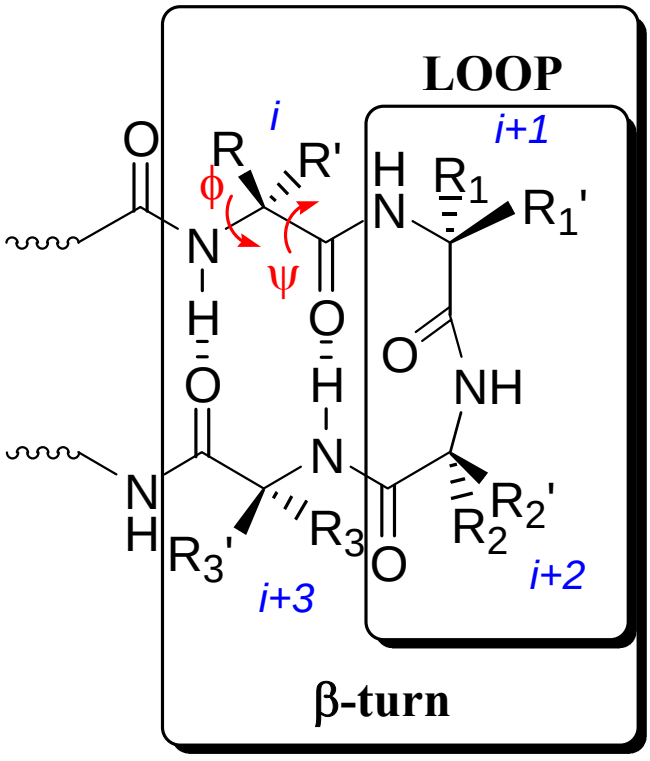

Figure 1.1. Schematic of β-turn and dihedral angles associated with a β-turn involving consecutive amino acid residues.

studying β-turn formation and stability. Early studies investigated the preference and turn potential of amino acid residues in nucleating various turn types. The primary approach in designing β-turns is to exploit backbone conformational constraints (ϕ, ψ torsion angles). Ramachandran discovered that van der Waals interactions restrict free ϕ,ψ rotation, thereby limiting available protein conformational space,[34, 35] thus turn motifs are classified based on local backbone conformational constraints and the distance between αC^{i} and αC^{i+3}.[11, 33, 36-38] While type-I and type-II β-turns are commonly found in many proteins, their mirror images, type-I' and type-II' β-turns (inverse turns), are common to β-hairpin peptides because they form a left-handed turn that is complementary to the natural right-handed twist of antiparallel β-sheets.[31, 36, 38-41] Specific turn types that are common to β-hairpin peptides will be elaborated in Chapter 2 of this dissertation.

1.4 PEPTIDE-BASED THERAPEUTICS

There has been increased interest in the design of pharmacological targets capable of inhibiting and/or altering amyloid aggregation and fibril formation.[13,16] The strategic rationale of most "therapeutic agents" is that they are capable of mitigating amyloid aggregation while remaining nontoxic to cell lines. In a more biologically related scheme, ideal therapeutic targets should be able to cross the blood-brain barrier (BBB) and resist proteolytic degradation. To date, a myriad of different approaches targeting Aβ amyloid aggregation and fibril formation have been proposed. Many studies have explored inhibition of endoproteolytic enzymes,[42-45] while others have employed the use of antibodies,[15, 17, 46-48] senile plaque-associated biological molecules (SPAM),[43, 49] small molecules,[50-52] and peptides[15, 53] to interfere with amyloid aggregation. This dissertation focuses primarily on the use of peptide-based mitigators of Aβ fibril formation.

The use of peptides in drug design offers many advantages. They provide for rational design strategies, have extremely high specificity, and have highly developed methods for analyzing different modes of action using various instrumental techniques. Despite the significance of peptide-based drugs, there are drawbacks associated with the use of these particular compounds. They cannot be delivered to local targets because they do not readily cross the BBB, thus gaining access to required sites of action is highly unlikely. In addition, peptides are subject to proteolysis and are rapidly inactivated by enzymes; therefore, administering peptide-based drugs is problematic. However, peptides have been used therapeutically to treat diabetes (insulin), multiple sclerosis (Cop-1), and hypertension (ACE inhibitors) and are excellent candidates for potential pharmacological targets.[54]

Aβ peptide mitigator design strategies were derived from an increased understanding of the Aβ primary sequence and its aggregation mechanisms. From mutagenesis studies of Aβ, it has been shown that the hydrophobic core, KLVFF, serves as a key sequence in the self-assembly of Aβ.[55, 56] The KLVFF peptide sequence forms amorphous aggregates, does not aggregate to form fibrils,[55] but this sequence is capable of binding to and inhibiting formation of Aβ fibrils. Thus, a number of groups have investigated peptides related to this sequence as a recognition element for Aβ and have investigated peptides containing this hydrophobic core as possible mitigators of aggregation and/or as Aβ fibril dissolution agents. These newly developed peptides are of particular interest because they are particularly hydrophobic and they adopt predominately random-coiled conformations which could interfere with β-sheet assemblies associated with Aβ fibrils. Recent studies by Ferreira[10, 48] suggest that the stability of Aβ fibrils is due to hydrophobic interactions. This hypothesis contributed to the design of the highly hydrophobic yet soluble AMY peptide

mitigators of Aβ amyloidal aggregation and fibril formation that will be discussed in detail in Chapter 4 of this dissertation.

1.5 REFERENCES

1. Karle, I. L.; Kaul, R.; Rao, R. B.; Raghothama, S.; Balaram, P. Stereochemical analysis of higher α,α-dialkylglycine containing peptides. Characterization of local helical conformations at dipropylglycine residues and observation of a novel hydrated multiple β-turn structure in crystals of a glycine rich peptide. *J. Am. Chem. Soc.* **1997,** 119, 12048-12054.

2. Kaul, R.; Banumathi, S.; Velmurugan, D.; Ravikumar, K.; Rao, R. B.; Balaram, P. Context-dependent conformation of diethylglycine residues in peptides. *J. Peptide Res.* **2000,** 55, 271-278.

3. Awasthi, S. K.; Shankaramma, S. C.; Raghothama, S.; Balaram, P. Solvent-induced β-hairpin to helix conformational transition in a designed peptide. *Biopolymers* **2001,** 58, 465-476.

4. Kaul, R.; Banumathi, S.; Velmurugan, D.; Balaji Rao, R.; Balaram, P. Conformational choice at α,α-di-*N*-propylglycine residues: helical or fully extended structures? *Biopolymers* **2000,** 54, 159-167.

5. Toniolo, C.; Crisma, M.; Formaggio, F.; Peggion, C. Control of peptide conformation by the Thorpe-Ingold effect (C^{α}-tetrasubstitution). *Biopolymers* **2001,** 60, 396-419.

6. Lansbury, P. T. Evolution of amyloid: What normal protein folding may tell us about fibrillogenesis and disease. *Proc. Natl. Acad. Sci. U. S. A.* **1999,** 96, 3342-3344.

7. Gregersen, N.; Bross, P.; Vang, S.; Christensen, J. H. Protein misfolding and human disease. *Annu. Rev. Genomics Hum. Genet.* **2006,** 7, 103-124.

8. Dobson, C. M. Protein folding and misfolding. *Nature* **2003,** 426, 884-890.

9. Baker, D. A surprising simplicity to protein folding. *Nature* **2000,** 405, 39-42.

10. Ferreira, S. T.; De Felice, F. G. Protein dynamics, folding and misfolding: from basic physical chemistry to human conformational diseases. *FEBS Lett.* **2001,** 498, 129-134.

11. Carrell, R. W. Cell toxicity and conformational disease. *Trends Cell Biol.* **2005,** 15, 574-580.

12. Howlett, D. R. Protein misfolding in disease: Cause or response? *Curr. Med. Chem.* **2003,** 3, 371-383.

13. Thompson, A. J.; Barrow, C. J. Recent developments in the understanding and treatment of neurodegenerative disorders involving protein conformational misfolding and amyloid formation. *Med. Chem. Rev.-online* **2005,** 2, 115-125.

14. Chow, M. K. M.; Lomas, D. A.; Bottomley, S. P. Promiscuous β-strand interactions and the conformational diseases. *Curr. Med. Chem.* **2004,** 11, 491-499.

15. Thompson, A. J.; Barrow, C. J. Protein conformational misfolding and amyloid formation: characteristics of a new class of disorders that include Alzheimer's and Prion diseases. *Curr. Med. Chem.* **2002,** 9, 1751-1762.

16. Lin, J.-C.; Liu, H.-L. Protein conformational diseases: from mechanisms to drug designs. *Curr. Drug Discov. Technol.* **2006,** 3, 145-53.

17. Bucciantini, M.; Calloni, G.; Chiti, F.; Formigli, L.; Nosi, D.; Dobson, C. M.; Stefani, M. Prefibrillar amyloid protein aggregates share common features of cytotoxicity. *J. Biol. Chem.* **2004,** 279, 31374-31382.

18. Bitan, G., Structural study of metastable amyloidogenic protein oligomers by photo-induced cross-linking of unmodified proteins. In *Amyloid, Prions, and Other Protein Aggregates, Pt C*, **2006**; Vol. 413, pp 217-236.

19. Gorman, P. M.; Chakrabartty, A. Alzheimer β-amyloid peptides: Structures of amyloid fibrils and alternate aggregation products. *Biopolymers* **2001,** 60, 381-394.

20. Bitan, G.; Fradinger, E. A.; Spring, S. M.; Teplow, D. B. Neurotoxic protein oligomers - what you see is not always what you get. *Amyloid* **2005,** 12, 88-95.

21. Tycko, R. Molecular structure of amyloid fibrils: insights from solid-state NMR. *Q Rev. Biophy.* **2006,** 39, 1-55.

22. Ramirez-Alvarado, M.; Blanco, F. J.; Niemann, H.; Serrano, L. Role of β-turn residues in β-hairpin formation and stability in designed peptides. *J. Mol. Biol.* **1997,** 273, 898-912.

23. Muñoz, V.; Thompson, P. A.; Hofrichter, J.; Eaton, W. A. Folding dynamics and mechanism of β-hairpin formation. *Nature* **1997,** 390, 196-199.

24. Haque, T. S.; Little, J. C.; Gellman, S. H. Stereochemical requirements for β-hairpin formation: Model studies with four-residue peptides and depsipeptides. *J. Am. Chem. Soc.* **1996,** 118, 6975-6985.

25. Haque, T. S.; Gellman, S. H. Insights on β-hairpin stability in aqueous solution from peptides with enforced type-I' and type-II' β-turns. *J. Am. Chem. Soc.* **1997,** 119, 2303-2304.

26. Stanger, H. E.; Gellman, S. H. Rules for antiparallel β-sheet design: D-Pro-Gly is superior to L-Asn-Gly for β-hairpin nucleation. *J. Am. Chem. Soc.* **1998,** 120, 4236-4237.

27. Schenck, H. L.; Gellman, S. H. Use of a designed triple-stranded antiparallel β-sheet to probe β-sheet cooperativity in aqueous solution. *J. Am. Chem. Soc.* **1998,** 120, 4869-4870.

28. Gronenborn, A. M.; Filpula, D. R.; Essig, N. Z.; Achari, A.; Whitlow, M.; Wingfield, P. T.; Clore, G. M. A novel, highly stable fold of the immunoglobulin binding domain of streptococcal protein-G. *Science* **1991,** 253, 657-61.

29. Ilyina, E.; Mayo, K. H. Multiple native-like conformations trapped via self-association-induced hydrophobic collapse of the 33-residue β-sheet domain from platelet factor 4. *Biochem. J* **1995,** 306, 407-19.

30. Ilyina, E.; Milius, R.; Mayo, K. H. Synthetic peptides probe folding initiation sites in platelet factor-4: stable chain reversal found within the hydrophobic sequence LIATLKNGRKISL. *Biochemistry* **1994,** 33, 13436-44.

31. Chou, K. C.; Blinn, J. R. Classification and prediction of β-turn types. *J. Protein Chem.* **1997,** 16, 575-595.

32. Hutchinson, E. G.; Thornton, J. M. A revised set of potentials for β-turn formation in proteins. *Protein Sci.* **1994,** 3, 2207-16.

33. Suat Kee, K.; Jois, S. D. S. Design of β-turn based therapeutic agents. *Curr. Pharm. Design* **2003,** 9, 1209-1224.

34. Ramachandran, G. N.; Ramakrishnan, C.; Sasisekharan, V. Stereochemistry of polypeptide chain configurations. *J. Mol. Biol.* **1963,** 7, 95.

35. Ramachandran, G. N.; Sasisekharan, V. Conformation of polypeptides and proteins. *Adv. Protien Chem.* **1968,** 23, 283-438.

36. Mohle, K.; Gussmann, M.; Hofmann, H. J. Structural and energetic relations between β-turns. *J. Comput. Chem.* **1997,** 18, 1415-1430.

37. Ball, J. B.; Hughes, R. A.; Alewood, P. F.; Andrews, P. R. β-Turn topography. *Tetrahedron* **1993,** 49, 3467-3478.

38. Wilmot, C. M.; Thornton, J. M. Analysis and prediction of the different types of β-turn in proteins. *J. Mol. Biol.* **1988,** 203, 221-232.

39. Gunasekaran, K.; Ramakrishnan, C.; Balaram, P. β-Hairpins in proteins revisited: Lessons for de novo design. *Protein Eng.* **1997,** 10, 1131-1141.

40. Hilario, J.; Kubelka, J.; Syud, F. A.; Gellman, S. H.; Keiderling, T. A. Spectroscopic characterization of selected β-sheet hairpin models. *Biopolymers* **2002,** 67, 233-236.

41. Stotz, C. E.; Topp, E. M. Applications of model β-hairpin peptides. *J. Pharm. Sci.* **2004,** 93, 2881-2894.

42. Bishop, G. M.; Robinson, S. R. Physiological roles of amyloid-β and implications for its removal in Alzheimer's disease. *Drugs and Aging* **2004,** 21, 621-630.

43. Iversen, L. L.; Mortishiresmith, R. J.; Pollack, S. J.; Shearman, M. S. The toxicity in vitro of β-amyloid protein. *Biochem. J* **1995,** 311, 1-16.

44. Hardy, J.; Selkoe, D. J. Medicine - The amyloid hypothesis of Alzheimer's disease: Progress and problems on the road to therapeutics. *Science* **2002,** 297, 353-356.

45. Adessi, C.; Soto, C. β-Sheet breaker strategy for the treatment of Alzheimer's disease. *Drug Dev. Res.* **2002,** 56, 184-193.

46. Kayed, R.; Head, E.; Thompson, J. L.; McIntire, T. M.; Milton, S. C.; Cotman, C. W.; Glabe, C. G. Common structure of soluble amyloid oligomers implies common mechanism of pathogenesis. *Science* **2003,** 300, 486-489.

47. Dumoulin, M.; Last, A. M.; Desmyter, A.; Decanniere, K.; Canet, D.; Larsson, G.; Spencer, A.; Archer, D. B.; Sasse, J.; Muyldermans, S.; Wyns, L.; Redfield, C.; Matagne, A.; Robinson, C. V.; Dobson, C. M. A camelid antibody fragment inhibits the formation of amyloid fibrils by human lysozyme. *Nature* **2003,** 424, 783-788.

48. Defelice, F. G.; Ferreira, S. T. Physiopathological modulators of amyloid aggregation and novel pharmacological approaches in Alzheimer's disease. *Anais Da Academia Brasileira De Ciencias* **2002,** 74, 265-284.

49. Morgan, C.; Colombres, M.; Nunez, M. T.; Inestrosa, N. C. Structure and function of amyloid in Alzheimer's disease. *Prog. Neurobio.* **2004,** 74, 323-349.

50. Lee, K. H.; Shin, B. H.; Shin, K. J.; Kim, D. J.; Yu, J. A hybrid molecule that prohibits amyloid fibrils and alleviates neuronal toxicity induced by β-amyloid (1-42). *Biochem. Biophys. Res. Commun.* **2005,** 328, 816-823.

51. Findeis, M. A. Approaches to discovery and characterization of inhibitors of amyloid β-peptide polymerization. *Biochim. Biophys. Acta-Mol. Basis Dis.* **2000,** 1502, 76-84.

52. Findeis, M. A.; Musso, G. M.; Arico-Muendel, C. C.; Benjamin, H. W.; Hundal, A. M.; Lee, J. J.; Chin, J.; Kelley, M.; Wakefield, J.; Hayward, N. J.; Molineaux, S. M. Modified-peptide inhibitors of amyloid β-peptide polymerization. *Biochemistry* **1999,** 38, 6791-6800.

53. Schwarzman, A. L.; Tsiper, M.; Gregori, L.; Goldgaber, D.; Frakowiak, J.; Mazur-Kolecka, B.; Taraskina, A.; Pchelina, S.; Vitek, M. P. Selection of peptides binding to the amyloid β-protein reveals potential inhibitors of amyloid formation. *Amyloid* **2005,** 12, 199-209.

54. Edwards, C. M. B.; Cohen, M. A.; Bloom, S. R. Peptides as drugs. *QJM-Mon. J. Assoc. Physicians* **1999,** 92, 1-4.

55. Tjernberg, L. O.; Naslund, J.; Lindqvist, F.; Johansson, J.; Karlstrom, A. R.; Thyberg, J.; Terenius, L.; Nordstedt, C. Arrest of β-amyloid fibril formation by a pentapeptide ligand. *J. Biol. Chem.* **1996,** 271, 8545-8548.

56. Hilbich, C.; Kisterswoike, B.; Reed, J.; Masters, C. L.; Beyreuther, K. Substitutions of hydrophobic amino-acids reduce the amyloidogenicity of Alzheimers-disease β-A4 peptides. *J. Mol. Biol.* **1992,** 228, 460-473.

CHAPTER 2.

IMPACT OF α,α-DISUBSTITUTED AMINO ACIDS ON β-HAIRPIN FOLDING*

2.1 INTRODUCTION

α-Helices and β-sheets are the most common secondary structural conformational motifs associated with proteins. Elucidation of factors contributing to structural stability is fundamental for the development of biologically active molecules.[1] Many protein-protein interactions are mediated by β-strands from one protein interacting with β-strands from another protein. Thus there has been an increased interest in understanding the factors that stabilize and destabilize β-sheet structures in proteins. There is a clear understanding of structural stability for α-helical systems due to well-established peptide model systems and the highly cooperative nature of α-helix folding. However, β-sheet models have been more difficult to study due to their rapid self-association in aqueous environments. Some success was seen with β-sheet peptides excised from proteins such as ubiquitin, tendemistate, GB1, etc.,[2] but most required the addition of organic solution to give significant β-hairpin structures. Breakthroughs in the development of autonomously folding peptide β-sheet models in aqueous solution have centered on the use of turn elements in forming anti-parallel β-hairpin peptides.[3]

The most common proteinogenic β-turns are the type-I and type-II turns (refer to Table 2.1 for ϕ/ψ torsion angles).[3] These sequences generally are less likely to nucleate isolated β-hairpins, as their native right-handed turn is not compatible with the preferred right handed twist of anti-parallel β-strands. A much smaller number of four-residue turns in proteins are the "mirror image" type-I' and type-II' turns. From a design perspective, type-I' and type-II' with

* Reprinted by permission of John Wiley and Sons Inc.

Asx-Gly and Gly-Asx in the *i+1* and *i+2* positions of a β-turn, take advantage of the propensity of Gly, Asn, and Asp to exist in left-handed helical conformations that are highly disfavored for most proteinogenic residues.[4-6] A key discovery allowing for the preparation of stable β-hairpin peptides was that DPro-Xxx sequences incorporated in the *i+1* and *i+2* positions have been shown to facilitate type-I' and type-II' turns while the corresponding LPro-Xxx sequences led to unfolded peptides.[4-8] A number of other non-proteinogenic residues, such as Pro-DPro[9, 10] (or DPro-Pro) and DPro-Aib,[11] have been identified as forming highly stabilized "mirror image" β-turns stabilizing β-hairpins. A large body of work now explores the use of these turn sequences in the stabilization of protein-based or *de novo* designed β-hairpins.

Searle and coworkers reported that local backbone constraints are vital in determining gross pattern shifts (δHα upfield and downfield chemical shifting[12]), but backbone torsion angles are not determinants to magnitude changes associated with Hα shifts when characterizing proteins. Effects such as geometry, orientation, and location of relative strands are more pressing factors.[13] Cross-strand interactions such as hydrogen bonding[14] and hydrophobic interactions[15] between antiparallel sheets play vital roles in forming stable β-hairpins, but there contribution to sheet stability was unclear. Recently, Waters,[16-20] Searle,[21-23] Gellman,[4, 24, 25] and Cochran[26, 27] groups have made apparent the importance of diagonal/cross-strand interaction to β-sheet stability based on heighten enthalpic and entropic effects which serves as driving forces towards β-sheet stability.

This chapter will explore the use of the α,α-disubstituted amino acids (ααAAs) α-aminoisobutyric acid (Aib, B), diisobutylglycine (Dibg, U), and dipropylglycine (Dpg, J) in both the β-strand portions of β-hairpin peptides and as β-turn inducers at the *i+1* position of β-hairpin

peptides. It was hypothesized that α,α-disubstituted amino acids such as Aib might serve as excellent inducers of the type-I' β-turn due to their propensity to stabilize helical peptides as a

Table 2.1. Standard β-turn motifs and their conformational constraints

Turn Type	Dihedral Angle (degrees)			
	ϕ_{i+1}	ϕ_{i+2}	ψ_{i+1}	ψ_{i+2}
Type-I	-60	-90	-30	0
Type-I'	+60	+90	+30	0
Type-II	-60	+80	+120	0
Type-II'	+60	-80	-120	0

Table 2.1. Canonical dihedral angles associated with type I/I' and type II/II' β-turns. See Hutchinson and Thornton (Protien Sci. **1994**, 3, 2207-16) for origin of dihedral angle values.

result of their steric preference for gauche dihedral angles (±30-60°).[28, 29] Although Aib is known to favor helical conformations,[30] a crystallographic characterization revealed that Aib-DAla incorporated at the *i+1* and *i+2* positions is capable of nucleating type-I' β-turns.[12, 30, 31] Dpg, along with its more bulky ααAA counterparts, have been known to stabilize both helical and extended (β-sheet-like) conformations and is speculated to induce β-turn formations.[28-30, 32]

The synthesis of four analogs (Figure 2.1) of the Gellman peptide $(\Omega^{D}PG)^{5}$ with substitutions at the *i+1* and *i+2* positions of the β-turn (Table 2.2) and their solution conformational analysis by CD will be discussed. Additionally, two peptides, one containing the Aib-Gly turn and the other containing the Aib-DAla turn was further characterized by NMR and restrained molecular dynamics. To date, only one group has utilized an ααAA-Xxx sequence to induce a β-hairpin in an acyclic peptide, but this structural study was by X-ray crystallography and CD in organic solvents.[12]

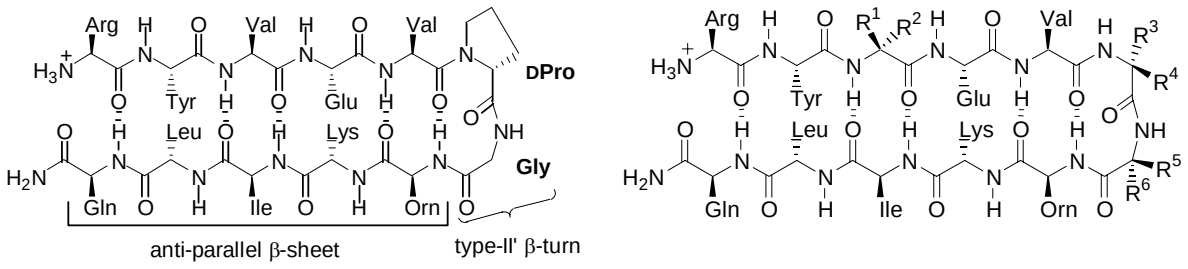

Figure 2.1. Schematic of Ω^{D}PG peptide, which is known to fold in a type-II' β-hairpin in aqueous solution, and hairpin model peptide synthesized to probe for ααAA nucleation on β-motifs. Table 2.2 defines the amino acids incorporated into the turn portion (*i+1* and *i+2* residues) of the β-turn.

Table 2.2. Peptide models (ΩXZ) used to probe nucleation

Variants	*i+1*	*i+2*	R^1	R^2	R^3	R^4	R^5	R^6
Ω^{D}PG	^{D}Pro	Gly	Val	H	---	---	H	H
ΩBG	Aib	Gly	Val	H	CH_3	CH_3	H	H
ΩAG	Ala	Gly	Val	H	CH_3	H	H	H
ΩB^{D}A	Aib	^{D}Ala	Val	H	CH_3	CH_3	H	CH_3
ΩJG	Dpg	Gly	Val	H	Pr	Pr	H	H
ΩUG	Dibg	Gly	Val	H	iBu	iBu	H	H

2.2 EXPERIMENTAL

Protected Fmoc-amino acid derivatives and Fmoc-PAL-PEG-PS, supports (initial loading 0.18-0.22 mmol/g) for peptide synthesis were mainly from Applied Biosystems (Framingham, MA). Additional supplier of protected derivatives was Nova Biochem (Darmstadt, Germany). Piperidine (Pip), 1,8-Diazabicyclo[5.4.0]undec-7-ene (DBU), and triisopropylsilane (TIPS) were

purchased from Aldirch (Milwaukee, WI). Trifluoroacetic acid (TFA) and *N*,*N*-diisopropylethylamine (DIEA) were from Fisher (Pittsburgh, PA), and phenol crystals were purchased from Mallinckrodt (St. Louis, MI). 1-Hydroxybenzotriazole (HOBt), N-[(1H-benzotriazol-1-yl)(dimethylamino)methylene]-N-methylmethanaminium tetrafluoroborate (TBTU), *N*-[(dimethylamino)-1*H*-1,2,3-triazolo[4,5-*b*]pyridin-1-yl-methylene]-*N*-methylmethanaminium hexafluorophosphate *N*-oxide (HATU), and 7-azabenzotriazolyoxytris(pyrrolidino) phosphonium hexafluorophosphate (PyAOP) were from Applied Biosystems.

2.2.1 AMINO ACID SYNTHESIS

The synthesis of Fmoc-Dpg-OH (**3**) followed protocols previously outlined (Scheme 2.1).[33-36]

Scheme 2.1. Synthetic route of *N*-terminal protected ααAA dipropylglycine- Dpg.

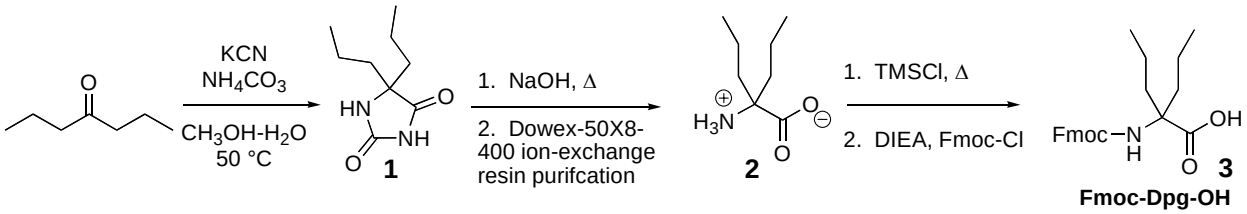

2.2.1.1. SYNTHESIS OF 5,5-DIPROPYLHYDANTOIN (1)

5,5-Dipropylhydantoin (**1**) was prepared following a Bucherer-Bergs protocol that was previously outlined for other ketones.[33, 37, 38] A solution of 4-heptanone (20 g, 175.2 mmol), potassium cyanide (24 g, 367.6 mmol), and ammonium carbonate (37.2 g, 385.2 mmol) in CH_3OH (100 mL) and H_2O (100 mL) was heated at 50 ºC in a capped vessel for 36 hours. The precipitated solid was filtered and washed with small portion of water and dried in air. The

hydantoin was obtained as off-white powder (28.4 g, 88%). ^{1}H (250 MHz, CD3SOCD3) δ: 10.52 (s, 1H), 7.84 (s, 1H), 1.62-1.43 (m, 4H), 1.42-1.22 (m, 2H), 1.21-1.02 (m, 2H), 0.97-0.85 (t, 6H).

2.2.1.2 SYNTHESIS OF 2,2-DIPROPYLGLYCINE (2)

The hydantoin **1** (25 g, 136 mmol) was suspended in 5 N NaOH (272 mL, 1.36 mol) and heated under reflux for 40 hours. The mixture was cooled, acidified to pH 6.5 with concentrated HCl, and filtered. The filtrate was dried by removal of the solvent under *vacuo* and washed with small portion of acetone to remove the unreacted hydantoin. Both the filtrate and the solid that precipitated out upon acidification were extracted with warm ethanol for several times. Dipropylglycine was obtained by removal of ethanol *in vacuo*. The white solid was further purified using Dowex 50X8-400 ion exchange resin to remove inorganic salts that formed as a result of acidification. The ion exchange resin was activated by rinsing the resin with 6 N HCl followed by rinsing with water until the eluent was neutral. Dipropylglycine, was dissolved in 6 N HCl, added to the cationic exchange resin, and rinsed with water (2 L) to remove all inorganic salts. The resin was then washed with 2 N NH_4OH (1 L) to remove the amino acid from the resin (8.0 g, 37%). Anal. Calcd for $C_{23}H_{27}NO_4$: C, 60.35; H, 10.76; N, 8.80; Found: C, 60.51; N, 10.64; N, 8.80. ^{1}H (250 MHz, CD_3SOCD_3) δ: 7.34(s, 2H), 1.55-1.10 (m, 8H), 0.88-0.78 (t, 6H).

2.2.1.3 N^{α}-(9-FLUORENYLMETHOXYCARBONYL)-2,2-DIPROPYLGLYCINE (3)

Following the procedure of Bolin,[39] a suspension of **2** (3 g, 18.83 mmol) in a mixture of dry CH_2Cl_2 (45 mL) and trimethylsilyl chloride (4.76 mL, 37.66 mmol) was heated under reflux for 2 hours. The mixture was cooled in an ice bath, then DIEA (6.49 mL, 37 mmol) and Fmoc chloride (4.64 g, 18.60 mmol) were added in succession. The solution was stirred with cooling for 30 minutes and then warmed to room temperature. After stirring for 24 h, CH_2Cl_2, was removed *in vacuo*. The resulting oil was dissolved in deionized water (50 mL) and extracted

with ethyl acetate (50 mL). After separation, the aqueous layer was again extracted with ethyl acetate (2 x 50 mL). The combined organic layers were dried over $MgSO_4$ and concentrated under reduced pressure, giving white solid product **3** (3.67 g, 57%). ^1H (250 MHz, CD_3SOCD_3) δ: 10.68 (s, 1H), 7.91-7.88 (d, 2H), 7.71-7.69 (d, 2H), 7.44-7.29 (m, 4H), 6.95 (s, 1H), 4.28-4.21 (m, 3H), 1.76-1.74 (m, 4H), 1.20-1.10 (m, 2H), 0.86-0.82 (m, 6H). Anal. Calcd for $C_{23}H_{27}NO_4$(381.45): C, 74.42; H, 7.13; N, 3.67. Found: C, 72.57; H, 7.30; N, 3.80.

2.2.2 PEPTIDE SYNTHESIS AND PURIFICATION

All peptides were synthesized by standard solid-phase Fmoc chemistry on Fmoc-PAL-PEG-PS (Peptide Amide Linker)-resin (0.2 mmol, 0.18 mmol/g loading) in continuous-flow mode on a Pioneer Peptide Synthesizer. The side-chain protected amino acid derivatives utilized were Fmoc-Arg(Pbf)-OH, Fmoc-Gln(Trt)-OH, Fmoc-Glu-(tBu)-OH, Fmoc-Lys(Boc)-OH, and Fmoc-Orn(Boc)-OH. Unless indicated otherwise, molar equivalents are given over resin-bound amine. Standard Fmoc amino acid coupling chemistry utilized four equivalents each of amino acid, TBTU, and HOBt (final concentration of each = 0.25 M) dissolved in 0.5 M DIEA in DMF for 1 hr, except where noted. Alternative methods for difficult couplings used four equivalents each of amino acid and HATU (final concentration of each = 0.25 M) dissolved in 0.5 M DIEA in DMF for 1 hr or four equivalents each of amino acid and PyAOP (final concentration of each = 0.25 M) dissolved in 0.5 M DIEA in DMF for 1 hr at 50 °C. Couplings involved minimal preactivation time. Washings between reactions were carried out with DMF. For heated couplings, the normal resin column was fitted with a 100 mm OMNI column jacket (6331, OMNI Fit), which allowed for the column to be heated at 50 °C with a Lauda Model WK230 circulating waterbath. Fmoc group deprotection was accomplished using Pip-DBU-DMF (1:1:48) for 5 min. Once peptide assembly was complete, peptide was cleaved from the solid

support using Reagent B (88:5:5:2 TFA:phenol:water:TIPS).[40] Approximately 10 mL of cleavage solution was added to 500 mg of resin and allowed to shake for 2 h then filtered. The resin was rinsed with 2 mL of TFA and the added to the cleavage filtrate. The filtrate was placed on a rotavapor at a temperature of 35 °C to reduce the amount of TFA to approximately half the original volume. The remaining filtrate was precipitated by a dropwise addition into a ten-fold excess of cold ether. The peptide was allowed to precipitate at -27 °C for 24 h. The peptide/ether solution was then placed in a centrifuge at a speed of 4 x 1,000 rpms. The resulting pellet was washed (3 times) followed by drying for 4 h under vacuum.

HPLC was performed on one of three systems: (1) Waters 600E multisolvent delivery system with a Model 486 tunable detector controlled by Empower Software, detection at 220 nm; (2) Waters 625 pump with a Model 996 diode array detector controlled by Millennium software, detection from 200-400 nm; (3) Waters Deltaprep system with detection at 220 nm. Three different columns were used for analysis and purification of peptides: (**Column A**) analytical HPLC was performed using a Vydac analytical C-18 (5 μm, 300 Å) reversed-phase column (218TP54, 4.6 x 250 mm) at 1 mL/min; (**Column B**) analytical and semi-preparative chromatography was performed on a Delta-Pak C_4 (15 μm, 100 Å) reversed-phase column (8 x 100 mm), at 1 mL/min; (**Column C**) preparative HPLC was performed on a Waters Delta-Pak C_4 (15 μm, 100 Å) reversed-phase cartridge (25 × 10 mm) in a radial compression module at 15 mL/min. Linear gradients of 0.1% aqueous TFA in H_2O (v/v) (Buffer A) and 0.1% TFA in CH_3CN (v/v) (Buffer B) were utilized in all HPLC. See Figure 2.2 for details of the gradients. Fractions from semi-preparative and preparative HPLC were analyzed by matrix-assisted laser desorption ionization-time of flight (MALDI-TOF) on a Bruker Proflex III instrument with XMASS software.

Amino acid analysis was performed on a Dionex AAA-Direct system composed of a GS50 Gradient Pump, an AS50 Autosampler, and an ED50 Electrochemical Detector. Peptides were hydrolyzed in 1 mL Pierce vacuum hydrolysis tubes using 6 N HCl for 24 h at 110 °C. Hydrolyzates were separated on a microbore anion exchange column, AminoPac PA10, (2 × 250 mm) with a ternary gradient of deionized water, 0.25 M sodium hydroxide and 1.0 M sodium acetate. Quantitation was performed with Pierce Amino Acid Standard H (Dionex, AminoPac PA1), diluted to produce a 4-level calibration curve of 18 amino acids from 50-200 picomoles and including norleucine as an internal standard, using PeakNet software. Table 2.3 summarizes the purification and characterization of Ω^{D}PG and the turn ΩXZ peptides.

2.2.3 CIRCULAR DICHROISM MEASUREMENTS.

All measurements were carried out using an Aviv Circular Dichroism Spectrometer Model 62DS with Igor plotting software. CD spectra were the average of three scans made at 1.00 nm intervals acquired from 260 nm to 190 nm (UV absorbance range). Samples were prepared from a dilution of stock peptide sample (~1 mM) and NaOAc buffer (100 mM, pH = 3.8) in water to acquire a working solution of 50-500 μM peptide concentration in NaOAc (1 mM pH = 3.8). The spectrum of NaOAc buffer (1x) was used as the background subtraction in all experiments.

2.2.4 NMR ANALYSIS

2.2.4.1 PEPTIDE NMR SPECTROSCOPY

ΩBG and ΩB^{D}A were dissolved in 200 mM sodium deuterioacetate buffer, containing 10% D_2O at pH 3.8 (uncorrected for isotopic effect). NMR spectra of ΩBG and ΩB^{D}A (1 mM) were recorded at 278.1 K on a 600 MHz Varian Inova 4-channel NMR spectrometer operating at 600.13 MHz. 1-D ^{1}H spectra acquired in a range of temperatures from 278.1 to 306.1 K were

used to calculate temperature coefficients for the amide protons. Water signal was suppressed by applying a WATERGATE pulse sequence.[41] Resonance assignments were performed using 2-D-TOCSY and ^{1}H/^{1}H-ROESY experiments. NMR samples [U^3]-Ω^{D}PG and [J^3]-Ω^{D}PG consisted of 1 mM peptide in 100 mM sodium deuterioacetate buffer containing 10% D_2O, pH 3.8. Measurements were performed at 278.1 K on a 500 MHz Brucker NMR spectrometer.

2.2.4.2 NMR STRUCTURE DETERMINATION

Intra- and interresidue dipolar contacts for the SNN-PEP/DMT complex were identified using a 2-D ROESY spectrum (400 ms mixing time), and the structures were calculated using X-PLOR.25. Structures were calculated using simulated annealing from an extended structure at an initial temperature (T_i) of 1000 K with 12000 high steps, 6000 cooling steps, and a step size of 5 fs to generate 100 conformers. Final structure refinement was carried out by gradually introducing van der Waals radii and Lennard-Jones potentials on the 100 structures using a T_i of 300 K, 100,000 cooling steps, and a step size of 1 fs. Subsequently, twenty lowest energy conformers were selected with violations less than 0.3 Å and the final structures were visualized using the MOLMOL software package.[42]

2.3 RESULTS AND DISCUSSION

2.3.1 ααAAS AS β-TURN DETERMINANTS

2.3.1.1 PEPTIDE SYNTHESIS AND CHARACTERIZATION

Peptides synthesized are shown in Figure 2.1 and the *i+1* and *i*+2 residues of the β-turn are defined in Table 2.2. The syntheses of Ω^{D}PG, first introduced by Gellman,[5] and an unfolded peptide standard ΩAG were readily accomplished using standard coupling protocols with TBTU/HOBt/DIEA as the activator. These two peptides were of high crude purity (98% and 85%, respectively) and were readily purified to homogeneity ≥ 99% (Table 2.3, entries 1 and 2).

For the synthesis of ΩBG, it was anticipated that the coupling of Aib and the following amino acid (Val-5) would be challenging so a double coupling HATU/DIEA protocol for these residues was employed. This initial synthesis of ΩBG was found to be only 22% pure (Figure 2.2 A; blue line, full length product has t_R of 32.3 min). The impurity at t_R of 30.6 min had a mass of 1303.44 due to a deletion of Val-5, located at the *N*-terminal side of the ααAA residue. Thus, the HATU was effective at incorporation of the Aib, but only moderately effective at coupling the branched Val residue to the *N*-terminus of Aib. The Hammer laboratory and other groups have noted that most difficult couplings in ααAA-containing sequences are the ones onto the amino group of the ααAA.[36, 43] One method used to address difficulties in coupling is heating the coupling reactions at 50 ºC.[34, 36] Thus, ΩBG was synthesized a second time by double coupling of the Aib and Val-5 residue using activation with the HOAt-based phosphonium reagent PyAOP and DIEA at 50 ºC. ΩBG synthesized by this method was found to be 93% pure (Figure 2.2 A, red line), where the peptide due to Val deletion was no longer detectable. ΩB^DA was also synthesized using PyAOP activations for the Aib and Val-5 at an elevated temperature of 50 °C and resulted in a clean chain assembly (Table 2.3, entry 4) with minimal impurities detected by UV absorbance (Figure 2.2 B, red line). The Dpg-containing peptide ΩJG was synthesized using PyAOP activation as well, but HPLC (Figure 2.2 C, red line, desired ΩJG at t_R of 32.5 min) showed that for this bulkier ααAA containing peptide, modified conditions were not effective. The major side-product at t_R of 27.7 min had a mass corresponding to deletion of all amino acid residues to the *N*-terminal side of the Dpg (Val, Glu, Val, Tyr, and Arg). An adequate amount of ΩJG was isolated for solution characterization; therefore, further improvements in the synthesis were not pursued. Alternate methods that utilize symmetrical anhydrides, mixed anhydrides, in combination with heating and non-polar solvents have been

Table 2.3. Purification and MALDI-MS data of Ω^{D}PG and ΩXZ turn variants.

Entry	Peptide	Calculated $[M+H]^+$	Observed MALDI-MS	Crude Purity	t_R (min)	Peptide content
1	Ω^{D}PG	1415.76	1415.71	98%	14.92	60%
2	ΩAG	1389.72	1389.45	85%	13.49	85%
3	ΩBG	1403.75	1403.60	93%	14.85	74%
4	ΩB^{D}A	1417.77	1418.24	79%	12.57	58%
5	ΩJG	1458.65	1458.68	43%	17.17	63%
6	ΩUG	1488.70	1488.68	88%	n/a	n/a

B = Aib; J = Dpg; U = Dibg. HPLC crude purities were determined from the area peak integration ratios from analytical HPLC. Purity determinations were performed using a PDA detection ranging from 200-400 nm. Retention times (t_R) correspond to the analytical HPLC of pure compounds. Amino acid analysis (AAA) was used to determine net peptide content. Refer to Appendix B for HPLC chromatograms and MALDI-MS spectra.

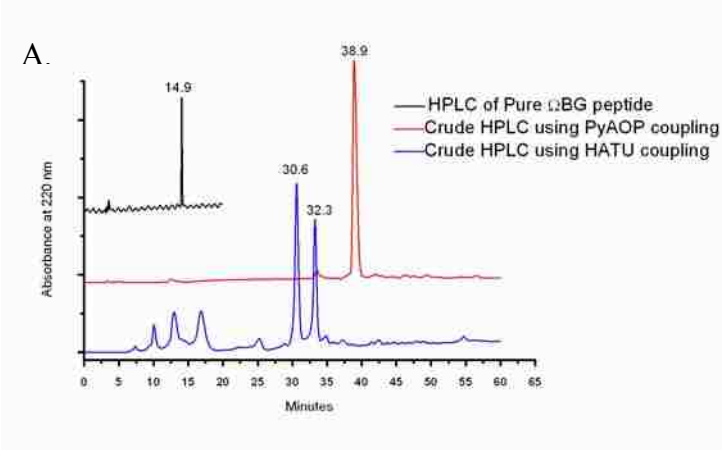

Figure 2.2. Analytical HPLC chromatograms of ΩXZ variants. Two columns were used for peptide analysis: Column A (black) and Column B (red and blue). See 2.2.2 Peptide Synthesis and Purification for details. Buffer conditions: A: H_2O and 0.1% TFA (v/v); B: CH_3CN and 0.1% TFA (v/v), at 1 mL/min (A) ΩBG crude peptide synthesized with HATU activation for Aib and Val-5 coupling (blue) with a gradient of 10% B to 70% B over 60 min; t_R(ΩBG) of 32.3 min. The peak at 30.6 min occurred due to a Val-5 deletion from the peptide sequence. The ΩBG crude peptide, using PyAOP activation at 50 °C for Aib and Val-5 coupling (red), was separated using a gradient of 10% to 27% B over 60 min followed by a ramp from 27% to 37% B over 10 min (total gradient time 70 min); t_R (ΩBG) of 38.9 min. Pure ΩBG with PyAOP activation at 50 °C (black) was analyzed using a gradient of 10% B to 30% B over 20 min. (Figure 2.2 cont'd.)

B.

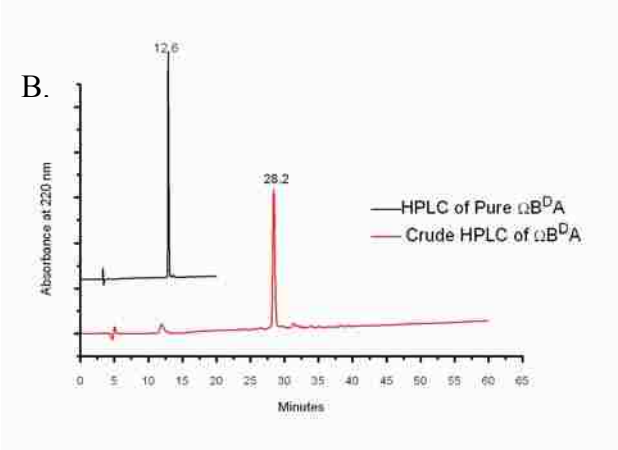

C.

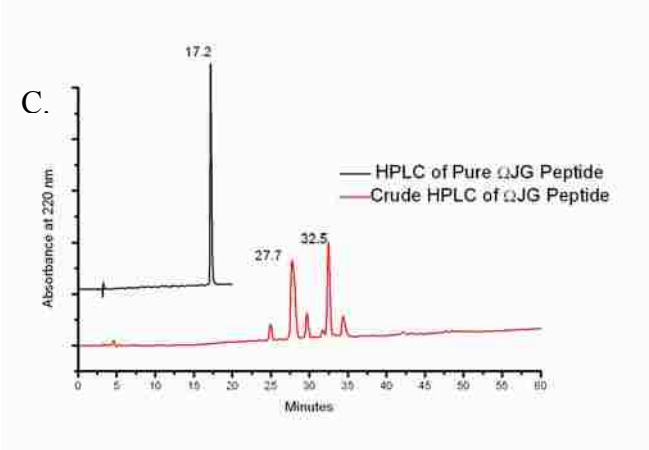

(B) Crude ΩB^{D}A (red) synthesized using PyAOP activation at 50 °C for Aib and Val-5 coupling, gradient of 10% B to 70% B over 60 min; pure ΩB^{D}A (black), gradient of 10% B to 35% B over 20 min. (C) Analytical chromatogram of crude peptide ΩJG (red); t_R (ΩJG) of 32.5 min. The peak at 27.7 min occurred due to the deletion of Arg-1, Tyr-2, Val-3, Glu-4, and Val-5. Pure ΩJG (black) with homogeneity (>99%); gradient of 10% B to 35% B over 35 min.

developed that might increase the yield of this peptide or other homologs.[34, 36] In the synthesis of ΩUG, PyAOP activation was used for the coupling of Dibg-6 to Gly-7. Coupling of Val-5 to the *N*-terminal-side of Dibg occurred via a doubling coupling of amino acid symmetrical anhydride.

2.3.1.2 CIRCULAR DICHROISM

Circular dichroism (CD) spectroscopy represents a facile instrumental method used to monitor secondary structure.[44, 45] A negative band at approximately 217 nm ($n \rightarrow \pi^*$ transitions) and a positive band at 197 nm ($\pi \rightarrow \pi^*$ transitions) is characteristic of β-sheet secondary structures.[46, 47] Additionally, β-turns have their own CD signatures, which have been studied through the use of model cyclic and linear peptides. Type-I/II' turns typically have an α-helical-like CD, while type-I'/II turns have β-sheet-like conformations. Thus, the CD spectra of hairpin peptides containing these turn types will be a conglomerate of both the sheet and turn components.

CD spectra of Ω^DPG and the ΩXZ turn variants (25 °C, 50 μM) are shown in Figure 2.3. CD data showed that Ω^DPG had a β-sheet conformation (data consistent with Gellman[5]). As expected, the ΩAG peptide had a random coil conformation, as indicated by the negative band at 195 nm; this peptide was not studied further and served as an unfolded comparison for the other β-sheet peptides. In contrast, ΩBG and ΩB^DA produced CD spectra that strongly indicated β-sheet conformations (maxima around 200 nm; minima around 215 nm). ΩJG and ΩUG, having almost identical CD curves, also produces a β-sheet secondary structure that was less ordered than the Aib homologues. It was expected that the ααAA-Xxx hairpins would nucleate type-I/I' β-turns based on previous data derived from lowest energy conformations (backbone constraints), crystal structure determination, and detailed NMR analysis of other systems.[11, 30, 48] Thus, if the CD spectra are a mixture of turn and sheet components, it was somewhat surprising

to see the strong similarity in the CD data of Ω^{D}PG (type-II' β-turn) and ΩBG and ΩB^{D}A (putative type-I' β-turn). The difference in the CD band for the more bulky ααAAs turn systems (J, U) could be indicative of the nucleation of a differing β-turn.

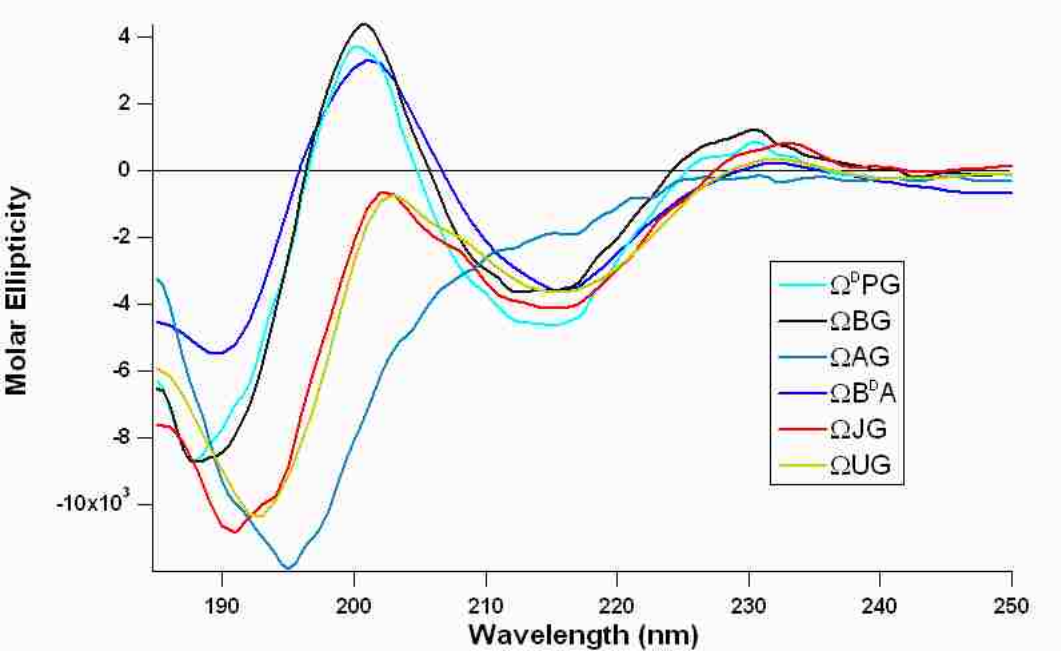

Figure 2.3. CD spectrum of Ω^{D}PG (DPro-Gly) overlayed with spectra of ΩXZ turn variants. Table 2.1 outlines turn designations. Scans were taken at 50 μM peptide concentration in 1 mM NaOAc buffer; pH 3.8 at 25 °C. Molar ellipticity- [θ] units: deg cm^2 $dmol^{-1}$.

To test the aggregation behavior of the β-hairpin forming peptides, their CD spectra were measured over a concentration range of 50 μM-500 μM. The CD of Ω^{D}PG did not vary significantly over a 10-fold concentration range (Figure 2.4 A), which indicates that Ω^{D}PG is not changing aggregation state over this concentration range. This is consistent with the analytical ultracentrifugation results of Gellman that showed Ω^{D}PG was monomeric at NMR concentrations (~1 mM). The ααAA-hairpin peptides also showed no significant changes in CD intensity with a 10-fold increase in concentration (Figure 2.4 B, C, D), also indicating these

peptides do not change aggregation state over this concentration range and that they have a low propensity for aggregation.

The DPro-Gly, Aib-Xxx, and Dpg-Gly hairpins were also thermally stable over a range of temperatures from 5 °C to 55 °C (Figure 2.4 E, F, G, H). This data is shown also in Figure 2.5 as molar ellipticity at various maxima and minima in the spectra is plotted versus temperature. In general, the data showed that the model hairpin peptides exhibited little signs of thermal denaturating up to 55 °C. Also, the temperature denaturating curves were generally linear, thus suggesting the "denaturation" lacked cooperativity.

The temperature dependent CD (Figure 2.4 F) of the Aib-Gly turn peptide showed a systematic decrease in β-sheet character at 202 nm, but the n→π* transitions at 218 nm were almost identical. Figure 2.5 B shows the thermal denaturation of ΩBG at various molar ellipticities. Comparable to Ω^{D}PG, ΩBG lacked thermal denaturating. Both remain linear with a minimal decrease in slope over a wide temperature range. Additionally ΩBG was ^{13}C=O labeled at key positions and its thermal stability was measured.[49, 50] Isotope-edited IR revealed that the Aib-Gly turn inducer partially unfolds (partial transition to random coil) at elevated temperatures up to 95 °C, but upon cooling, a reversible coil to sheet transition was observed. This reversiblility was a result of incomplete protein unfolding due to the stability of the Aib-Gly turn sequence.

The thermal denaturation experiment of the Aib-DAla turn (Figure 2.5 C) suggested that this β-hairpin was stable showing no signs of thermal denaturation. As temperature increased, this peptide became more folded at 25 °C followed by minimal to no unfolding at higher temperatures. The thermal denaturation studies of ΩJG suggest that substitution of more bulky ααAA Dpg could possibly have a negative effect on β-sheet stability (Figure 2.4 H). As

temperature increased, there was a systematic decrease in β-sheet character (232 nm and 202 nm, Figure 2.5 D) suggesting partial protein unfolding at higher temperatures. This is in line with the expected ability of Dpg to stabilize both helical (turn-like) conformations and extended conformations.[28, 30]

2.3.1.3 NMR ANALYSIS

While CD spectroscopy gives some idea of the overall fold of the peptide, to get more detailed structural information, NMR experiments on two of the ααAA-containing peptides, ΩBG and ΩB^DA, were performed. NMR studies were not performed on the more bulky turn sequences, ΩJG and ΩUG, because they displayed signs of self-assembly at concentrations above 400 μM. With the aid of 2-D TOCSY and ROESY experiments, most of the H resonances in ΩBG could be assigned (Table 2.4). Wishart *et al.*[51, 52] and Dyson and Wright *et al.*[53, 54] have shown that $\Delta\delta_{H\alpha}$ depends on the secondary structure of proteins and local backbone torsion angles. Using equation 2.1, peptides could be characterized as α-helical or β-sheet relative to upfield and downfield δHα shifts, respectively, as compared to their random coiled values.[51, 52, 55] Figure 2.6 summarizes the chemical shift index (A-$\Delta\delta_{H\alpha}$, B-$\Delta\delta_{NH}$; Equation 2.1) for Ω^{D}PG, ΩBG, and ΩB^DA. This is a widely used method probe for indication of protein secondary structure. Eight of the twelve residues of ΩBG and ΩB^DA show a downfield shift suggestive of β-strand formation, similar to Ω^{D}PG. The $\Delta\delta_{H\alpha}$ data supports the hypothesis that Aib-Gly and Aib-DAla can form β-turns, which are capable of initializing β-strand motifs and producing an autonomously folded hairpin domain. Further evidence of the folding of ΩBG and ΩB^DA were obtained by measurement of through-space interactions by 2-D ROESY experiments suggesting that both hairpin models induce a type-I' β-turn. Similar through-space

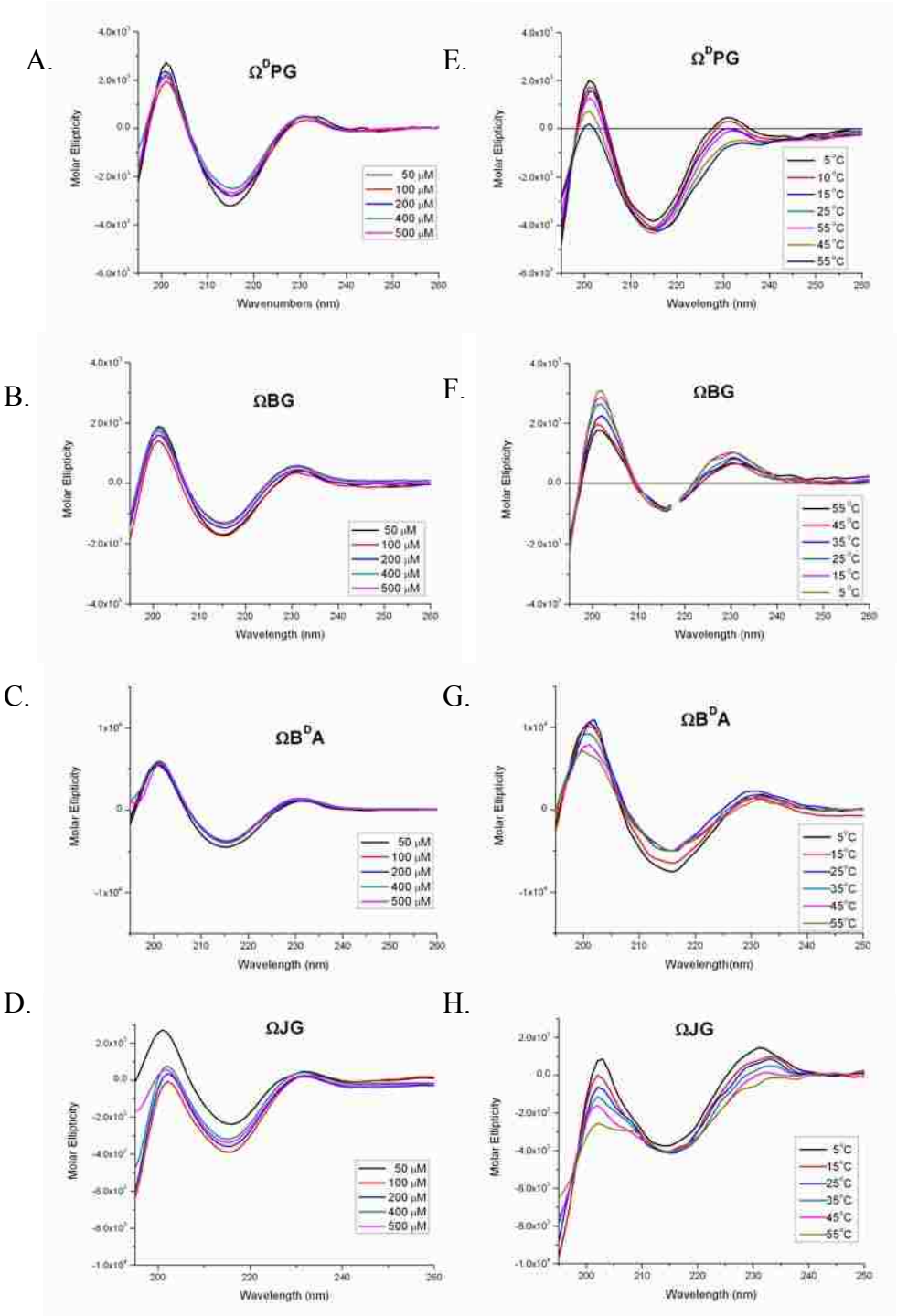

Figure 2.4. Concentration studies (50 μM -500 μM peptide) (A) Ω^{D}PG, (B) ΩBG, (C) ΩB^{D}A, and (D) ΩJG . Temperature analysis (50 μM peptide, 5 °C -55 °C) of (E) Ω^{D}PG, (F) ΩBG, (G) ΩB^{D}A, and (H) ΩJG. All CD spectra were taken in l mM NaOAc; pH 3.8. Molar ellipticity-$[\theta]$ units: deg cm^2 $dmol^{-1}$.

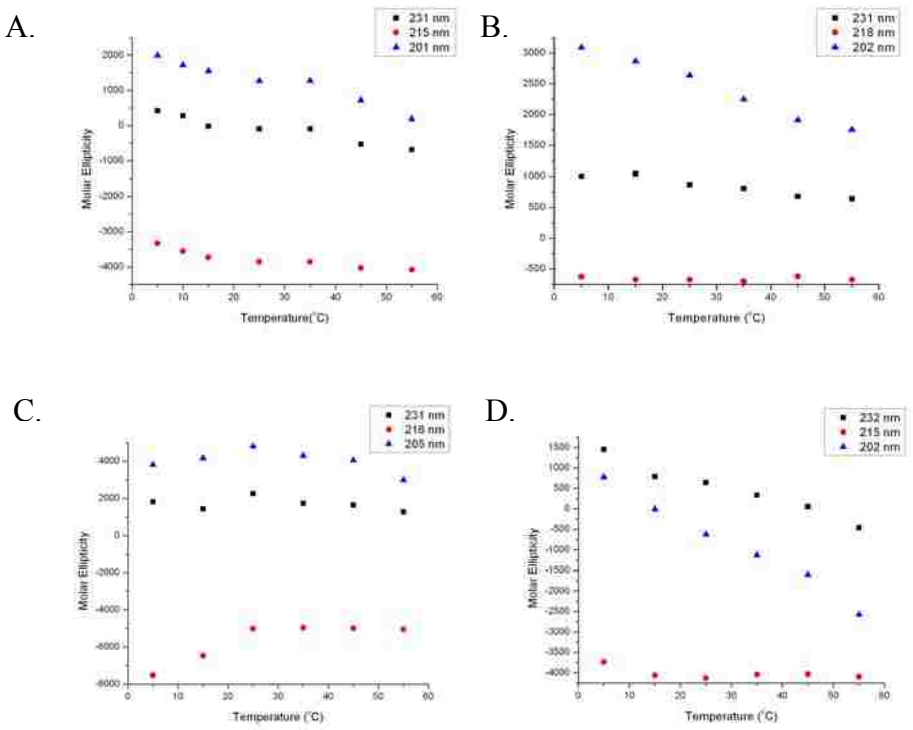

Figure 2.5. Thermal denaturation plots of (A) Ω^{D}PG; (B) ΩBG; (C) ΩB^{D}A; and (D) ΩJG. Temperature range from 5 ºC to 55 ºC taken at 5 ºC-10 ºC intervals. Data extracted from molar ellipticity values at given wavelengths. Molar ellipticity- [θ] units: deg cm^2 $dmol^{-1}$.

Table 2.4. NMR assignments of Hα of ΩYZ peptide variants

Assignment	RC (Wishart-C)	Ω^{D}PG	ΩBG	ΩB^{D}A
R1	4.32	3.96	4.031	4.1
Y2	4.43	5.02	5.141	5.23
V3	4.11	4.22	4.343	4.53
E4	4.24	4.76	4.926	4.45
V5	4.11	4.46	4.159	4.2
X6		4.28	-	-
G7	3.88	3.88, 3.66	3.632, 4.002	4.3
O8	4.23	4.47	4.591	4.6
K9	4.23	4.42	4.521	4.57
I10	4.09	4.34	4.451	4.4
L11	4.35	4.04	4.129	5.09
Q12	4.28	4.18	4.269	4.25
δGlyHα		0.22	0.37	

Gly values are the difference between the two diastereotopic Hα hydrogens.

$$\Delta\delta_{H\alpha} = (\delta_{H\alpha}^{\text{observed}} - \delta_{H\alpha}^{\text{random coil}}) \qquad \text{(Equation 2.1)}$$

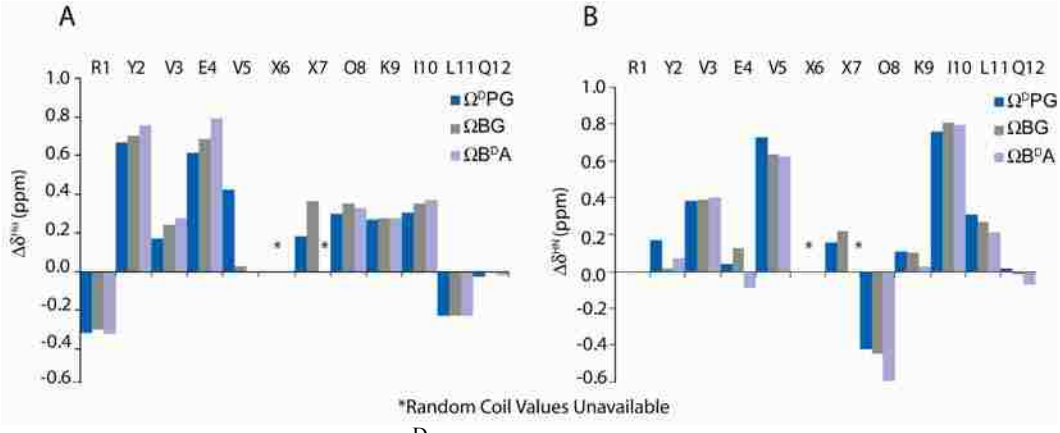

Figure 2.6. Chemical shift index of Ω^{D}PG (blue, data collected by Gellman), ΩBG (grey) and ΩB^{D}A (cyan) at 3.5 mM in 100 mM aqueous sodium deuterioacetate buffer, pH 3.8 (9:1 H_2O: D_2O), 278 K. (A) $\Delta\delta_{H\alpha}$ chemical shift index. (B) $\Delta\delta_{NH}$ chemical shift index. Values were determined using Equation 2.1 utilizing the random coil values of Wishart. Gly values are the difference between the two diastereotopic Hα hydrogens.

interactions were observed by Gellman and coworkers in the Ω^{D}PG peptide including interstrand NH-NH NOEs as well as side-chain/side-chain interactions suggesting a turn aligning the two antiparallel strands in close proximity. The NH-Gly^{7} —> Hβ-Glu^{4} also supports a more folded orientation. A number of "diagonal" side-chain/side-chain ROEs, including Hγ-Gln^{12} —> H$\tilde{\gamma}$Val^{3}, Hβ/δ-Lys^{9} —> H$\tilde{\gamma}$Tyr^{2}, along with the , Hβ-Gln^{12} —> H$\tilde{\alpha}$Tyr^{2}, suggest a twisted hairpin.

An overlay of the backbone for the three peptides (Figure 2.7) resulted in a RMSD ~0.4 Å, for the average minimized structures. Moreover, ΩBG and ΩB^{D}A adopt a [2:4] type-I' β-turn with a left-handed twist (see Masterson et al.[56] for complete list of defined torsion angles) with only small differences in the lengths of the backbone hydrogen bonds. The structure of Ω^{D}PG shows longer hydrogen bonds, while ΩB^{D}A and ΩBG show more uniform lengths along the

peptide backbone. This apparent discrepancy could be explained by the different protocols used for the structural refinement calculations.

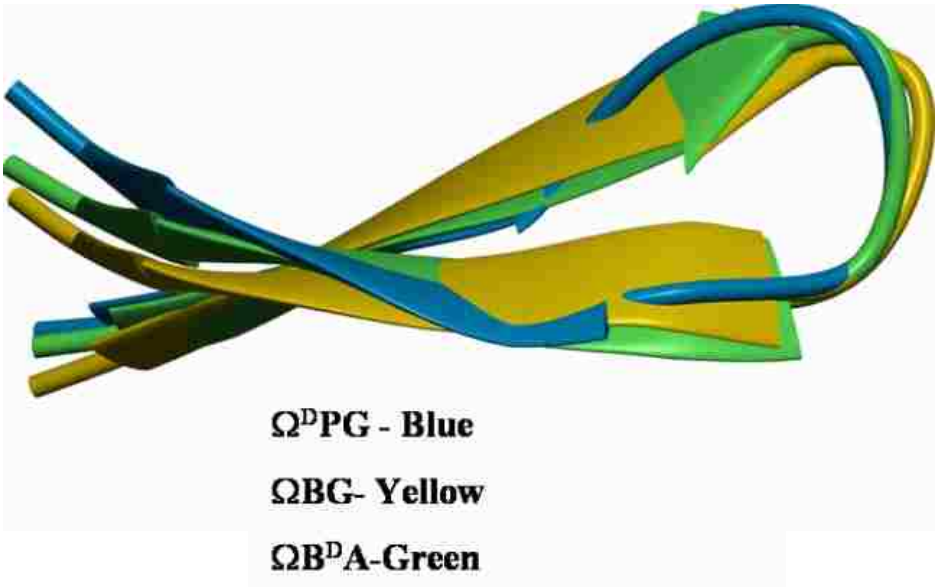

Figure 2.7. Superposition of Ω^{D}PG, ΩBG, and ΩB^{D}A backbone. Structure determinations were calculated using XPLOR.2.5.

2.3.2 EFFECTS OF αα AAs IN β-STRANDS

The use of ααAAs in stabilizing β-sheet conformations is not completely understood. Wang et al.[57] suggest that Aib and its more bulky ααAA homologues have conformational preferences depending on local peptide sequence. This occurs because the higher dialkylated amino acids conformations are strongly dependent on sequence and the solvating environment. Thus, it is imperative to design peptide models that define specific context-dependent factors stabilizing ααAAs in a desired conformational space. Section 2.3.1 of this chapter has highlighted the importance of ααAAs in stabilizing β-turns; here, the importance of amino acid sequencing relative to peptide primary structure and cross-strand interactions will be investigated

using ααAAs. To study local preferences, Dpg and Dibg have been incorporated into position-3 of the β-strand portion of the previously studied, Ω^{D}PG peptide.

The UV-monitored continuous flow synthesis cycle indicated successful deprotection steps, rapid release and elimination of the UV absorbing Fmoc protecting group, and wash cycles for all amino acids prior to the coupling of Tyr-2 and Arg-1 for [J^3]-Ω^{D}PG. PyAOP/DIEA was used as the activating agent with an amino acid double coupling at 50°C for the coupling of Dpg-3 ([J^3]-Ω^{D}PG) and Dibg-3 ([U^3]-Ω^{D}PG) to Glu-4 and for the coupling of Tyr-2 to Dpg-3 ([J^3]-Ω^{D}PG). This was performed because previous studies by Fu et al.[36] suggest that elevated temperatures at the *N*-acylated coupling site of ααAAs results in better product yields due to the use of phosphonium-based coupling agents and higher molecule to molecule interactions as a result of heating. In the synthesis of [U^3]-Ω^{D}PG, Tyr-2 was double coupled to the peptide sequence via amino acid symmetrical anhydride coupling. The HPLC chromatogram of [J^3]-Ω^{D}PG displayed two distinct peaks with t_R of 54.5 min and t_R of 56.8 min (Appendix B-1). MALDI-MS corresponding to the peak with t_R of 54.5 min suggested that residues Tyr-2 and Arg-1 did not couple to the peptide chain. The peak with t_R of 56.8 min had a mass corresponding to [J^3]-Ω^{D}PG (Appendix B-2; calc peaks-1456 mass units with *m/z* observed peaks $[M+Na]^+$ at 1478 mass units and $[M+K]^+$ at 1500 mass units; homogeneity > 99% determined by analytical HPLC). The HPLC chromatogram of [U^3]-Ω^{D}PG had a major peak at t_R of 38.5 min and a crude peptide content (determined by integration of peak area) of 83%. MALDI-MS data of the peak corresponding to t_R of 38.5 min revealed the mass unit of the desired peptide sequence, calculated m/z 1486.7, observed m/z 1486.2. Amino acid analysis (AAA) measurements were not performed on [U^3]-Ω^{D}PG and AAA results for [J^3]-Ω^{D}PG were inconclusive.

Circular dichroism measurements of Ω^{D}PG, [J^{3}]-Ω^{D}PG, and [U^{3}]-Ω^{D}PG were assayed in 1mM NaOAc buffer (pH 3.8). Ω^{D}PG is a well established autonomously folding β-hairpin used to study amino acid propensities in stabilizing β-sheet secondary structures and was used as a control peptide to assess the relative β-sheet character of [J^{3}]-Ω^{D}PG and [U^{3}]-Ω^{D}PG. It was hypothesized that the β- and γ-branching of Dpg and Dibg would increase β-sheet formation. The CD spectrum of Ω^{D}PG (Figure 2.8, black) was characteristic of a β-sheet conformation. The CD spectrum of [J^{3}]-Ω^{D}PG (Figure 2.8, green) displayed the presence of a less structured β-sheet (minimum at 219 nm) with the presence of random coil (negative ellipticity below 200 nm) contributions while the CD spectrum of [U^{3}]-Ω^{D}PG (Figure 2.8, red) indicated a more ordered β-sheet conformation as compared to the Ω^{D}PG control peptide. The less ordered CD band for [J^{3}]-Ω^{D}PG and the more ordered secondary structure for [U^{3}]-Ω^{D}PG suggest that the ααAAs (Dpg, J and Dibg, U) contribute to β-sheet formation and stability in a context- and sequence-dependent manner.

With the use of 2-D NMR techniques (ROESY and TOSCY), peptide conformations, with respect to neighboring amino acid residues, were observed (Figure 2.9). Dyson and Wright random coil standards were chosen as they take into account the nearest neighbor effects of other residues, most nobably Pro and aromatic residues.[53, 54] A downfield shift in the Hα chemical shift deviation (Figure 2.9) for eight of the nine amino acids measured (more folded secondary structure for seven residues), suggests [U^{3}]-Ω^{D}PG formed a more ordered β-sheet conformation. This is in good agreement with CD data (Figure 2.8). Experimental results suggest that Dibg had a higher propensity to promote a β-sheet conformation in aqueous buffer when strategically placed in the β-strand region of a β-hairpin peptide. CD spectroscopy and NMR analysis of the

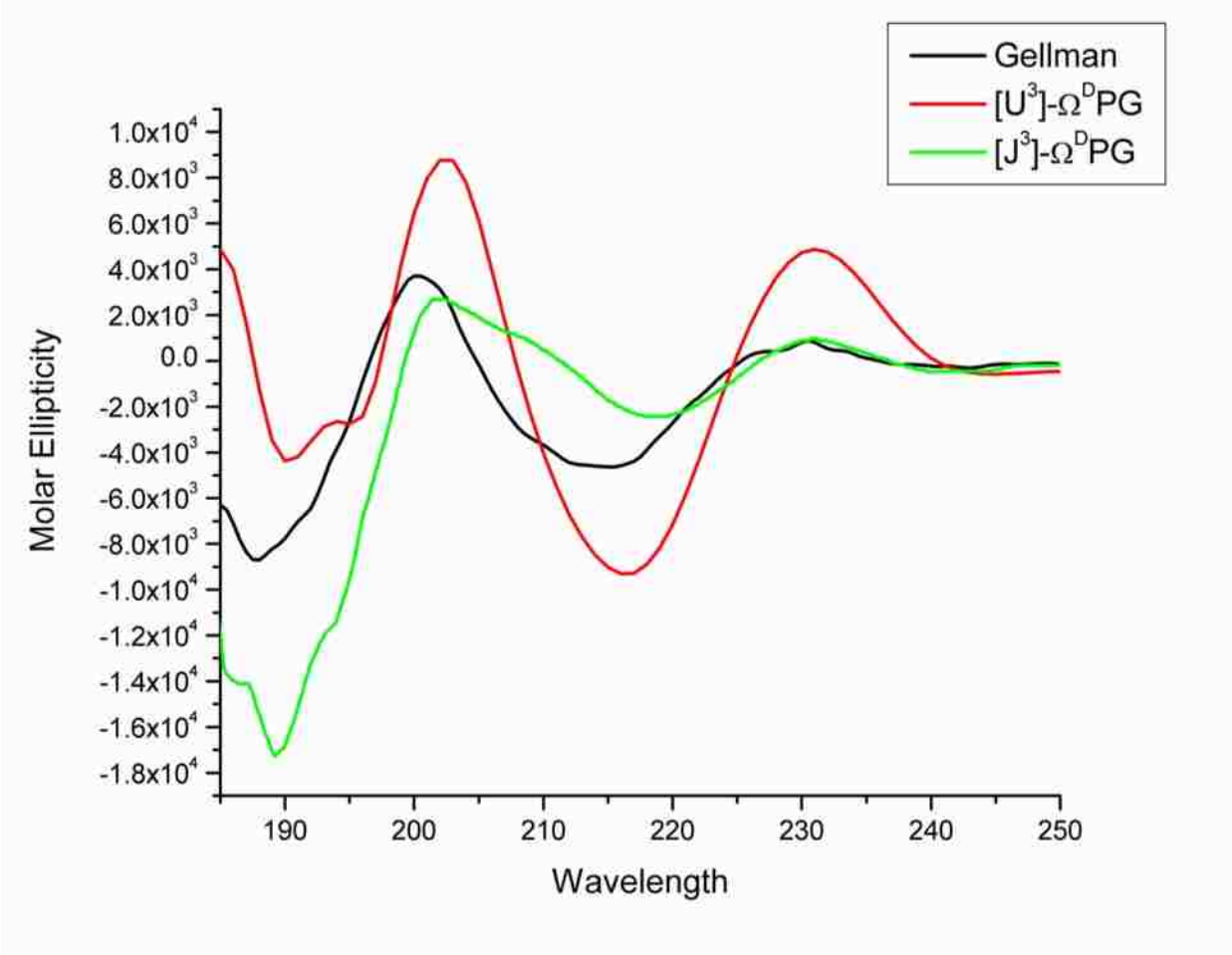

Figure 2.8. CD spectrum of Ω^{D}PG, [J^{3}]-Ω^{D}PG, and [U^{3}]-Ω^{D}PG. Scans were taken in 1mM NaOAc buffer, pH 3.8, (peptide concentration, 0.1mM). Molar ellipticity- [θ] units: deg cm^{2} $dmol^{-1}$.

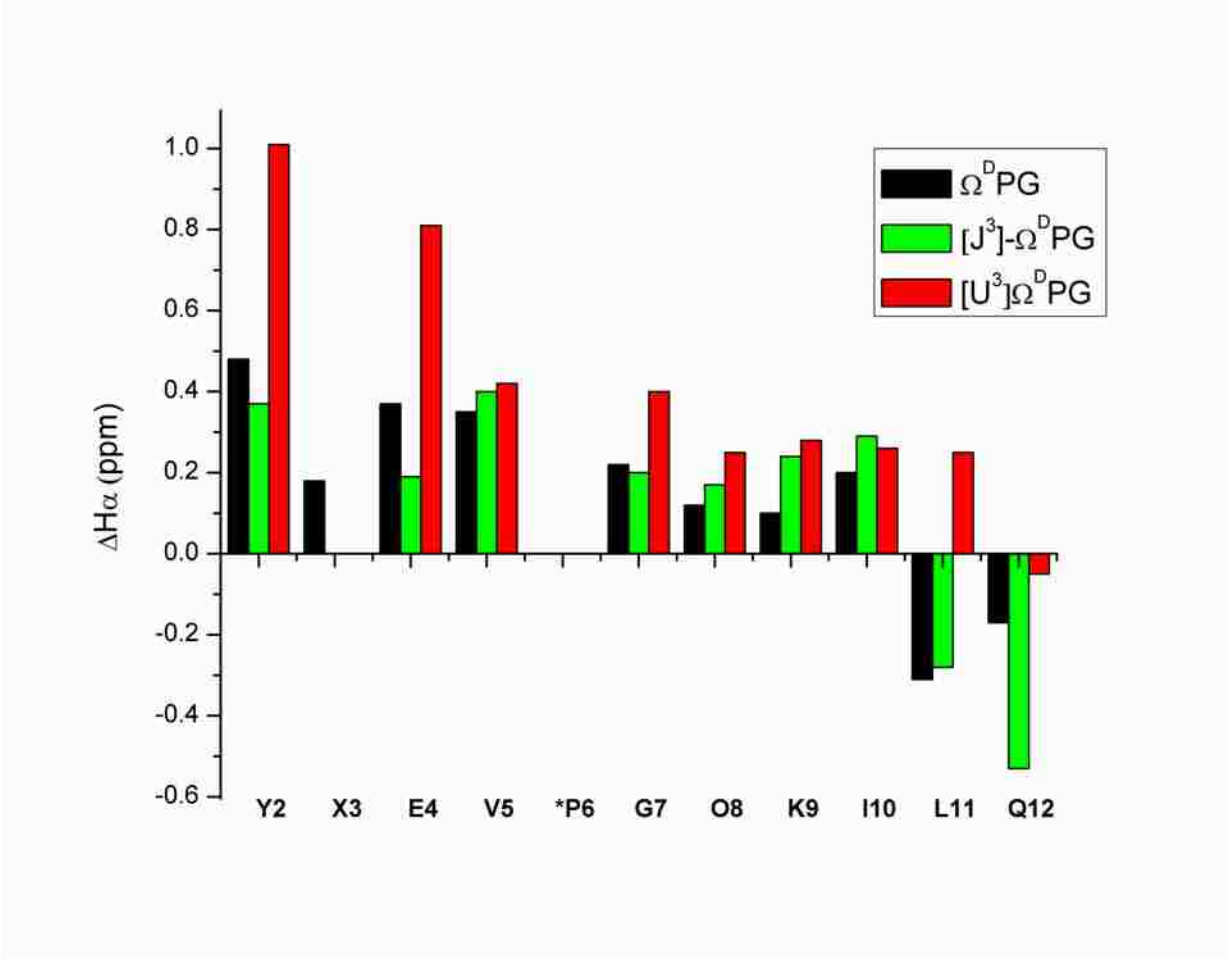

Figure 2.9. Chemical shift index of Ω^{D}PG (black), [J^3]-Ω^{D}PG (green), and [U^3]-Ω^{D}PG (red) at 3.5 mM in 100 mM aqueous sodium deuterioacetate buffer, pH 3.8 (9:1 H_2O: D_2O), 278.1 K. $\Delta\delta_{H\alpha}$ values were determined utilizing the random coil values of Dyson and Wright (Equation 2.1). Gly values are the difference between the two diastereotopic α-hydrogens.

Hα chemical shift deviation for [J^3]-Ω^{D}PG suggests that Dpg containing peptides form less ordered β-sheet conformations relative to their positioning in β-strands and β-turns (*i+1* residue).

2.4 CONCLUSION

The Asn-Gly and DPro-Gly hairpins have been studied extensively. DPro-Gly turns have been proven to have superiority in hairpin nucleation in aqueous buffer compared to Asn-Gly. It was proposed that Aib-Xxx and ααAA-Gly turns would nucleate type-I'/II' β-turns. CD and NMR analysis support the hypothesis that Aib-Xxx turns are sufficient in the nucleation of type-

I' β-hairpins. The stereochemical effects of amino acid residues in the *i+2* position of the β-turn are under further investigation. CD data and CD based thermal denaturation studies suggest that more bulky side-chain groups (larger than methyl groups) in the β-turn moderately destabilize the β-sheet secondary structures.

Dpg containing peptides form less ordered β-sheet conformations when Dpg is incorporated into both the *i+1* position of a β-turn and β-strand portions of β-hairpin peptides. This would suggest that Dpg is nucleating a differing turn type. Dibg containing peptides form less ordered β-sheets when Dibg is located in the *i+1* position of a β-turn (section 2.3.1.2), but Dibg is an excellent promoter of β-sheet formation relative to its positioning in β-strands. This emphasizes the importance of side-chain interactions in stabilizing β-sheet conformations. More in depth CD and NMR structural analysis is needed to fully understand the local conformational preferences of ααAAs in β-sheets.

2.5 REFERENCES

1. Kelly, J. W. The environmental dependency of protein folding best explains prion and amyloid diseases. *Proc. Natl. Acad. Sci. U. S. A.* **1998,** 95, 930-932.

2. Searle, M. S. Peptide models of protein β-sheets: design, folding and insights into stabilising weak interactions. *J. Chem. Soc., Perkin Trans. 2* **2001**, 1011-1020.

3. Hutchinson, E. G.; Thornton, J. M. A revised set of potentials for β-turn formation in proteins. *Protein Sci.* **1994,** 3, 2207-16.

4. Haque, T. S.; Gellman, S. H. Insights on β-hairpin stability in aqueous solution from peptides with enforced type-I' and type-II' β-turns. *J. Am. Chem. Soc.* **1997,** 119, 2303-2304.

5. Stanger, H. E.; Gellman, S. H. Rules for antiparallel β-sheet design: D-Pro-Gly is superior to L-Asn-Gly for β-hairpin nucleation. *J. Am. Chem. Soc.* **1998,** 120, 4236-4237.

6. Gunasekaran, K.; Ramakrishnan, C.; Balaram, P. β-Hairpins in proteins revisited: lessons for de novo design. *Protein Eng.* **1997,** 10, 1131-1141.

7. Raghothama, S. R.; Awasthi, S. K.; Balaram, P. β-Hairpin nucleation by Pro-Gly β-turns. Comparison of D-Pro-Gly and L-Pro-Gly sequences in an apolar octapeptide. *J. Chem. Soc., Perkin Trans. 2* **1998**, 137-144.

8. Haque, T. S.; Little, J. C.; Gellman, S. H. Stereochemical requirements for β-hairpin formation: Model studies with four-residue peptides and depsipeptides. *J. Am. Chem. Soc.* **1996,** 118, 6975-6985.

9. McElroy, A. B.; Clegg, S. P.; Deal, M. J.; Ewan, G. B.; Hagan, R. M.; Ireland, S. J.; Jordan, C. C.; Porter, B.; Ross, B. C.; Ward, P.; Whittington, A. R. Highly potent and selective heptapeptide antagonists of the Neurokinin Nk-2 receptor. *J. Med. Chem.* **1992,** 35, 2582-2591.

10. Chalmers, D. K.; Marshall, G. R. Pro-D-NMe-amino acid and D-Pro-NMe-amino acid: simple, efficient reverse-turn constraints. *J. Am. Chem. Soc.* **1995,** 117, 5927-37.

11. Aravinda, S.; Harini, V. V.; Shamala, N.; Das, C.; Balaram, P. Structure and assembly of designed β-hairpin peptides in crystals as models for β-sheet aggregation. *Biochemistry* **2004,** 43, 1832-1846.

12. Aravinda, S.; Shamala, N.; Rajkishore, R.; Gopi, H. N.; Balaram, P. A crystalline β-hairpin peptide nucleated by a type-I' Aib- D-Ala β-turn: Evidence for cross-strand aromatic interactions. *Angew. Chem. Int. Edit.* **2002,** 41, 3863-3865.

13. Sharman, G. J.; Griffiths-Jones, S. R.; Jourdan, M.; Searle, M. S. Effects of amino acid φ,ψ propensities and secondary structure interactions in modulating Hα chemical shifts in peptide and protein β-sheet. *J. Am. Chem. Soc.* **2001,** 123, 12318-12324.

14. Griffiths-Jones, S. R.; Maynard, A. J.; Sharman, G. J.; Searle, M. S. NMR evidence for the nucleation of a β-hairpin peptide conformation in water by an Asn-Gly type-I' β-turn sequence. *Chem. Commun.* **1998**, 789-790.

15. DeGrado, W. F.; Lear, J. D. Induction of peptide conformation at apolar water interfaces. 1. A study with model peptides of defined hydrophobic periodicity. *J. Am. Chem. Soc.* **1985,** 107, 7684-9.

16. Tatko, C. D.; Waters, M. L. Selective aromatic interactions in β-hairpin peptides. *J. Am. Chem. Soc.* **2002,** 124, 9372-9373.

17. Tatko, C. D.; Waters, M. L. The geometry and efficacy of cation-π interactions in a diagonal position of a designed β-hairpin. *Protein Sci.* **2003,** 12, 2443-2452.

18. Tatko, C. D.; Waters, M. L. Investigation of the nature of the methionine-π interaction in β-hairpin peptide model systems. *Protein Sci.* **2004,** 13, 2515-2522.

19. Rashkin, M. J.; Waters, M. L. Unexpected substituent effects in offset π–π stacked interactions in water. *J. Am. Chem. Soc.* **2002,** 124, 1860-1861.

20. Kiehna, S. E.; Waters, M. L. Sequence-dependence of β-hairpin structure: Comparison of a salt bridge and an aromatic interaction. *Protein Sci.* **2003,** 12, 2657-2667.

21. Sharman, G. J.; Searle, M. S. Dissecting the effects of cooperativity on the stabilization of a de novo designed three stranded anti-parallel β-sheet. *Chem. Commun.* **1997**, 1955-1956.

22. Sharman, G. J.; Searle, M. S. Cooperative interaction between the three strands of a designed antiparallel β-sheet. *J. Am. Chem. Soc.* **1998,** 120, 5291-5300.

23. Maynard, A. J.; Sharman, G. J.; Searle, M. S. Origin of β-hairpin stability in solution: structural and thermodynamic analysis of the folding of a model peptide supports hydrophobic stabilization in water. *J. Am. Chem. Soc.* **1998,** 120, 1996-2007.

24. Espinosa, J. F.; Gellman, S. H. A designed β-hairpin containing a natural hydrophobic cluster. *Angew. Chem. Int. Edit.* **2000,** 39, 2330-2333.

25. Syud, F. A.; Stanger, H. E.; Gellman, S. H. Interstrand side chain-side chain interactions in a designed β-hairpin: Significance of both lateral and diagonal pairings. *J. Am. Chem. Soc.* **2001,** 123, 8667-8677.

26. Cochran, A. G.; Skelton, N. J.; Starovasnik, M. A. Tryptophan zippers: stable, monomeric β-hairpins. *Proc. Natl. Acad. Sci. U. S. A.* **2001,** 98, 5578-5583.

27. Russell, S. J.; Blandl, T.; Skelton, N. J.; Cochran, A. G. Stability of cyclic β-hairpins: asymmetric contributions from side-chains of a hydrogen-bonded cross-strand residue pair. *J. Am. Chem. Soc.* **2003,** 125, 388-395.

28. Karle, I. L.; Kaul, R.; Rao, R. B.; Raghothama, S.; Balaram, P. Stereochemical analysis of higher α,α-dialkylglycine containing peptides. Characterization of local helical conformations at dipropylglycine residues and observation of a novel hydrated Multiple β-turn structure in crystals of a glycine rich peptide. *J. Am. Chem. Soc.* **1997,** 119, 12048-12054.

29. Toniolo, C.; Crisma, M.; Formaggio, F.; Peggion, C. Control of peptide conformation by the Thorpe-Ingold effect (C^{α}-tetrasubstitution). *Biopolymers* **2001,** 60, 396-419.

30. Kaul, R.; Banumathi, S.; Velmurugan, D.; Balaji Rao, R.; Balaram, P. Conformational choice at α,α-di-*N*-propylglycine residues: helical or fully extended structures? *Biopolymers* **2000,** 54, 159-167.

31. Awasthi, S. K.; Shankaramma, S. C.; Raghothama, S.; Balaram, P. Solvent-induced β-hairpin to helix conformational transition in a designed peptide. *Biopolymers* **2001,** 58, 465-476.

32. Kaul, R.; Banumathi, S.; Velmurugan, D.; Ravikumar, K.; Rao, R. B.; Balaram, P. Context-dependent conformation of diethylglycine residues in peptides. *J. Peptide Res.* **2000,** 55, 271-278.

33. Hammarstroem, L. G. J.; Fu, Y.; Vail, S.; Hammer, R. P.; McLaughlin, M. L. A convenient preparation of an orthogonally protected Cα,α-disubstituted amino acid analog of lysine: 1-tert-butyloxycarbonyl-4-((9-fluorenylmethyloxycarbonyl)amino)-piperidine-4-carboxylic acid. *Org. Syn.* **2005,** 81, 213-224.

34. Fu, Y.; Etienne, M. A.; Hammer, R. P. Facile Synthesis of α,α-Diisobutylglycine and anchoring its erivatives onto PAL-PEG-PS resin. *J. Org. Chem.* **2003,** 68, 9854-9857.

35. Fu, Y.; Hammarstroem, L. G. J.; Miller, T. J.; Fronczek, F. R.; McLaughlin, M. L.; Hammer, R. P. Sterically hindered $C^{\alpha,\alpha}$-disubstituted α-amino acids: Synthesis from α-nitroacetate and incorporation into peptides. *J. Org. Chem.* **2001,** 66, 7118-7124.

36. Fu, Y.; Hammer, R. P. Efficient acylation of the *N*-terminus of highly hindered $C^{\alpha,\alpha}$-disubstituted amino acids via amino acid symmetrical anhydrides. *Org. Lett.* **2002,** 4, 237-240.

37. Wysong, C. L.; Yokum, T. S.; McLaughlin, M. L.; Hammer, R. P. Controlling peptide structure. *Chem. Tech.* **1997,** 27, 26-33.

38. Wysong, C. L.; Yokum, T. S.; Morales, G. A.; Gundry, R. L.; McLaughlin, M. L.; Hammer, R. P. 4-Aminopiperidine-4-carboxylic ccid: A cyclic α,α-disubstituted amino acid for preparation of water-soluble highly helical peptides. *J. Org. Chem.* **1996,** 61, 7650-7651.

39. Bolin, D. R.; Sytwu, II; Humiec, F.; Meienhofer, J. Preparation of oligomer-free *N*-alpha-Fmoc and *N*-alpha-urethane amino-acids. *Int. J. Pept. Protein Res.* **1989,** 33, 353-359.

40. Sole, N. A.; Barany, G. Optimization of solid-phase synthesis of [Ala8]-dynorphin A. *J. Org. Chem.* **1992,** 57, 5399-403.

41. Piotto, M.; Saudek, V.; Sklenar, V. Gradient-tailored excitation for single-quantum NMR-spectroscopy of aqueous-solutions. *J. Biomol. NMR* **1992,** 2, 661-665.

42. Koradi, R.; Billeter, M.; Wuthrich, K. MOLMOL: A program for display and analysis of macromolecular structures. *J. Mol. Graph.* **1996,** 14, 51-&.

43. Martin, L.; Ivancich, A.; Vita, C.; Formaggio, F.; Toniolo, C. Solid-phase synthesis of peptides containing the spin-labeled 2,2,6,6-tetramethylpiperidine-1-oxyl-4-amino-4-carboxylic acid (TOAC). *J. Peptide Res.* **2001,** 58, 424-432.

44. Johnson, C. W., Jr. Protein seconday structure and circular dichorism: A practical guide. *Protiens* **1990,** 7, 205-214.

45. Perczel, A.; Park, K.; Fasman, G. D. Analysis of the circular dichroism spectrum of proteins using the convex constraint algorithm: a practical guide. *Anal. Biochem.* **1992,** 203, 83-93.

46. Sreerama, N.; Woody, R. W. Computation and analysis of protein circular dichroism spectra. *Methods Enzymol.* **2004,** 383, 318-351.

47. Woody, R. W. Circular dichroism of peptides and proteins. *Circ. Dichroism* **1994**, 473-496.

48. Balaram, P. De novo design: backbone conformational constraints in nucleating helices and β-hairpins. *J. Peptide Res.* **1999,** 54, 195-199.

49. Setnicka, V.; Huang, R.; Thomas, C. L.; Etienne, M. A.; Kubelka, J.; Hammer, R. P.; Keiderling, T. A. IR study of cross-strand coupling in a β-hairpin peptide using isotopic labels. *J. Am. Chem. Soc.* **2005,** 127, 4992-4993.

50. Huang, R.; Setnicka, V.; Etienne, M. A.; Kim, J.; Kubelka, J.; Hammer, R. P.; Keiderling, T. A. Cross-strand coupling of a β-hairpin peptide stabilized with an Aib-Gly turn studied using Isotope-edited IR spectroscopy. *J. Am. Chem. Soc.* **2007,** 129, 13592-13603.

51. Wishart, D. S.; Sykes, B. D.; Richards, F. M. Relationship between nuclear-magnetic-resonance chemical-shift and protein secondary structure. *J. Mol. Biol.* **1991,** 222, 311-333.

52. Wishart, D. S.; Sykes, B. D.; Richards, F. M. The chemical shift index: a fast and simple method for the assignment of protein secondary structure through NMR spectroscopy. *Biochemistry* **1992,** 31, 1647-51.

53. Schwarzinger, S.; Kroon, G. J.; Foss, T. R.; Chung, J.; Wright, P. E.; Dyson, H. J. Sequence-dependent correction of random coil NMR chemical shifts. *J. Am. Chem. Soc.* **2001,** 123, 2970-8.

54. Merutka, G.; Dyson, H. J.; Wright, P. E. Random coil ^{1}H chemical shifts obtained as a function of temperature and trifluoroethanol concentration for the peptide series GGXGG. *J. Biomol. NMR* **1995,** 5, 14-24.

55. Wuthrich, K., *NMR of Proteins and Nucleic Acids*. John Wiley and Sons, New York: 1986; p 304 pp.

56. Masterson, L. R.; Etienne, M. A.; Porcelli, F.; Barany, G.; Hammer, R. P.; Veglia, G. Nonstereogenic α-aminoisobutyryl-glycyl dipeptidyl unit nucleates type-I' β-turn in linear peptides in aqueous solution. *Biopolymers* **2007,** 88, 746-753.

57. Wang, J. Design, synthesis, and conformational studies of peptides containing chiral and achiral α,α-disubstituted amino acids. PhD Dissertation, Louisiana State University, Baton Rouge, 2007.

CHAPTER 3.

INTRODUCTION TO ALZHEIMER'S DISEASE*

3.1 THE HISTORY OF ALZHEIMER'S DISEASE

One of the most prevalent protein conformational diseases is Alzheimer's disease (AD). AD was first described in 1907 by Bavarian psychiatrist Alois Alzheimer.[1, 2] Alzheimer described the clinical observations of a 51-year old woman's behavioral symptoms as complete helplessness having increased imbecility with continual increase in the lapse of metacognition as her illness progressed. In the post-mortem autopsy of the patient's brain, Alzheimer noticed extensive pathological changes such as a shrunken cortex[3] and distinguishable fibrils combined in thick bundles located on the surface of neuronal cells.[4] Alzheimer characterized this disease as progressive pre-senile dementia with cortex atrophy. In 1910, this disease was officially named Alzheimer's disease due to the detailed description of Auguste's brain by the Bavarian neuropsychiatrist.[5]

3.2 AD IMPACT ON SOCIETY

Alzheimer's disease is the most common form of dementia and is the 7th leading cause of death in America. Unfortunately, the death toll associated with this disease is on the rise; AD is one of only two causes of death, the other being hypertension, to increase in ranking as a leading cause of death in the past five years.[6] In 2000, approximately 4.5 million Americans were diagnosed with AD. Today, 5 million Americans suffer with this disease and by the middle of the current century, 14 million are predicted to be diagnosed.[7, 8] The reported statistics only take into account the documented cases within the US population. Worldwide, approximately more than 30 million people are speculated to have this degenerative disease.

With increasing technology over the past century, the distinguishable fibrils and thick bundles initially reported by Alzheimer have been identified as being composed of amyloid protein

* Reprinted by permission of The American Chemical Society.

aggregates, mostly consisting of the β-amyloid protein (Aβ). The amyloid hypothesis states that "accumulation of Aβ in the brain is the primary influence driving AD pathogenesis";[9, 10] therefore, current research seeks to understand the causative role of the Aβ in the onset of AD.

3.3 IDENTIFICATION OF THE β-AMYLOID PEPTIDE

The initial identification of Aβ primary sequence, a highly hydrophobic peptide, 39-43 amino acids in length, was obtained by Glenner and Wong in 1984,[11] when they extracted Aβ extracted from both senile plaques and blood vessels and characterized this highly complex protein via Edman degradation and amino acid analysis (AAA).[10-12] Based on oligonucleotide probes which complemented the Aβ peptide gene, scientists later discovered the gene responsible for encoding Aβ. Subsequent work by Kang et al.[13] lead to the cloning of the ubiquitously expressed transmembrane type-1 glycoprotein known as the amyloid precursor protein (APP).[2, 9, 14] APP is cleaved in vivo by the α-, β-, and γ-secretases. Cleavage of APP with the α-secretase enzyme produces non-amyloidegenic fragments of Aβ. Normal secretion of the *N*-terminal fragment of Aβ occurs while the *C*-terminal fragment remain anchored to the cell membrane. Further cleavage with γ-secretase then releases the inactive bound *C*-terminal fragment out of the cell. However, cleavage using the β-sercetase results in the *N*-terminal cleavage of Aβ from APP and subsequent cleavage with the γ-secretase result in the release of the *C*-terminal side of Aβ from APP. Sequential proteolytic processing of APP with the β- and γ-secretases lead to the production of the two neurotoxic isoforms of Aβ, $A\beta_{1\text{-}40}$ (most abundant) and $A\beta_{1\text{-}42}$ (second most abundant), (Figure 3.1).[3, 9, 10, 15]

3.4 Aβ AGGREGATION

Under normal physiological conditions, Aβ proteins are soluble and have been detected in normal human plasma (nm concentrations). Aβ is naturally produced in both the blood and

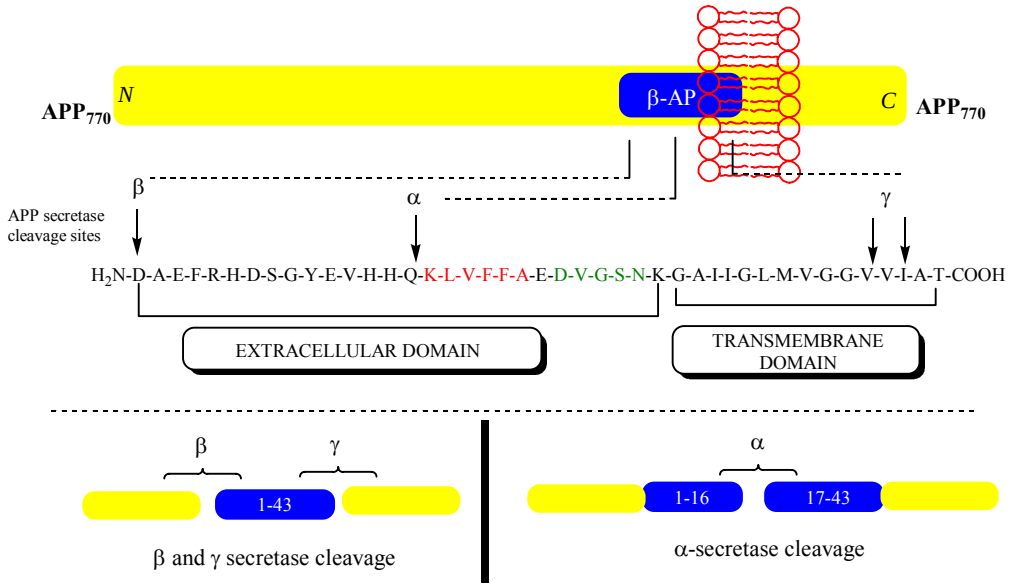

Figure 3.1. Proteolytic cleavage of Aβ from the Amyloid Precursor Protein (APP) by the α-, β-, and γ-secretases. Cleavage of APP with the α-secretase produces two inactive fragments of Aβ. However, cleavage with β-secretase followed by cleavage with the γ-sercetase results in the release of full length Aβ from APP producing the two neurotoxic isoforms of Aβ, $A\beta_{1\text{-}40}$ and $A\beta_{1\text{-}42}$.

brain of all humans and normally, it is fully catabolised, secreted, and released from cells before it can be deposited.[15-17] However, the abnormal secretion of Aβ from APP in vivo leads to the formation of Aβ two neurotoxic isoforms.

The fibrillogenesis process of Aβ has been under investigation in order to identify the neurotoxic entities associated with AD and for the development of medicinal strategies to target these neurotoxins. In one of the first experiments assessing the aggregation behavior Aβ, Jarrett and Lansbury[18-20] observed a delay period where supersaturated aqueous protein solutions (200 μM -250 μM) remained clear for days followed by protein nucleation where insoluble fibrils were rapidly formed resulting in viscous and turbid solutions. The lag phase associated with the thermodynamic solubility (amyloid stability) suggested that monomer dissolution to ordered peptide aggregates was slow and thermodynamically unfavored and formation of a stable nucleus

or addition of nuclei (seeding of solutions) served as a template for spontaneous fibril growth. These findings lead to the assumption that the nucleation step is the rate-determining step in fibril formation, thus introducing the widely accepted nucleation-dependent polymerization mechanism (Figure 3.2).[18-20]

Lomakin et al.[21, 22] showed that Aβ fibrillogensis was dependent on initial protein concentration. Using light scattering techniques, they observed that if Aβ protein concentration was greater than its critical micelle concentration (cmc; ~25 μM),[23, 24] spontaneous and reversible self-assembly of monomers to micelle was established followed by rapid fibril formation. In contrast, if Aβ protein concentration was below its cmc, no micelles were formed and the predominate pathway was a heterogeneous nucleation process seeded by preformed aggregates or impurities not Aβ itself. Lomakin's model provided the theory that once the Aβ nucleus was formed (micelle acting as nuclei), fibril elongation was dependent on monomer concentration.

Harper and Lansbury[25, 26] agreed with the nucleation-dependent polymerization aggregation model, but was one of the first to discover differences between $A\beta_{1-40}$ and $A\beta_{1-42}$ aggregation kinetics and identified a structural intermediate that was found to play an important role in the fibrillogenesis process of Aβ. In agreement with Jarrett[18-20] and Lansbury,[27, 28] they noted that $A\beta_{1-42}$ nucleated more quickly than $A\beta_{1-40}$. The increased hydrophobicity of the *C*-terminus was responsible for the faster aggregation kinetics rather than initial concentration of full length Aβ as suggested by Lomakin et al.[21] Harper et al.[25, 26, 29] also observed three important events dealing with the observation of an intermediate species named "protofibril" using AFM. First, protofibril elongation was slower than fibril elongation which supports initial models that suggests nucleation is slow and polymerization is fast. To further study the

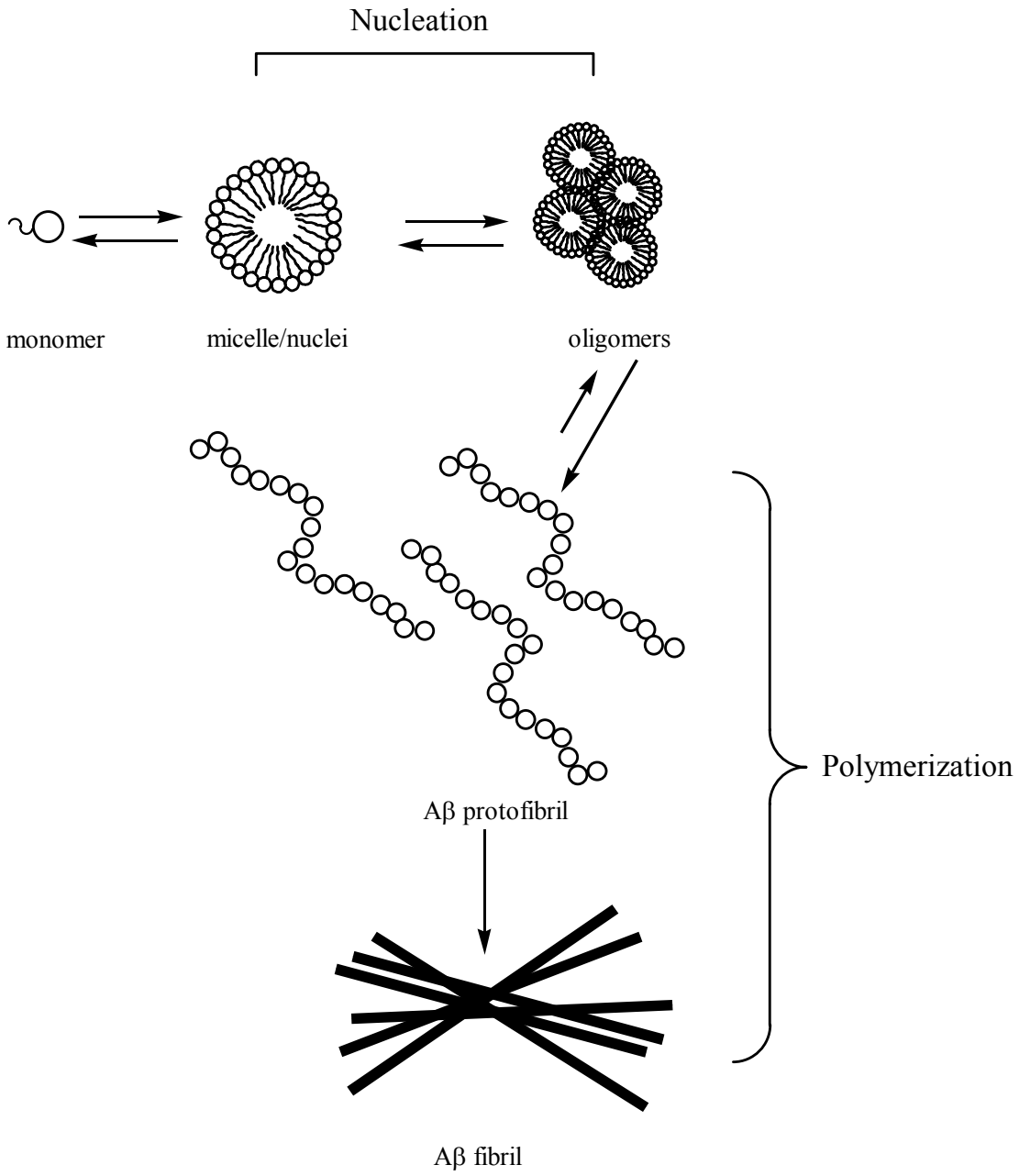

Figure 3.2. Two step nucleation-dependent polymerization mechanism of fibril formation derived from Bitan et al. *PNAS*, **96**, 6020-24 (1999).

protofibrils role in the nucleation-dependent pathway, the group tested the efficiency of protofibril-to-fibril conversion and discovered that protofibrils were on-pathway precursors to fibrils. Secondly, there was a distinct difference in the diameter of the relative protofibrils and fibrils depending on time and concentration. Thirdly, there appeared to be an overlap of

protofibrils (3-4 nm in height, 30-200 nm in length) where two or more long protofibrils become intertwined forming ordered branched or unbranched rigid type-1 fibrils (7-10 nm in height; range from 100 nm to greater than 1 μm in length). This new information was paramount because it now suggested that protofibrils play a vital role in the assembly of Aβ fibrils and development of therapeutics agents targeting the protofibril-to-fibril transition could be effective at altering AD progression.

Using size exclusion chromatography (SEC), light scattering, and EM, Walsh et al[30, 31] also studied the Aβ protofibril described by Harper. Walsh and colleagues discovered that the protofibril intermediate was in equilibrium with low-weight Aβ (LWAβ; monomer, and dimer material), was capable of binding Congo-red and thioflavin-T (ThT) just as mature fibrils, and a contain β-sheet secondary structure similar to mature fibrils. Although the protofibril intermediate was found to be in equilibrium with LWAβ, LWAβ had disorder random-coil conformations using CD spectroscopy and both had distinguishable morphologies. An important discovery was in the biological activity of the protofibril. Protofibrils, just as fibrils, perturbed neuronal metabolism and could be implemented as an initial indicator of neuronal dysfunction. LWAβ was ruled out as contributing to cell death because it exhibited no cytotoxicity in cortical neurons.[31] Ambiguity lies between whether protofibrils or fibrils contribute to AD cytotoxicity and neurodegenerative conditions. More recently, scientists have evidence to believe that protofibrils (soluble oligomers) correlate strongly with memory impairment[7] and are the primary species contributing to neuronal death.[32-36]

To characterize the initial stages of Aβ fibrillogenesis, photo-induced cross-linking of unmodified protein (PICUP), first introduced by Fancy et al.,[37-39] proved to be an ideal method for determining Aβ oligomer size distributions.[40] The basis of the PICUP experiment was

oligomers of Aβ would be "frozen" at a given state due to covalent cross-linking with a tris-bipyridyl Ru (II) complex. The oligomers could then be analyzed in order to determine the oligomerization state just before cross-linking. PICUP studies revealed that LWAβ consist of materials ranging from monomers to hexamers[40] (tetramer termination with $A\beta_{1-40}$ and hexamer termination with $A\beta_{1-42}$)[41, 42] in rapid equilibrium rather than the monomer/dimer state previously reported.[31] It was also determined that $A\beta_{1-40}$ aggregation proceeds via the previously described nucleation-dependent pathway, but $A\beta_{1-42}$ aggregation pathway contains a prenucleation mechanism. The monomers, dimers, and small oligomers (trimer) of $A\beta_{1-42}$ are in equilibrium with one another. Self-assembly of these initial intermediates forms a paranucleus (tetramer to hexamers) that nucleates larger unstructured oligomer formation (nonamers to dodecamers/octadecamers) followed by nucleation and polymerization of protofibrils to mature fibrils. Although $A\beta_{1-40}$ has been more extensively studied in vitro and in vivo, proteinacious deposits of $A\beta_{1-42}$ are more commonly found in AD diseased brains. Because $A\beta_{1-40}$ and $A\beta_{1-42}$ exhibit two distinct aggregation pathways, it is imperative to identify the differences in aggregation and regulate both formation and progression the intermediates associated with both pathways.[15, 41]

3.5 $A\beta_{1-40}$ FIBRIL SUPRASTRUCTURE

Fibrils are paracrystalline quaternary assemblies (Figure 3.3) that show Congo-red birefringence, show β-sheet secondary structures in CD and FTIR, and have a cross-β motif in X-ray diffraction.[27, 43, 44] Several models have been proposed; all suggest the Aβ fibril consists of parallel or antiparallel β-sheet assemblies. Parallel β-sheet alignments have been observed in longer segmented $A\beta_{1-40}$[44-46] and $A\beta_{10-35}$,[47, 48] whereas antiparallel β-sheet alignments have been found in smaller, more hydrophobic peptide segments, $A\beta_{16-22}$,[49] $A\beta_{11-25}$,[50] and $A\beta_{34-42}$[51] using

solid-state NMR techniques. Full-length $A\beta_{1-40}$ has also shown antiparallel sheet alignments, but the structural characterization was based on ambiguous IR data (amide-I band signals).[27, 45]

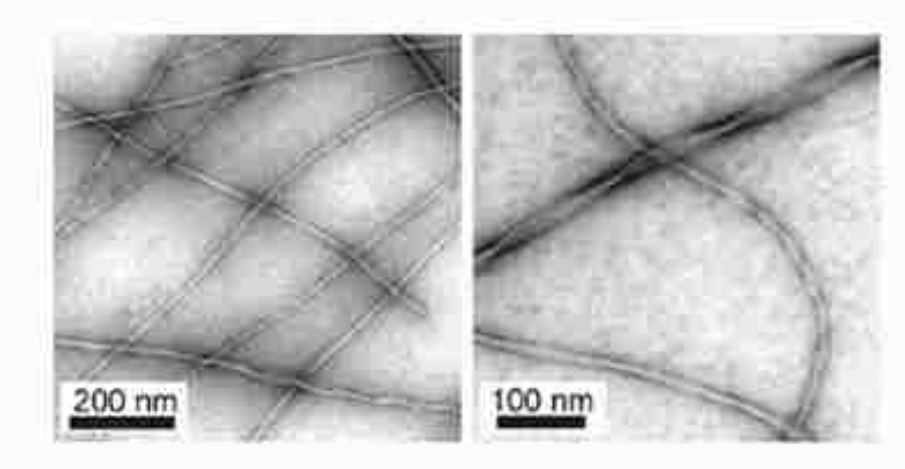

Figure 3.3. Electron microscopy image of Aβ fibrils. Aβ fibrils are typically 7-10 nm in height and range from 100 nm to greater than 1μm in length. Image was taken from Progress in Nuclear Magnetic Resonance Spectroscopy, **42**, 53-68 (2003).

Using 2-D $^{15}N/^{13}C$ (CO, Cα, and Cβ labeling) chemical shift correlation spectroscopy, it was determined that amino acid residues 12-24 and 30-40 from full-length $A\beta_{1-40}$ orient in β-strand conformations, where the average $\phi = -135° \pm 25°$ and $\psi = 140° \pm 20°$, while the first 10 residues are fairly unstructured.[43-47, 52, 53] Residues 25-29 (GSNKG) make up the 180° bend that aligns the two strands. NMR and molecular modeling studies (Figure 3.4) show that Aβ fibrils form two in-registry parallel β-sheets having a β-turn (not indicative of a β-hairpin[45, 52]) that is stabilized by side-chain interactions (salt-bridge formation) between residues 23 (aspartic acid) and 28 (lysine).[43, 46, 52, 54, 55] Protofilaments are stabilized through intermolecular hydrophobic contacts between residues 30-40 and 16-22 of each monomer unit (Figure 3.4 b).[43] This hydrophobic contact along with electrostatic interactions further stabilize the structure in the cross β-motif (Figure 3.4 a) as fibrils grow because all polar and charged residues are located on the exterior (non-contact) portion of the motif.[43, 46, 52]

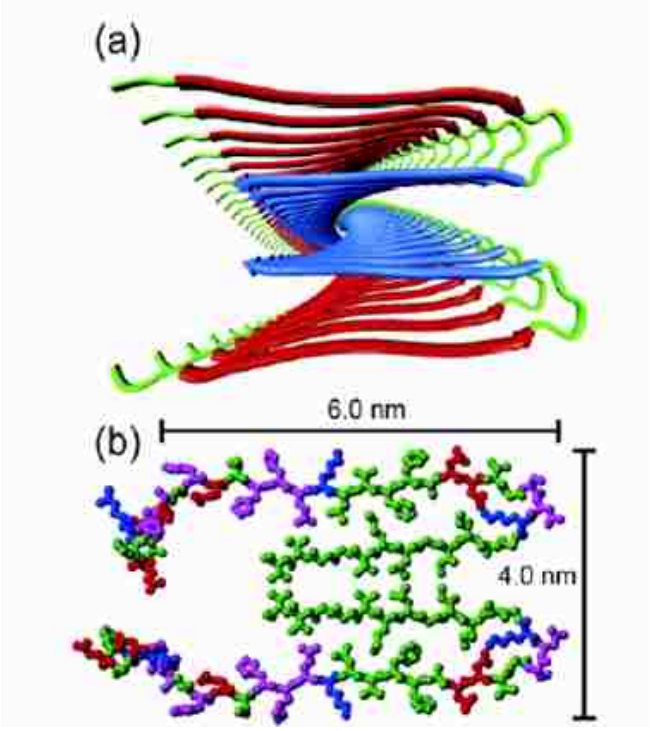

Figure 3.4. Supramolecular structure of Aβ fibril. (A) Cross β-sheet motif. (B) Monomer addition of Aβ stabilized by side-chain hydrophobic interactions. Image was taken from *Biochemistry*, **42**, 3151-3159 (2003).

3.6 CONCLUSION

AD is a progressive and degenerative disease that directly affects over 30 million people worldwide. There is no cure for this fatal and debilitating condition. Researchers are investigating ways to slow the progression of AD and develop possible medicinal agents targeting Aβ aggregation. Monomeric Aβ, LWAβ, and oligomers (tetramer-decamers) are believed to pose no direct threat to neurological functions. However, formation of the protofibril intermediate is believed to cause neurodegeneracy. Although there is currently no structural representation of nonfibrillar aggregate materials, a well defined structure of the Aβ fibril does exists. Understanding specific interactions that stabilize the Aβ fibril structure is important for the development of biologically active molecules that have the potential to prevent or mitigate protein misfolding.

3.7 REFERENCES

1. Selkoe, D. J. Alzheimers-disease - in the beginning. *Nature* **1991,** 354, 432-433.

2. Selkoe, D. J. Amyloid protein and Alzheimers-disease. *Sci.Am.* **1991,** 265, 40-47.

3. Ingram, V. Alzheimer's disease. *Am. Sci.* **2003**, 289, 1-9.

4. Alzheimer, A.; Stelzmann, R. A.; Schnitzlein, H. N.; Murtagh, F. R. An English translation of Alzheimer's 1907 paper, "Uber eine eigenartige Erkankung der Hirnrinde". *Clin. Anat.* **1995,** 8, 429-31.

5. Gorman, P. M.; Chakrabartty, A. Alzheimer β-amyloid peptides: Structures of amyloid fibrils and alternate aggregation products. *Biopolymers* **2001,** 60, 381-394.

6. In *National Center for Health Statistics of the Centers for Disease Control*, http://www.seniorjournal.com/NEWS/Health/6-04-20 AlzheimersClimbs.html: 2004.

7. Walsh, D. M.; Selkoe, D. J. Deciphering the molecular basis of memory failure in Alzheimer's disease. *Neuron* **2004,** 44, 181-193.

8. http://www.alz.org/alzheimers_disease_alzheimer_statistics.asp, Alzheimer's Facts and Figures. In 2007.

9. Iversen, L. L.; Mortishiresmith, R. J.; Pollack, S. J.; Shearman, M. S. The toxicity in vitro of β-amyloid protein. *Biochem. J* **1995,** 311, 1-16.

10. Hardy, J.; Selkoe, D. J. Medicine - The amyloid hypothesis of Alzheimer's disease: Progress and problems on the road to therapeutics. *Science* **2002,** 297, 353-356.

11. Glenner, G. G.; Wong, C. W. Alzheimers-disease: Initial report of the purification and characterization of a novel cerebrovascular amyloid protein. *Biochem. Biophys. Res. Commun.* **1984,** 120, 885-890.

12. Soto, C.; Branes, M. C.; Alvarez, J.; Inestrosa, N. C. Structural determinants of the Alzheimers amyloid β-peptide. *J. Neurochem.* **1994,** 63, 1191-1198.

13. Kang, J.; Lemaire, H. G.; Unterbeck, A.; Salbaum, J. M.; Masters, C. L.; Grzeschik, K. H.; Multhaup, G.; Beyreuther, K.; Mullerhill, B. The precursor of Alzheimers disease amyloid-A4 protein resembles a cell-surface receptor. *Nature* **1987,** 325, 733-736.

14. Selkoe, D. J. Amyloid β-protein and the genetics of Alzheimer's disease. *J. Biol. Chem.* **1996,** 271, 18295-18298.

15. Kirkitadze, M. D.; Kowalska, A. Molecular mechanisms initiating amyloid β-fibril formation in Alzheimer's disease. *Acta Biochim. Pol.* **2005,** 52, 417-423.

16. Bishop, G. M.; Robinson, S. R. Physiological roles of amyloid-β and implications for its removal in Alzheimer's disease. *Drugs and Aging* **2004,** 21, 621-630.

17. Lazo, N. D.; Grant, M. A.; Condron, M. C.; Rigby, A. C.; Teplow, D. B. On the nucleation of amyloid β-protein monomer folding. *Protein Sci.* **2005,** 14, 1581-1596.

18. Jarrett, J. T.; Berger, E. P.; Lansbury, P. T., The *C*-terminus of the β-protein is critical in amyloidogenesis. In *Alzheimers Disease: Amyloid Precusor Proteins, Signal Transduction, and Neuronal Transplantation*, New York Acad Sciences: New York, **1993**; Vol. 695, pp 144-148.

19. Jarrett, J. T.; Berger, E. P.; Lansbury, P. T. The carboxy terminus of the β-amyloid protein is critical for the seeding of amyloid formation. Implications for the pathogenesis of Alzheimers disease. *Biochemistry* **1993,** 32, 4693-4697.

20. Jarrett, J. T.; Lansbury, P. T. Amyloid fibril formation requires a chemically discriminating nucleation event. Studies of an amyloidogenic sequence from the bacterial protein Osmb. *Biochemistry* **1992,** 31, 12345-12352.

21. Lomakin, A.; Chung, D. S.; Benedek, G. B.; Kirschner, D. A.; Teplow, D. B. On the nucleation and growth of amyloid β-protein fibrils: Detection of nuclei and quantitation of rate constants. *Proc. Natl. Acad. Sci. U. S. A.* **1996,** 93, 1125-1129.

22. Lomakin, A.; Teplow, D. B.; Kirschner, D. A.; Benedek, G. B. Kinetic theory of fibrillogenesis of amyloid β-protein. *Proc. Natl. Acad. Sci. U. S. A.* **1997,** 94, 7942-7947.

23. Soreghan, B.; Kosmoski, J.; Glabe, C. Surfactant properties of Alzheimer's Aβ peptides and the mechanism of amyloid aggregation. *J. Biol. Chem.* **1994,** 269, 28551-28554.

24. Garzon-Rodriguez, W.; Sepulveda-Becerra, M.; Milton, S.; Glabe, C. G. Soluble amyloid Aβ-(1-40) exists as a stable dimer at low concentrations. *J. Biol. Chem.* **1997,** 272, 21037-21044.

25. Harper, J. D.; Lieber, C. M.; Lansbury, P. T. Atomic force microscopic imaging of seeded fibril formation and fibril branching by the Alzheimer's disease amyloid-β protein. *Chem. Biol.* **1997,** 4, 951-959.

26. Harper, J. D.; Wong, S. S.; Lieber, C. M.; Lansbury, P. T. Observation of metastable Aβ amyloid protofibrils by atomic force microscopy. *Chem. Biol.* **1997,** 4, 119-125.

27. Lansbury, P. T. In pursuit of the molecular-structure of amyloid plaque. New technology provides unexpected and critical information. *Biochemistry* **1992,** 31, 6865-6870.

28. Lansbury, P. T. The molecular mechanism of amyloid formation in Alzheimer's disease. *Eur. J. Med. Chem.* **1995,** 30, S621-S633.

29. Harper, J. D.; Wong, S. S.; Lieber, C. M.; Lansbury, P. T. Assembly of Aβ amyloid protofibrils: An in vitro model for a possible early event in Alzheimer's disease. *Biochemistry* **1999,** 38, 8972-8980.

30. Walsh, D. M.; Lomakin, A.; Benedek, G. B.; Condron, M. M.; Teplow, D. B. Amyloid β-protein fibrillogenesis. Detection of a protofibrillar intermediate. *J. Biol. Chem.* **1997,** 272, 22364-22372.

31. Walsh, D. M.; Hartley, D. M.; Kusumoto, Y.; Fezoui, Y.; Condron, M. M.; Lomakin, A.; Benedek, G. B.; Selkoe, D. J.; Teplow, D. B. Amyloid β-protein fibrillogenesis: Structure and biological activity of protofibrillar intermediates. *J. Biol. Chem.* **1999,** 274, 25945-25952.

32. Bucciantini, M.; Calloni, G.; Chiti, F.; Formigli, L.; Nosi, D.; Dobson, C. M.; Stefani, M. Prefibrillar amyloid protein aggregates share common features of cytotoxicity. *J. Biol. Chem.* **2004,** 279, 31374-31382.

33. Bucciantini, M.; Giannoni, E.; Chiti, F.; Baroni, F.; Formigli, L.; Zurdo, J. S.; Taddei, N.; Ramponi, G.; Dobson, C. M.; Stefani, M. Inherent toxicity of aggregates implies a common mechanism for protein misfolding diseases. *Nature* **2002,** 416, 507-511.

34. Kayed, R.; Head, E.; Thompson, J. L.; McIntire, T. M.; Milton, S. C.; Cotman, C. W.; Glabe, C. G. Common structure of soluble amyloid oligomers implies common mechanism of pathogenesis. *Science* **2003,** 300, 486-489.

35. Kokubo, H.; Kayed, R.; Glabe, C. G.; Yamaguchi, H. Soluble Aβ oligomers ultrastructurally localize to cell processes and might be related to synaptic dysfunction in Alzheimer's disease brain. *Brain Res.* **2005,** 1031, 222-228.

36. Fifre, A.; Sponne, I.; Koziel, V.; Kriem, B.; Potin, F. T. Y.; Bihain, B. E.; Olivier, J. L.; Oster, T.; Pillot, T. Microtubule-associated protein MAP1A, MAP1B, and MAP2 proteolysis during soluble amyloid β-peptide-induced neuronal apoptosis: Synergistic involvement of calpain and caspase-3. *J. Biol. Chem.* **2006,** 281, 229-240.

37. Fancy, D. A. Elucidation of protein-protein interactions using chemical cross-linking or label transfer techniques. *Curr. Opin. Chem. Biol.* **2000,** 4, 28-33.

38. Fancy, D. A.; Kodadek, T. Chemistry for the analysis of protein-protein interactions: Rapid and efficient cross-linking triggered by long wavelength light. *Proc. Natl. Acad. Sci. U. S. A.* **1999,** 96, 6020-6024.

39. Fancy, D. A.; Kodadek, T. Chemistry for the analysis of protein-protein interactions: Rapid and efficient cross-linking triggered by long wavelength light. *Proc. Natl. Acad. Sci. U. S. A.* **2000,** 97, 1317-1317.

40. Bitan, G.; Lomakin, A.; Teplow, D. B. Amyloid β-protein oligomerization: Prenucleation interactions revealed by photo-induced cross-linking of unmodified proteins. *J. Biol. Chem.* **2001,** 276, 35176-35184.

41. Bitan, G.; Kirkitadze, M. D.; Lomakin, A.; Vollers, S. S.; Benedek, G. B.; Teplow, D. B. Amyloid β-protein (Aβ) assembly: Aβ 40 and Aβ 42 oligomerize through distinct pathways. *Proc. Natl. Acad. Sci. U. S. A.* **2003,** 100, 330-335.

42. Bitan, G.; Vollers, S. S.; Teplow, D. B. Elucidation of primary structure elements controlling early amyloid β-protein oligomerization. *J. Biol. Chem.* **2003,** 278, 34882-34889.

43. Tycko, R. Insights into the amyloid folding problem from solid-state NMR. *Biochemistry* **2003,** 42, 3151-3159.

44. Tycko, R. Molecular structure of amyloid fibrils: insights from solid-state NMR. *Q Rev. Biophy.* **2006,** 39, 1-55.

45. Balbach, J. J.; Petkova, A. T.; Oyler, N. A.; Antzutkin, O. N.; Gordon, D. J.; Meredith, S. C.; Tycko, R. Supramolecular structure in full-length Alzheimer's β-amyloid fibrils: Evidence for a parallel β-sheet organization from solid-state nuclear magnetic resonance. *Biophys. J.* **2002,** 83, 1205-1216.

46. Tycko, R. Applications of solid state NMR to the structural characterization of amyloid fibrils: Methods and results. *Prog. Nucl. Magn. Reson. Spectrosc.* **2003,** 42, 53-68.

47. Benzinger, T. L. S.; Gregory, D. M.; Burkoth, T. S.; Miller-Auer, H.; Lynn, D. G.; Botto, R. E.; Meredith, S. C. Propagating structure of Alzheimer's β-amyloid(10-35) is parallel β-sheet with residues in exact register. *Proc. Natl. Acad. Sci. U. S. A.* **1998,** 95, 13407-13412.

48. Benzinger, T. L. S.; Gregory, D. M.; Burkoth, T. S.; Miller-Auer, H.; Lynn, D. G.; Botto, R. E.; Meredith, S. C. Two-dimensional structure of β-amyloid(10-35) fibrils. *Biochemistry* **2000,** 39, 3491-3499.

49. Balbach, J. J.; Ishii, Y.; Antzutkin, O. N.; Leapman, R. D.; Rizzo, N. W.; Dyda, F.; Reed, J.; Tycko, R. Amyloid fibril formation by Aβ(16-22), a seven-residue fragment of the Alzheimer's β-amyloid peptide, and structural characterization by solid state NMR. *Biochemistry* **2000,** 39, 13748-13759.

50. Petkova, A. T.; Buntkowsky, G.; Dyda, F.; Leapman, R. D.; Yau, W. M.; Tycko, R. Solid state NMR reveals a pH-dependent antiparallel β-sheet registry in fibrils formed by a β-amyloid peptide. *J. Mol. Biol.* **2004,** 335, 247-260.

51. Lansbury, P. T.; Costa, P. R.; Griffiths, J. M.; Simon, E. J.; Auger, M.; Halverson, K. J.; Kocisko, D. A.; Hendsch, Z. S.; Ashburn, T. T.; Spencer, R. G. S.; Tidor, B.; Griffin, R. G. Structural model for the β-amyloid fibril based on interstrand alignment of an antiparallel-sheet comprising a *C*-terminal peptide. *Nat. Struct. Biol.* **1995,** 2, 990-998.

52. Petkova, A. T.; Ishii, Y.; Balbach, J. J.; Antzutkin, O. N.; Leapman, R. D.; Delaglio, F.; Tycko, R. A structural model for Alzheimer's β-amyloid fibrils based on experimental constraints from solid-state NMR. *Proc. Natl. Acad. Sci. U. S. A.* **2002,** 99, 16742-16747.

53. Tycko, R., Characterization of amyloid structures at the molecular level by solid state nuclear magnetic resonance spectroscopy. In *Amyloid, Prions, and Other Protein Aggregates, Pt C*, **2006**; Vol. 413, pp 103-122.

54. Thompson, L. K. Unraveling the secrets of Alzheimer's β-amyloid fibrils. *Proc. Natl. Acad. Sci. U. S. A.* **2003,** 100, 383-385.

55. Luhrs, T.; Ritter, C.; Adrian, M.; Riek-Loher, D.; Bohrmann, B.; Doeli, H.; Schubert, D.; Riek, R. 3-D structure of Alzheimer's amyloid-β(1-42) fibrils. *Proc. Natl. Acad. Sci. U. S. A.* **2005,** 102, 17342-17347.

CHAPTER 4.

STOICHIOMETRIC INHIBITION OF AMYLOID β-PROTEIN AGGREGATION WITH PEPTIDES CONTAINING ALTERNATING $C^{\alpha,\alpha}$-DISUBSTITUTED AMINO ACIDS[†‡]

4.1 AMY PEPTIDE DESIGN

The Aβ fibril cross β-sheet structure is stabilized by intrastrand and interstrand hydrogen bonding between two parallel β-sheets and by side-chain interactions (hydrophobic/electrostatic) (Figure 3.4). This stability is a driving force for dimerization that leads to Aβ self-association and fibril formation. Designing peptides that could prevent or interfere with these favorable interactions from one putative face would not prevent dimerization, but could prevent additional extended peptides from adding to sheet-like structures.

A number of research groups have investigated peptides related to the hydrophobic core of Aβ (residue 16-22, Lys-Leu-Val-Phe-Phe-Ala-Glu; KLVFFAE) as potential blockers of Aβ aggregation and fibrillogenesis (Figure 4.1). Their approach relied on self-recognition of the hydrophobic core with inhibitor compounds and the adaptation of specific conformational changes of Aβ with their proposed inhibitors to limit toxicity. Soto and coworkers used the recognition sequence, but incorporated L-Proline, due to its "β-sheet breaking" capabilities, within in the hydrophobic core of Aβ and found that this inhibitor was able to convert Aβ fibrils to amorphous aggregates and inhibit toxicity in vitro.[1-3] Murphy et al.[4-6] used a strategy where they designed peptides that bind to the hydrophobic core of Aβ and facilitate fibril formation by increasing the rate of Aβ aggregation. In addition, their peptides decreased Aβ cytotoxicity using PC-12 cell lines. Researchers at the University of Chicago employed the use of *N*-methylated amino acids to prevent fibril formation. Their study was based on the replacement of the peptide

[†] Reprinted by permission of The American Chemical Society
[‡] Reprinted by permission of Springer

backbone amide proton, which stablizes β-sheets via intrastrand/interstrand hydrogen bonding, with methyl groups. *N*-methyl amino acids form tertiary amides favoring trans-conformations; thus, peptides incorporating methylated amino acids are torsionally constrained to adopt β-strand conformations.[7] Meredith et al. described inhibitors, where *N*-methylated amino acids were used in alternating positions of the hydrophobic core of Aβ that were adequate at blocking fibril formation, disassembled pre-formed fibrils, and were resistant to proteolytic digestion.[8, 9] They also found that the alternating positioning of *N*-methylated amino acids was crucial for fibril inhibition because their peptides were designed so that when in β-strand conformations, one hydrogen bonding face would be blocked. Chalifour[10] and Tjernberg[11] studied the stereoselective effects of Aβ hydrophobic core with the two most neurotoxic isoforms. The rationale for their study was D-amino acids would create peptide bonds that are resistant to proteolyisis, thus making peptide models favorable therapeutic targets. Their stereospecific results concluded that heterochiral stereospecificity is essential for inhibition. More recently, aminoisobutyric acid (Aib) have been incorporated in peptides derived from hIAPP, the protein responsible for fibril formation in type-II diabetes.[12] Aib is a helix promoting amino acid residue and compared to native protein controls, Aib containing peptides were capable of interfering with fibril formation and preventing the formation of β-sheet assemblies.

Herein, the use of peptide analogs containing α,α-disubstituted amino acids substituted into the hydrophobic core of Aβ and their interaction with Aβ in aqueous buffer will be presented. An alternating ααAA/L-amino acid design to give peptides that interact with Aβ by hydrogen bonding, but has one hydrogen bonding edge blocked due to side-chain interactions and steric hinderance, thus capping that facial side minimizing self-assembly has been utilized.

ααAAs are widely used in peptide design because of their structure-promoting effects.[13-19] Highly hydrophobic ααAAs with larger side-chain groups have been shown to stabilize extended

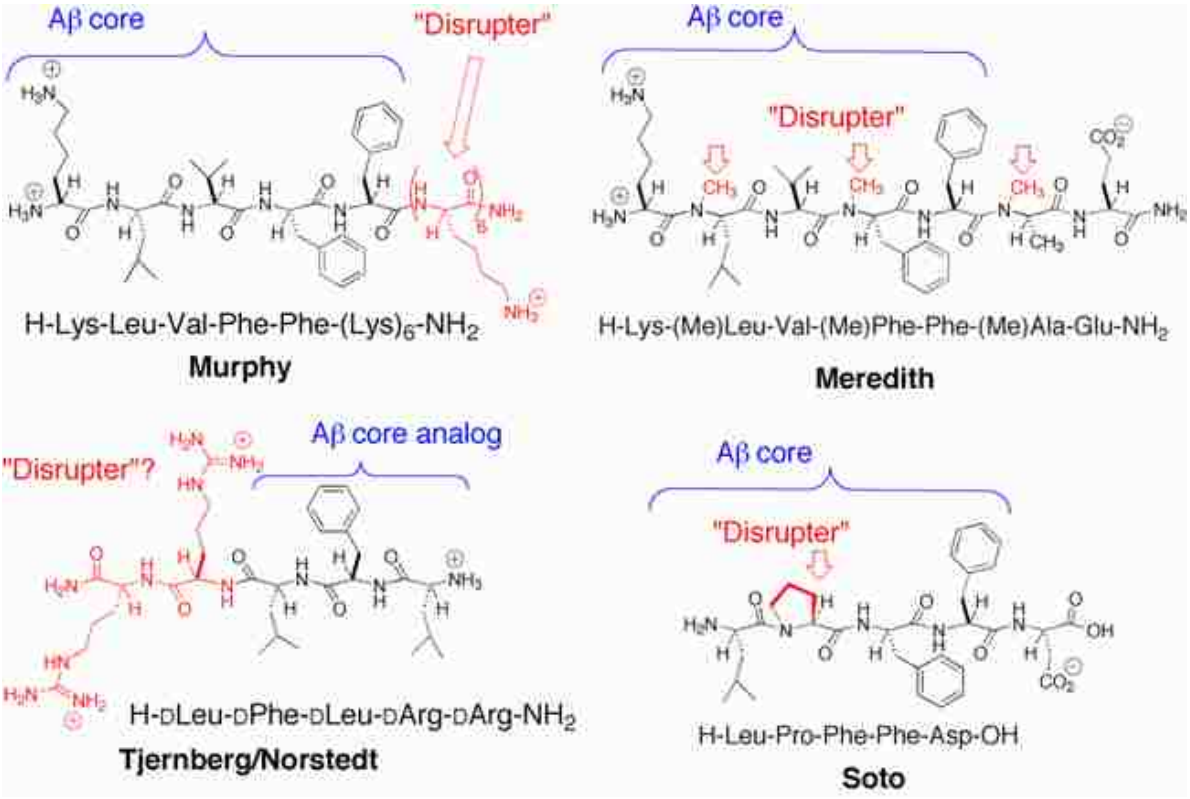

Figure 4.1. Peptidomimetic inhibitors of Aβ fibrillogenesis. Inhibitor design strategy takes advantage of Aβ hydrophobic core self-recognition for binding while introducing β-sheet disrupting elements within the peptide sequence.

conformations in homo-oligomers of diethylglycine,[14, 17] thus it was hypothesized that peptides designed in this manner (Scheme 4.1) might have strong affinity for β-sheet assemblies of Aβ and also prevent further aggregation by blocking one face of the assembly. The characterization of peptide mitigatiors using several physical techniques such as thioflavin-T (ThT) fluorescence spectroscopy, circular dichorism spectroscopy (CD), scanning force microscopy (SFM), and transmission electron microscopy (TEM) have been used to characterize the effects of peptide mitigators on Aβ aggregation and will also be discussed.

Scheme 4.1 Design of peptides with ααAAs as blockers of Aβ assembly.

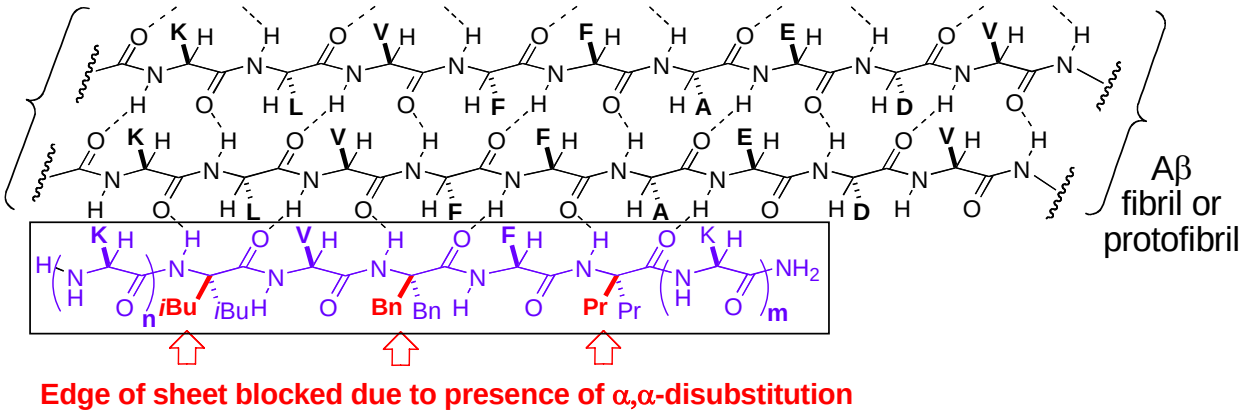

4.2 EXPERIMENTAL

4.2.1 PEPTIDE SYNTHESIS

The AMY peptides (Table 4.1) were synthesized using the following coupling and cleavage conditions. Standard Fmoc coupling was carried out using the following reagents unless otherwise noted: PyAOP, 4 equiv; DIEA, 8 equiv; Fmoc-amino acids, 4 equiv (0.3 M) in DMF with a coupling time of 24 h while shaking. Fmoc removal was carried out using DMF:piperidine:DBU (93:5:2) for 30 min while shaking. The *N*-terminus and *C*-terminus oligio-Lys chain was coupled to the resin bound peptide chain or the PAL-PEG-PS resin on a Pioneer Peptide Synthesizer using PyAOP in DMF. The remaining amino acid residues were manually incorporated into the sequence. Dpg, Phe, and Dbzg were incorporated into the peptide sequence using PyAOP/DIEA in DCE:DMF (1:1) at 50 ºC. The equiv of each reagent for coupling was as described above. Additionally, Dpg was coupled to resin bound support using bis(2-oxo-3-oxazolidinyl)phosphinic chloride (BOP-Cl) mixed anhydride coupling. The preformed mixed anhydride was prepared by treatment of Fmoc-Dpg-OH (1 equiv) with BOP-Cl (1 equiv) and DIEA (1 equiv) in CH_2Cl_2 for 2 h at 0 °C. The mixed anhydride was concentrated and coupled to PAL-PEG-PS resin in DCE-DMF (4:1) for 8 h. Capping of the resin to eliminate any

unreactive active sites was performed using acetic anhydride (0.2 M in 0.28 M DIEA). The Val residue was coupled to the *N*-terminus of Dbzg via amino acid symmetrical anhydride. The symmetrical anhydride was prepared by treatment of 2 equiv of Fmoc-Val-OH with 1 equiv of DCC in CH_2Cl_2 stirring at room temperature for 2 h followed by removal of the precipitated DCU by filtration. The symmetrical anhydride was concentrated, redissolved in the higher boiling DCE:DMF (9:1), and added for coupling of the amino acid residue to the resin-bound peptide chain. The reaction was carried out at 50 ºC for 24 h. Dibg was coupled to Val using HATU (4 equiv), HOAt (4 equiv), DIEA (8 equiv), and Fmoc-Dibg-OH (4 equiv, 0.3 M) in DCE:DMF (1:1) at 50 ºC. The first *N*-terminal Lys residue was coupled to Dibg via symmetrical anhydride coupling (as previously described) at 50 ºC. Additional Lys residues were automatedly attached to the peptide chain using standard Fmoc solid-phase peptide chemistry. Following final deprotection procedure, peptide cleavage from the solid support and side-chain deprotection was performed using a standard cleavage cocktail (Reagent B) of TFA:phenol:H_2O:TIPS (8.2:0.5:0.5:0.2) [20, 21] for 2 h while shaking followed by extraction in 30% acetic acid (HOAc) and chloroform (AMY-2). The filtrate concentrate was dissolved in cold 30% glacial acetic acid (HOAc) solution, diluted with two fold volume of chloroform, and the aqueous layer was extracted (3 times). The aqueous layer was concentrated and redissolve in 30% HOAc, frozen, and lyophilized to yield crude peptide. AMY-1, AMY-3, and AMY-4 were co-precipitated in cold Et_2O for 24 h at -27 °C. The precipitate was then washed with cold Et_2O and centrifuged at 4,000 rpm for 10 min (3 times). The supernatant was decanted and the remaining pellet was allowed to dry for 12 h yielding crude AMY-X product.

The HC-(hydrophobic core) peptides (Table 4.1) were synthesized using four equivalents of amino acid and activation with TBTU, HOBt, and DIEA at a final concentration of 0.2 M unless noted otherwise. The *N*MHC and HC-B_3 peptides were synthesized using PyAOP/DIEA

activation. A stepwise coupling of each amino acid was obtained using the standard solid-phase Fmoc coupling chemistry. A double coupling of each Aib residue and the *N*-terminal Aib residue (HC-B_3) and each *N*-methylated amino acid residue and the *N*-terminal *N*-methylated amino acid residue (*N*MHC) was performed at 50 ºC to maximize coupling yields. Peptide cleavages were performed using Reagent B. Following cleavage of the peptide from the solid support, the filtrate samples were combined and concentrated. Pre-purification of peptides were performed from an extraction using 30% HOAc and Et_2O (HC-K_6) or by co-precipitation in cold Et_2O at -27 °C for 24 h (HC-B_3 and *N*MHC).

4.2.2 PEPTIDE PURIFICATION AND CHARACTERIZATION

All peptide purification and characterization was performed using protocols previously described in Chapter 2 section 2.2.2. The peptides were purified using reversed-phase HPLC with linear gradients of 0.1% aqueous TFA in H_2O (v/v) (Buffer A) and 0.1% TFA in CH_3CN (v/v) (Buffer B). The molecular masses of the peptides were verified using MALDI-MS and the net peptide content of all peptides was determined using AAA. See Table 4.1 for HPLC, MALDI-MS, and AAA results.

4.2.3 $A\beta_{1\text{-}40}$ PEPTIDE AGGREGATION (MONOMERIC STARTING SOLUTIONS)

Lyophilized Aβ was dissolved in neat TFA at 1 mg/mL and sonicated for 10-15 min. TFA was then evaporated using using centrifugal evaporator at 30 mTorr (dark yellow oil). The resulting oil was dissolved in HFIP at 1 mg/mL and incubated at 37 °C for 1 h. HFIP was removed using centrifugal evaporator at 30 mTorr (white powder). The white powder was dissolved in HFIP at 1 mg/mL and incubated at 37 °C for 1 h. HFIP was then removed and the resulting white powder was lyophilized overnight. The white powder was then re-dissolved in 2 mM KOH and 2x PBS (100 mM, 300 mM NaCl, pH 7.4) at 1:1 mole ratio and centrifuged for 10 min at 13,000 g. Amino acid analysis was performed on the supernatant to verify peptide

concentration. Samples were stored in a freezer at -72 °C until ready for use. 1:1 molar ratio mixtures of Aβ:inhibitor (500 μM: 500 μM) were diluted 1:10 and allowed to co-incubate at 37 °C at various time intervals.

4.2.4 CIRCULAR DICHROISM MEASUREMENTS

All measurements were carried out using an Aviv Circular Dichroism Spectrometer Model 62DS with Igor plotting software. Samples were prepared by diluting 10x stock solution of $A\beta_{1-40}$ (500 μM) and 10x PBS (500 mM, 1.5 M NaCl) with ultra-pure deionized water to acquire a working solution of 50 μM Aβ in PBS (50 mM, 150 mM NaCl; pH 7.4). Prior to each dilution, individual 10x samples and water was filtered using a 0.02 micron Anatop filter (Whatman). For co-incubation experiments, Aβ was dissolved (as above) to yield 100 μM -500 μM solutions; inhibitor peptides were dissolved in water to yield solutions with concentrations ranging from 100 μM-500 μM. Working stock solutions were then diluted 10-fold and incubated at 37 °C over various time intervals. CD spectra were the average of three scans made at 1 nm intervals acquired from 260 nm to 190 nm (UV absorbance range) recorded at 25 °C. The spectrum of PBS buffer (10x) diluted in water was used as the background subtraction in all experiments.

4.2.5 SCANNING FORCE MICROSCOPY

All measurements were performed using the Nanoscope III Multimode SFM (tapping mode). Samples were adsorbed on atomically flat hydrophilic mica. Cleavage and exposure of interior mica planes (which are atomically flat over large areas and ideal for SFM imaging) was achieved by placing a razor blade in the middle of the sheet edge layers of a 1 cm^2 mica and separating the layers by gripping one side with a pair of tweezers. A sample aliquot of 5 μL was then placed on the freshly exposed mica and allowed to remain for 25 min, unless otherwise noted. After a 25 min adsorption step in most cases, the sample/substrate was rinsed with 400

μL of deionized water followed by tilting the substrate and placing its edge on a Kimwipe to wick away the water. The mica samples were then placed sample-exposed face up on a 15 mm metal specimen disc. When ready for imaging, each specimen disc was placed on top of the piezoelectric scanner of the SPM instrument and imaged using SFM tapping mode. Samples not immediately imaged were stored in semiconductor wafer containers under an ordinary lab ambient environment.

4.2.6 TRANSMISSION ELECTRON MICROSCOPY

Samples for TEM analysis were prepared by inverting the carbon-supported Cu coated grid on a 5 μL droplet of sample for approximately 30 sec. Excess solvent was wicked away and the grid was rinsed by inverting the deposited Cu grid on a 5 μL droplet of water for approximately 5-10 sec. The grid was stained with 2% uranyl acetate in 0.05 M HCl by inverting the Cu grid on a 5 μL droplet of filtered 2% uranyl acetate for 5-10 sec. The prepared grids were then placed in JEOL 100 CX transmission electron microscope at an electron acceleration voltage of 80 kV for imaging.

4.2.7 FLUORESCENCE MEASUREMENTS

Fluorescence spectroscopy was measured using a Fluostar Spectometer with Fluostar operating software with an excitation filter at 450 nm and an emission filter at 480 nm. Thioflavin-T (ThT) was dissolved in 10 molar excess of PBS (500 mM 1.5M NaCl, pH 7.4) to acquire a 10 molar excess stock solution (100 μM) of dye. 90 μL of peptide sample stock (peptide sample in buffer diluted with water) was diluted with 10 μL of dye stock solution to prepare fluorescence spectroscopy working solutions [25 μM Aβ or 25 μM Aβ/peptide mitigator (1:1 mol ratio) in PBS (50 mM 150 mM NaCl, pH 7.4) with 10 μM of ThT]. Aβ and Aβ/peptide mitigator solutions were diluted as previously described in section 4.2.4 Circular Dichroism Measurements and were allowed to incubate in a 96 well-plate for various time intervals.

4.2.8 NEURONAL CELL CULTURE

Primary rat cortical neuronal cells isolated from micro-surgically dissected regions of Sprague/Dawley or Fischer 344 rat were purchased form Genlantis (N200200). Tissue culture treated CoStar 96 well-plates were coated with poly-D-lysine (50 μg/mL) and neuronal cells were plated at a density of 2 x 10^4 cells/100 μL (per well) in Neurobasal medium (Invitrogen 211103) containing NGF-B27 supplement (Genlantis N200200) with 0.5 mM glutamine.[22] Cultures were allowed to differeniate for 4-5 days in a humidified incubator at 37 °C, 5% CO_2 before assaying with Aβ and Aβ/peptide mitigator solutions at various concentrations and time intervals.

4.2.9 CELL CULTURE (PC-12 CELLS)

PC-12 cells were grown in collagen-coated tissue culture plates in medium containing 81% RPMI Media 1640, 10% horse serum, 5% fetal bovine serum, 1% amino acid, 1% non-essential amino acids, 1% vitamins, 1% glutamine, with Primocin (200 μL/100 mL of media). Cultures were allowed to proliferate in a humidified incubator 37 °C, 5% CO_2 for 3-5 days. Cells were harvested from plates and re-suspended in collagen-coated 96 well-plates at a density of 5 x 10^4 cells/100 μL (per well). Plates were incubated at 37 °C for 24 h to allow for cell adhesion.

4.2.10 CELL VIABILITY ASSAYS

Mitochondrial function was evaluated via cell mediated reduction of 3-(4,5-dimethylthiazol-2-yl)-2,5 diphenyltetrazolium bromide (MTT).[23-26] Aβ fibril solutions were prepared by incubating Aβ for 1 week at 37 °C in PBS diluted in RPMI-supplemented cell culture media yielding final peptide concentrations of 5 μM-50 μM. Cells were co-incubated in 100 μL of freshly prepared RPMI-supplemented cell culture media or Neurobasal media

containing B27 NGF (0.5 mM glutamine) with fibril solutions at various concentrations (5 μM-50 μM) and time intervals (2 h-24 h) in a humidified incubator 37 °C, 5% CO_2. Following concentration- and/or time-dependent incubations, 15 μL of MTT stock solution was added to each well and allowed to incubate for 4 h. After 4 h, 100 μl of solubilizing solution, 50% DMF and 20% SDS at pH 4.7, was added to each well and allowed to incubate for 1 h followed by UV absorbance reading at 590 nm.

Cellular viability of neuronal cortical cells was measured fluorescently using a dye indicator resazurin. Mitochondrial function could also be evaluated via cell mediated reduction of the indicator dye. Viable cells have the ability to reduce resazurin to resofurin, which is highly fluorescent at 560 nm/ 590 nm (ex/em; CellTiter-Blue). Aβ fibril solutions were prepared as previously described above. Cells were incubated in 100 μL of freshly prepared Neurobasal media containing B27-NGF (0.5 mM glutamine) with fibril solutions at various concentrations (5 μM-50 μM) and time intervals (2 h-24 h) in a humidified incubator 37 °C, 5% CO_2. Following concentration- and/or time-dependent incubations, 20 μL of resazurin dye was added to each well and allowed to incubate for 4 h. After 4 h, fluorescence intensity was recorded, excitation at 570 nm and emission at 615 nm.

4.3 RESULTS AND DISCUSSION

4.3.1 SYNTHESIS OF AGGREGATION MITIGATORS

The most common approaches for the synthesis of the ααAAs have been the Strecker or Bucherer-Bergs synthetic routes. Dpg was synthesized via the Bucherer-Bergs synthetic route (Chapter 2 section 2.2.1) from a diketone precursor forming a hydantion that underwent hydrolysis to form an unprotected amino acid product that was *N*-terminally Fmoc-protected. Although this method was convenient for linear side-chains, synthesis of the more bulky and

sterically hindered side-chains via this route was problematic. Hydrolysis of the larger side-chain hydantoins to free amino acid is relatively impossible. For this reason, the use of more reactive glycine anion equivalents was explored.[27, 28] Ethyl nitroacetate was found to be a very useful synthon for the preparation of bulky amino acids. Diisobutylglycine (Dibg) was synthesized via a Pd-catalyzed diallylation of ethyl nitroacetate,[28] while dibenzylglycine (Dbg) was synthesized from the treatment of ethyl nitroacetate with DIEA followed by addition of an activated alkyl halide.[27] Following formation of the nitrosubstituted complex in both syntheses, both were reduced via hydrogenation over Raney Ni followed by hydrolysis and *N*-terminal Fmoc protection.

Difficulties associated with the incorporation of sterically hindered $C^{\alpha,\alpha}$-disubstituted amino acids into peptide sequences by standard amino acid coupling methods resulted in the exploration of alternative routes for synthesizing peptides containing these bulky amino acids. The synthesis of the "AMY" peptides used methods previously reported.[27-29] Incorporation of Dpg into the AMY-1 peptide sequence was facile using PyAOP at 50 °C. Unfortunately, incorporation of the more sterically hindered Dibg or Dbg to the *N*-terminus of unhindered amino acids proved to be more difficult. Fu investigated a series of coupling and activation strategies to access amide bond formation efficiencies and determined that more nonpolar solvent in the presence of uronium or phosphonium salt-activation improved coupling of ααAAs, Dibg and Dbg respectively, to peptide chains. One additional problem that existed in the addition of ααAA into peptide chains was *N*-acylation of the ααAA. Carbodiimide-mediated symmetrical anhydrides in nonpolar solvents proved to be more efficient at acylating the *N*-terminal residues.

AMY-2, AMY-3, and AMY-4 (Table 4.1) were synthesized using protocols similar to that of AMY-1. One major difference between AMY-1 and AMY-2 was a method of anchoring

Table 4.1. Peptide Mitigators of Amyloid-β protein. Primary sequence, purification, and characterization.

Peptide	Sequence	Calculated $[M+H]^+$	Observed MALDI-MS	t_R (min)	Peptide content
AMY-1	K**U**V**Z**F**J**K_6	1708.37	1709.54	22.95	51%
AMY-2	K_7**U**V**Z**F**J**	1708.42	1709.72	12.51	45%
AMY-3	K**U**V**Z**F**J**	939.64	939.41	20.32	n/a
AMY-4	K**U**V**Z**F**J**K	1067.74	1069.97	n/a	n/a
*HC-K_6	KLVFFK_6	1420.24	1420.64	13.65	67%
HC-B_3	K**B**V**B**F**B**K_6	1415.90	1414.68	15.53	65%
**N*MHC	K(MeL)V(MeF)F(MeA)E	894.36	896.85	22.88	66%

* Denotes peptides previously reported in literature used as control experiments. HC-K_6 is the peptide initially introduced by Murphy (Figure 4.1) and the *N*MHC peptide was initially described by Meredith (Figure 4.1). Refer to Appendix B for HPLC chromatograms and MALDI-MS spectra.

ααAA Dpg to the solid support was necessary. Fu et al.[28] reported that proper and efficient anchoring of the ααAA to the solid support was a critical step in peptide synthesis and was necessary for the prevention of deletion sequences which could complicate purification and overall peptide yields. Preformed mixed anhydrides from bis(2-oxo-3-oxazolidinyl)phosphinic chloride (BOP-Cl) and Fmoc-ααAA-OH reacted together was effective at anchoring the sterically hindered amino acids to the solid support. Table 4.1 lists the primary sequence of peptide mitigators of Aβ, where B=Aib, J=Dpg, U=Dibg, Z=Dbg, and Me=*N*-methylated. Also described is the purification and characterization using HPLC, MALDI-MS, and AAA. Peptides AMY-3 and AMY-4 were not used for any assays. AMY-3 was extremely hydrophobic and was not soluble in aqueous buffers, therefore excluded from all experiments. The purification of AMY-4 was problematic as a result of poor coupling yields. A major problem with AMY-4 was the deletion of Dpg from the peptide chain. The AMY-4 peptide did not have homogeneity > 95% as determined by analytical HPLC; therefore, it was excluded from further experimental assays. A double coupling procedure at elevated temperatures for the incorporation of Aib (HC-

B_3) and *N*-methylated amino acids (*N*MHC) was used because previous protocols determined that this method of coupling afforded efficient peptide bond formation.

4.3.2 CONFORMATIONAL STUDIES OF PEPTIDE MITIGATORS

Initial CD studies of each peptide analog in the absence of Aβ (Figure 4.2) was performed to determine their aggregation behavior. The interaction of Aβ with the peptide analogs will be discussed later in Chapter 4 section 4.3.3. It was speculated that the peptide analogs would bind and interact with Aβ through β-sheet assemblies, but this premise relied on each peptide analog interacting with Aβ via the hydrophobic core, KLVFF, and the peptide analogs not folding into sheet-like conformations themselves. The CD spectra of AMY-1 and AMY-2 peptides were characteristic of predominately random coil conformations (RC), as indicated by a large negative band near 192 nm. The large positive band near 200 nm and 215 nm is due to the aromatic contributions from Dbg.[30-34] HC-K_6 and HC-B_3 peptides also exhibited unstructured random coiled conformations (Figure 4.2), while the *N*MHC peptide exhibited a signature curve characteristic of a β-sheet conformation. The unusual red-shifted CD spectra (minimum at 227 nm instead of normal 220 nm for β-sheets) could be attributed to differences in electronic transitions due to *N*-methylated amino acids. The concentration study of all peptide migitators suggest that they displayed minimal aggregation at concentrations studied. AMY-1 and AMY-2 concentration dependent CD studies all exhibited isodochroitic points, but the absence of a conformational transition from random coil to β-sheet suggested these peptides lack a multi-step misfolding transition. The systematic concentration dependent decrease in random coil signal at wavelengths ranging from 192 nm to 200 nm with increasing concentration for each peptide occurred due to increased salt content (TFA salt from HPLC purification) in each peptide sample which distorts the CD signal at the lower wavelengths. Data derived from the

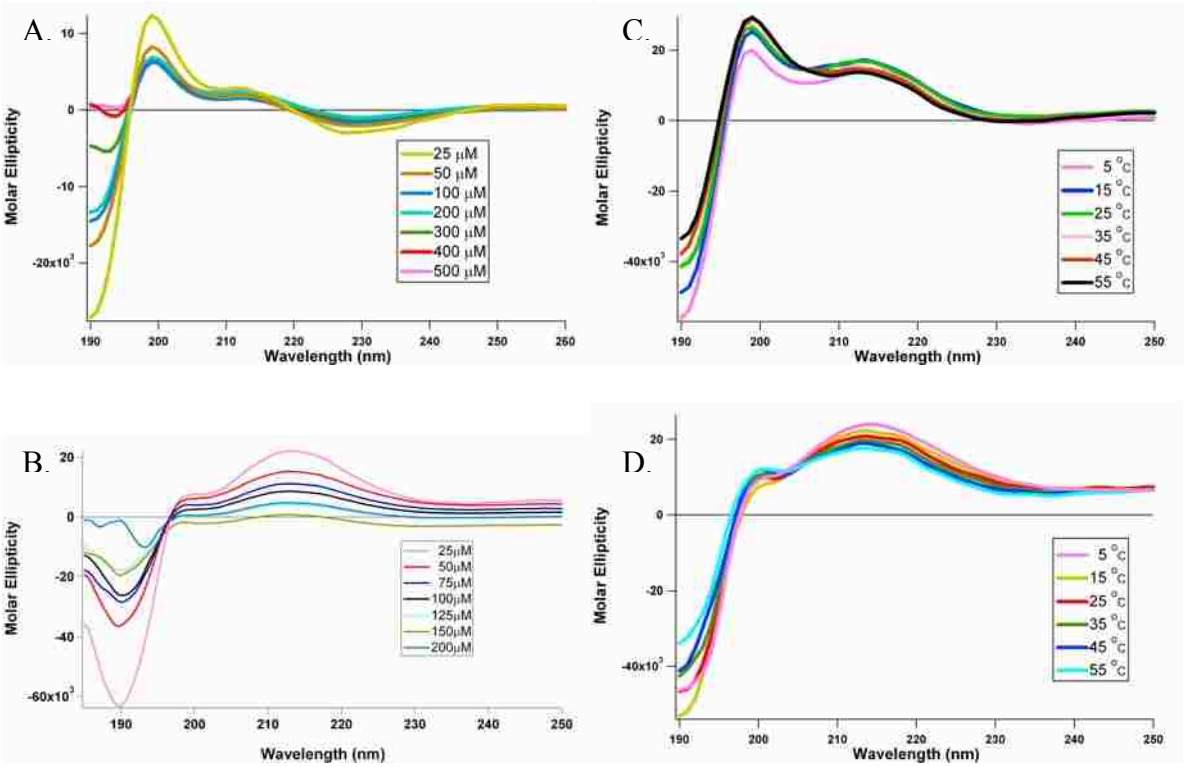

Figure 4.2. Concentration studies (25 μM-500 μM peptide) (A) AMY-1, (B) AMY-2. Temperature analysis (50 μM peptide, 5-55 °C) of (C) AMY-1, (D) AMY-2. All CD spectra were taken in 50 mM PBS (150 mM NaCl); pH 7.4. Molar Ellipticity -[θ] units: deg cm^2 dmol^{-1}. (Figure 4.2 cont'd.)

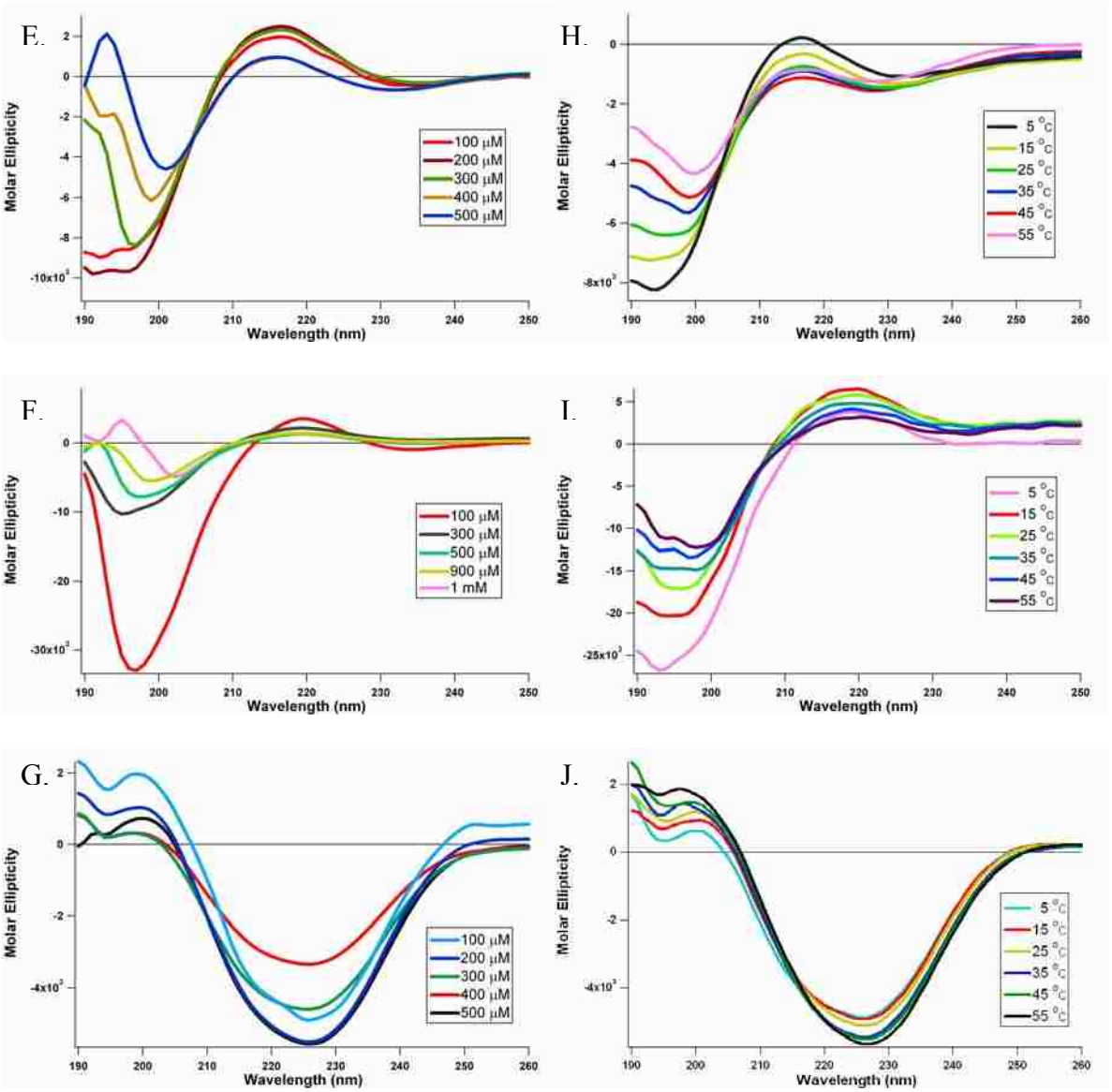

Concentration studies (100 µM-1 mM peptide) (E) HC-B_3, (F) HC-K_6, and (G) NMHC. Temperature analysis (50 µM peptide, 5-55 °C) of (H) HC-B_3, (I) HC-K_6, and (J) *N*MHC. All CD spectra were taken in 50 mM PBS (150 mM NaCl); pH 7.4. Molar Ellipticity- [θ] units: deg cm^2 $dmol^{-1}$.

thermal analysis of AMY-1, AMY-2, and *N*MHC peptides showed that each had superimposible CD bands at varying temperatures suggesting no thermal denaturation or unfolding of the peptide analogs from 5 °C to 55 °C. Although the HC-K_6 and HC-B_3 CD curves do not overlay, their secondary structures, at varying concentrations and temperatures, are consistent with one another. There was a systematic decrease in random coil signal at wavelengths ranging from 192 nm to 200 nm in both aggregation and thermal analysis as both the concentration and temperature increased. A clear isodichroitic point exists, but the absence of a conformational transition from the unstructured RC conformation to one that is more ordered suggests both peptides did not undergo a multi-step misfolding/unfolding process from a >10-fold concentration range and from low to elevated temperatures respectively.

4.3.3 PEPTIDE MITIGATORS AND THEIR INTERACTION WITH $A\beta_{1-40}$.

A significant problem associated with biophysical studies of synthetic Aβ is the time-dependent aggregation of Aβ in aqueous solution.[35] Polymorphism associated with subtle variations in Aβ fibril growth has lead to many inconsistencies in interpreting experimental results.[36, 37] Several factors such as peptide concentration, pH, ionic strength, amino acid primary sequence, and solvent systems have been found to affect in vitro studies of Aβ fibril formation. Controlling the initial aggregated state of the peptide is generally a challenge as synthetic Aβ is difficult to dissolve directly into physiological buffers.[38] The existence of pre-seeded material in commercially available Aβ from different manufacturers results in various initial aggregation states. Different lot batches produced by the same company also vary; therefore, obtaining monomeric starting solutions has been a main focus of a number of research laboratories as to ensure reliable and reproducible results. It is essential to understand the earliest phases of Aβ aggregation, including prenucleation and nucleation. Elucidating the

activity of protofibrillars and fibrils is essential for the development of therapies needed to interfere with neurotoxicity. To better study the early stages of aggregation, many groups follow protocols that involve the pre-dissolution of Aβ in organic solvents[39] such as: trifluoroacetic acid (TFA),[35] 2,2,2-trifluoroethanol (TFE),[40, 41] dimethyl sulfoxide (DMSO),[42, 43] and 1,1,1,3,3,5 hexafluoroisopropanol (HFIP),[44, 45] followed by dilution in aqueous buffer systems. Pre-dissolution using organic solvents is widely used due to their ability to dissolve pre-seeded material, promote α-helical conformations, and overcome solubility issues in physiological buffers. A modified protocol where Aβ was dissolved in organic solvents TFA and HFIP followed by dissolution in KOH and centrifugation to remove aggregated material was utilized to ensure monomeric stock solutions. Stock solutions were then diluted in PBS at various concentrations (5 μM-50 μM) to obtain working solutions. Using this protocol, monomeric starting solutions were assayed and monitored to study the effects of peptide anologs on Aβ aggregation.

The AMY-1 peptide (oligolysine unit on the *C*-terminus) greatly alters the progression of the β-sheet secondary structure associated with the Aβ protein. It was observed (Figure 4.3 A) after several days in aqueous buffer that Aβ protein, in the absence of peptide mitigator, has a conformational transition from random coil to β-sheet. This is followed by concomitant formation of approximately 4-7 nm-high protofibrils,[42, 43, 46, 47] as observed by scanning force microscopy (SFM; Figure 4.3 C). This is typical of the pattern that is observed where Aβ protein forms small oligomeric aggregates, then protofibrils that progress to mature fibrils (Figure 4.3 C displays one larger fibril among a plethora of protofibrils). Monomeric material is largely unstructured as evident by the random coil conformations illustrated by time zero solution (Figure 4.3 A purple curve) and mature fibrils (7-10 nm height; microns in length) contain

assemblies that have β-sheet conformations (Figure 4.3 A black and red curve) and are present in solutions incubated for 8 days while shaking (Figure 4.3 C). In contrast, equimolar mixtures of AMY-1 and Aβ lead to a complex and unusual CD curve that appears to become more β-sheet like as time progressed (Figure 4.3 B). Samples containing equimolar concentrations of AMY-1 and Aβ do not exhibit any protofibrillar material when examined with ex situ SFM after 8 days. All that is observed is a layer of protein adsorption onto the mica substrate (Figure 4.3 D). Dynamic light scattering suggests that the AMY-1/Aβ mixture contains particles ranging from 100-300 nm in size.[48] Typically, Aβ protein will form protofibrils that progress to fibrils, but in numerous experiments, AMY-1 significantly alters the pathway of Aβ assembly. Mixtures of AMY-1 and Aβ do not exhibit fibrillization or gellation after months at room temperature (Figure 4.4). TEM images of Aβ stored at room temperature for 4.5 months display large branched fibrillar structures (≥ 10 μm; Figure 4.4 A). SFM of this sample showed that the remaining material was composed of small fibrillar structures (Figure 4.4 B). More important, a sample of equimolar AMY-1 and Aβ stored at room temperature for 4.5 months show no sign of precipitate; TEM (Figure 4.4 C) and SFM images (Figure 4.4 D) display no signs of fibril formation and point only to the presence of globular, non-fibrillic protein aggregates. Even at sub-stoichiometric concentrations of AMY-1 (5 μM AMY-1: 50 μM Aβ) very little fibrillization of Aβ was found (Figure 4.4, E and F) for the same time period. AMY-2 (oligolysine unit on the *N*-terminus) behaves very differently than AMY-1. Mixtures of Aβ and AMY-2 solutions result in rapid (< 10 min) turbidity of the sample, which precludes CD analysis due to sample opaqueness. Microscopy studies of Aβ/AMY-2 (1:1 mole ratios) display large non-fibrillar aggregates on the order of ~1 μm (Figure 4.3 E) similar to H1 (KKKKKKGGQKLVFFAEDVG) peptide reported by Ghanta.[4]

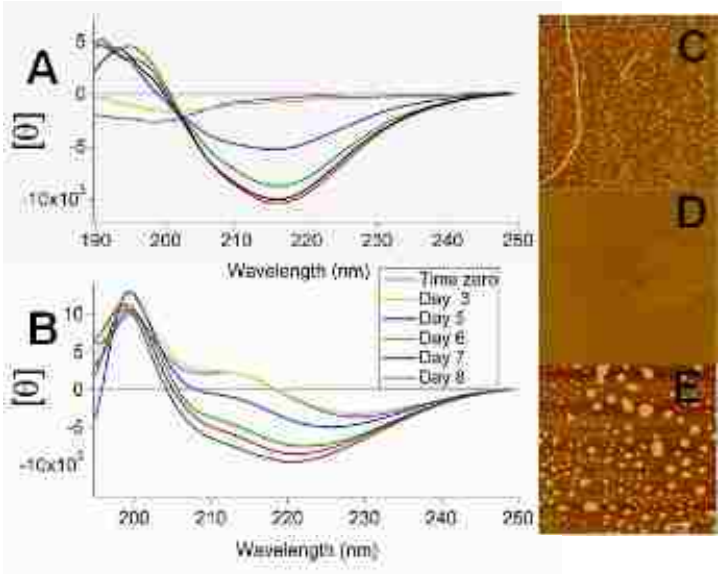

Figure 4.3. Aggregation of $A\beta_{1-40}$ mitigated by αα**A**A-based inhibitors. All incubations were performed in PBS (0.05 M NaH_2PO_4, 0.150 M NaCl, pH 7.4) and 37 °C. (A) CD of Aβ (50 μM) for t = 0-8 days; (B) CD of Aβ (50 μM) co-incubated with AMY-1 (50 μM) for t = 0-8 days; 10 μm x 10 μm ex situ tapping mode SFM images acquired on mica of (C) Aβ (50 μM) after 8 days, (D) Aβ (50 μM) and AMY-1 (50 μM) after 8 days, and (E) Aβ (50 μM) and AMY-2 (50 μM) for 1.5 h at 37 °C. [θ] units: deg cm^2 $dmol^{-1}$.

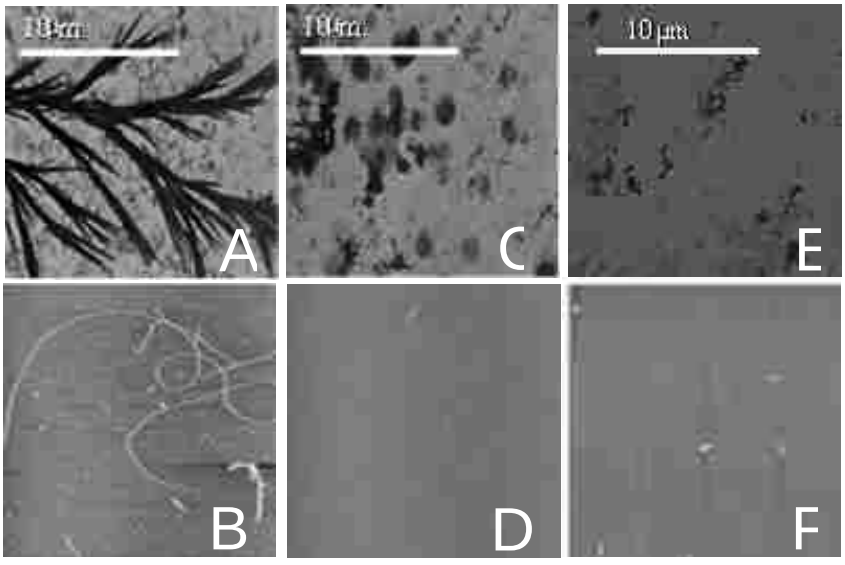

Figure 4.4. Effect of AMY-1 on $A\beta_{1-40}$ aggregation at varying inhibitor concentrations. A, C, and E are TEM images; B, D, and F are SFM images. Aβ (50 μM) incubated for 4.5 months at 25 °C in PBS; (A) and (B) Aβ alone; (C) and (D) with 50 μM AMY-1; (E) and (F) with 5 μM AMY-1. SFM images are 10 μm × 10 μm scans.

Small natural peptides, based on the hydrophobic core of Aβ, delay but do not stop imminent Aβ self-assembly and fibrillogenesis,[2, 3, 8, 9, 49] but the latter results suggest a very different mechanism for altering aggregation using AMY-1 than other peptide-based mitigators. Protein aggregates are stabilized suggesting that the aggregated states are trapped. This "trapness" could be a battle between conformations stabilized by intermolecular and intramolecular interactions.[50] What is the mechanism of the AMY inhibitors? We do know that AMY-1 and AMY-2 are very stable and do not aggregate in solution. In the presence of Aβ, one possibility is that the AMY-peptides are acting as non-specific cosurfactants that solubulize Aβ protein.[51] In this vein, surface activity analyses of the peptide mitigators were performed. The peptide AMY peptide mitigators do not show micellar-like activity up to millimolar (mM) concentrations, and they do not have significant surface activity at concentrations studied (50-100 μM).[52] The very different behavior of AMY-1 and AMY-2, which have the hydrophilic Lys tail on different termini, suggest some directionality to their interaction with Aβ. One way to rationalize this is to suggest a micelle with a hydrophobic core and a charged surface displaying the hydrophilic groups of Aβ and the Lys tails of AMY-1. AMY-2 may have the same directional interaction with Aβ, but displays the hydrophilic Lys tails to the inside of the micelle perhaps forming a bicelle or liposome-like structure that grows more quickly. An alternate hypothesis is that AMY-1 disrupts the propagation of intermolecular interactions necessary for the self-assembly of the hydrophobic *C*-terminal portion of Aβ.[53] Interfering with the propagation of favorable interactions that mediate the folding propensity of Aβ along with having one face capped due to ααAA steric contributions has the potential to reduce the formation of larger oligomer assemblies, thus producing smaller aggregate particles. The AMY-2/Aβ solutions do not proceed to mature fibrils because aggregation is capped due to ααAAs

steric contributions. However, AMY-2 disrupts only the hydrophilic *N*-terminal assembly of Aβ, which has less of an impact on aggregation.[54] As a result, AMY-2 leaves the *C*-terminus of Aβ accessible for nucleation that potentially leads to larger particle formation.

4.3.3.1 AMBIGUITY IN THIOFLAVIN-T FLUORESCENCE ASSAYS

Thioflavin-T (ThT) is a cationic benzothiazole dye that undergoes changes in its spectral properties as it binds to amyloid fibrils.[55-59] ThT is usually assayed at concentrations (10-100 μM) above its cmc (~4 μM); therefore, it forms micelles that bind to hydrophobic pockets/patches of Aβ fibrils and enhances the fluorescent signal as fibril growth occurs.[60] Preliminary studies using amylin protein (type-II diabeties Islet fibrils) were unsuccessful at binding ThT as the protein showed no increase in fluorescence signal as time progressed. The cationic dye was able to bind aggregates of Aβ protein (preliminary studies by Aucoin and Etienne) suggesting that ThT fluorescence is Aβ specific. Thus, ThT fluorescence assays were used to monitor Aβ fibril formation in conjunction with CD spectroscopy and TEM.

ThT results (Figure 4.5) were inconsistent with CD and TEM data. Under normal physiological conditions, Aβ has a lag-phase observed in fluorescence spectroscopy (emissions at 482 nm) due to the presence of monomeric material. As Aβ protein monomer self-associates and aggregate to form protofibrils and fibrils, an increase in ThT fluorescence is normally observed. However, CD analysis of aggregated Aβ solutions show β-sheet secondary structures and TEM images displayed protofibrils and fibril material while ThT fluorescence indicated the presence of a lag-phase. HC-K_6, was used as a peptide control and displayed characteristics consistent with literature. [5, 6, 61] CD analysis of HC-K_6 alone (Figure 4.2 F and I) showed that this peptide mitigator adopts a random coiled conformation. There were minimal differences in the CD spectra of HC-K_6 compared to a 1:1 molar mixtures of Aβ/HC-K_6 solutions at short term

incubations (0-72 hrs), but slight conformational changes occurred following 72 hrs. This change was attributed to the morphology changes that occurred in solution (formation of mature fibrils). The particle size distribution of aggregate material of Aβ and Aβ/HC-K_6 solutions (1:1) was monitored using DLS.[48] Aβ/HC-K_6 solutions increased the growth kinetics associated with fibril formation and formed fibrils with distinguishable morphologies which was also consistent with literature reports. Pallitto,[6] reported that HC-K_6 caused little or no reduction in ThT fluorescence signal; however, the fluorescence data presented in this dissertation is not consistent their findings. The HC-K_6 peptide (Figure 4.5 turquoise triangle) dramatically reduces fibrillogenesis for a prolonged period of time while fibrils were present in Aβ/HC-K_6 solutions at approximately 72 h (determined using TEM).

*N*MHC was also used as a control peptide. Its CD spectrum was predominately β-sheet and the peptide was highly soluble in aqueous solution. These results were consistent with the reported literature.[8, 9] In contrast to reported ThT results, *N*MHC was ineffective at halting fibril formation at concentrations assayed (1:1-10:1 mole ratios of mitigator:Aβ; conclusions determined by TEM images). Gordon et al. reported that this peptide was ineffective at reducing fibril formation at low Aβ:inhibitor ratios (<1:4), however, our ThT results indicate that at 1:1 mole ratio, a lag-phase (indicative of reduction in Aβ fibril formation compared to Aβ alone, Figure 4.5 black square-Aβ, green triangle- *N*MHC/Aβ solution) occurred for 82 h followed by rapid fibril formation. We were unable to reproduce the disassembly of pre-formed fibrils reported by Gordon at concentrations reported in literature. Differences in initial dissolution protocols of Aβ could contribute to the ambiguity associated with interpreting experimental results of control peptides.

Levine reports one important characteristic of this cationic dye is that it does not bind to

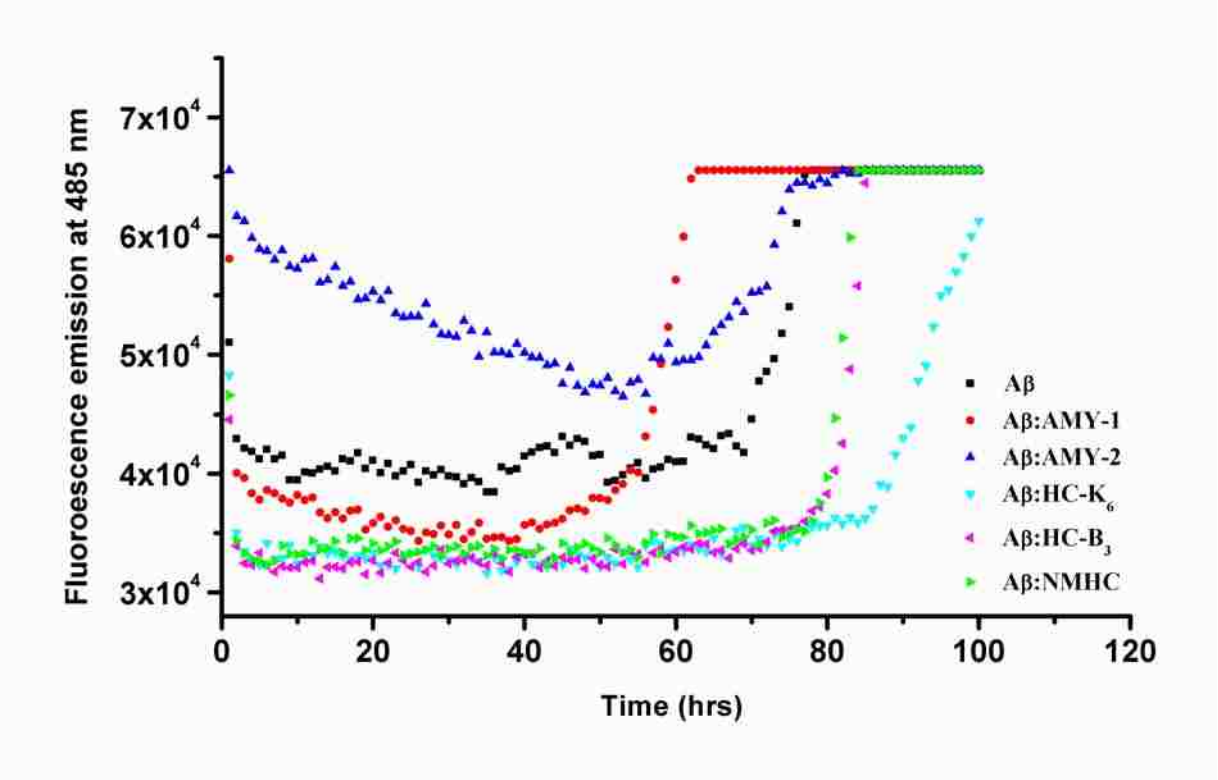

Figure 4.5 Thioflavin-T fluorescence assay measuring fibril growth of Aβ in the presence of peptide mitigators. Working solution contain 50 μM Aβ/peptide mitigator (1:1 mole ratio) in 50 mM PBS 150 mM NaCl (pH 7.4) using 10 μM ThT dissolved in PBS. Samples were heated continuously at 37°C and shaken 15 sec every 30 min in a 96 well-plate.

amorphous aggregates or monomer material, but does bind to protofibril material.[58] However, ThT fluorescence is not an effective experimental assay for monitoring fibril growth or disassembly because we and others[62] have shown that ThT is capable of binding amorphous aggregates as well as protofibrillar and fibrillar materials. It was expected that AMY-1 would reduce fibril formation due to the facial capping model of β-sheets. Although SFM images (Figure 4.4 B) supported this hypothesis with the absence of fibrillic material, ThT fluorescence of Aβ/AMY-1 solutions (Figure 4.5 red circle) had an initial reduction in fibril formation, but displayed increased fluorescence intensity compared to Aβ alone after approximately 60 h. The fast growth was initially thought to be a direct link with Aβ fibril formation but CD analysis

(Figure 4.3) and TEM (Figure 4.4) images of the AMY-1 (1:1) solution show amorphous aggregates that contain β-sheet secondary structures. Upon dissolution with Aβ, AMY-2 rapidly aggregates forming large globular aggregates that were capable of binding ThT. From preliminary CD and TEM studies, it was expected that AMY-2 would behave in a manner forming large hydrophobic aggregates whose aggregation kinetics would be faster than Aβ itself. AMY-2/Aβ solutions did form aggregates exceedingly faster than Aβ and exhibited enhanced fluorescence signals suggestive of rapid self-assembly and aggregate growth. SFM and TEM images of Aβ/AMY-2 solutions displayed the presence of large aggregate material after 60 h incubation and no sign of fibril formation. Thus it is hypothesized that ThT binding is not morphologically specific rather is driven by hydrophobic interactions and ionic interactions necessary to stabilize the ThT micelle binding to Aβ substructures.

4.3.4 Aβ CYTOTOXICITY

AD is characterized by the presence of extracellular deposits known as senile plaques. Senile plaques are localized to the cerebral cortex and/or hippocampus regions of the brain and have been associated with neurodegeneracy because affected regions of the brain are mostly responsible for increased brain functions including sensation, voluntary muscle movement, thought, reasoning, and memory function. These proteinacious plaques consist mostly of Aβ protein and have been implicated as a direct link between neuronal dysfunction and cell death. It is seemingly difficult to study Aβ aggregation in vivo; therefore, scientists have modeled Aβ aggregation using synthetic peptide forms of the neurotoxin to elucidate its mechanism and mode of action. More recently, in vitro and in vivo studies suggest that soluble intermediates (protofibrils) not mature fibrils are the cytotoxic species responsible for cell apoptosis and neurodegeneracy.[3, 63-68] Walsh and Selkoe[69] related neurodegeneracy and cytotoxicity to soluble oligomers stating that these intermediates mediate learning and memory and there is a direct link

to cytotoxicity and neurodegeneracy. In APP transgenic mice, protofibrillar materials contributed to neurotoxicity and progressive learning defects as well as declines in synaptic transmission. As Aβ aggregates forming diffusible plaques that build up on neuronal cells, neuronal impulse signals cannot be transmitted via axons and dendrites, thus activating microglail cells for a protective inflammatory response leading to synaptic dysfunction and cell apoptosis. [70, 71]

Although there are a myriad of proposed mechanisms by which Aβ protofibrils contribute to cytotoxicity in AD, the most explored method is cell apoptosis as a result of oxidative stress.[72, 73] It has been speculated that Aβ fibrils promote oxidative injuries that lead to cell apoptosis.[74] Cellular apoptosis can be localized to mitochondria dysfunction (change in structure and function). Typically a decrease in mitochondrial membrane potential is an early indicator of apoptosis. This apoptotic response, reduction in membrane potential, is also characterized by release of cystolic cytochrome c via reduction of cytochrome oxidase activating a cascade of events leading oxidative stress.[73, 75] Oxidative stress results from an imbalance between free radicals and antioxidants where a one electron dioxygen reduction occurs producing a reactive oxygen species (ROS) such as hydroxyl radicals ($OH^{\cdot}$), superoxide anions (O_2^{-}), and hydrogen peroxide (H_2O_2).[72, 76] During oxidative phosphorylation, (ATP production in mitochondria) an unpaired set of electrons are produced. These electrons interact with molecular oxygen, O_2, generating the superoxide anion O_2^{-}. The superoxide anion is detoxified with superoxide dismutase producing H_2O_2 that is either reduced to water (H_2O) or in the presence of free transition metals, forms the more reactive hydroxyl radicals ($OH^{\cdot}$). Generation of free radicals leads to lipid peroxidation and cell damage.[73, 77-79]

Antibodies have offered promising results in reducing the cytotoxic effects of oligomers both in vitro and in vivo, but studies have been limited to murine antibodies which are similar yet

different from human antibodies.[63, 69, 80-85] It is quite difficult to produce human antibodies against human tissue. For this reason, the use of peptidomimetics offers a more practical and less futile approach towards the discovery of pharmalogical targets of AD.

Ghanta[4] synthesized four peptides based on the hydrophobic core of Aβ (R1, R2, H1, H2) that contained a recognition element and a disrupting element and studied their ability to reduce Aβ toxicity in vitro using PC-12 cells. Peptides R1 (VFFAEDVG) and H2 (GQKLVFFAEDVGGaKKKKKK) did not readily aggregate and precipitate out of solution as H1 (KKKKKKGGQKLVFFAEDVG). They were also soluble in PBS, in contrast to R2 (LKVFFAEDVG); therefore, they were the only two peptides used to measure cytotoxicity. H2 and R1 were nontoxic to the PC-12 cell line, but in the presence of aged Aβ (fibrils imaged using TEM), H2 reduced toxicity at a two fold excess of mitigator peptide to Aβ. R1 was ineffective at reducing toxicity. One interesting feature of the hybrid peptide H2 was it did not decrease fibrillization as previous mention in section 4.3.3, rather it increased the rate of Aβ fibril formation forming nontoxic fibrils. The group further developed their synthetic design and synthesized more potent peptide mitigators by shortening the length of the peptide chain (reducing hydrophobicity) while maintaining the disrupting groups at either the *N* or *C*-terminus of the peptide chain. They found that peptide variants contain a disrupting element considerably decreased cytotoxicity as compared to their native counterparts (no disrupting group).[6] Hybrid peptides 16-20-K_6 and 16-20-E_6 were surprisingly potent Aβ fibril inhibitory compounds at extremely low doses, 1:100 and 1:1000 respectively (peptide mitigator:Aβ), being reported as some of most potent peptide mitigators to date.[5] Soto designed a β-sheet breaker peptide, iAβ5 (LPFFD), related to the hydrophobic core of Aβ that considerably inhibited Aβ fibril formation in vitro and in vivo for both neurotoxic isoforms of Aβ.[1-3] Using this same peptide, with a slight

modification to protect it against proteolytic degredation- iAβ5p (acetyl-LPFFD-amide), Chacon et. al[65] significantly increased spatial learning acquitions and reduce cognitive impairment and cerebral damage in transgenic mice. iAβ5p also blocked activation of astrocytes from becoming hypertropic glial cells (inflammatory responsive cells) in response to Aβ.

The ability of AMY peptide mitigators to reduce toxicity of Aβ fibril solutions in vitro using PC-12 cells was investigated. This cell line was of particular interest because of their synthesis, uptake, and storage of neurotransmittors. The PC-12 cell line is one that highly proliferates. Because the growth kinetics of these cells is not well known, an initial experiment to determine the rate of proliferation over 24 h was performed. It was imperative that reduction in metabolic activity was a result of Aβ fibril treatment and not cell apoptosis via environmental competition and that measured neuronal cell survival was a result of AMY peptides inhibitory activity and not cell nuclei growth. Initial studies assayed cells with a plating density of 0 cells/well-50,000 cell/well. Cells allowed to adhere for 24 h had no significant difference in metabolic activity compared to cells that we allowed to adhere for 8-12 h. As a result, the optimal cell plating density was 50,000 cells/well. At this level, cell apoptosis was trivial. 50 μM Aβ solutions were used to measure cytotoxicity in order to maintain a consistent molar concentration of aggregated material and to better compare and interpret Aβ toxicity data with results from other physical techniques previously used. Aggregated Aβ fibril samples, incubated for 7 days at 37 °C, were allowed to co-incubate with PC-12 cells for 0 h -24 h (Figure 4.6). Cell viability data, from time dependent cell co-incubation with Aβ, revealed that 24 h was the optimal exposure time aggregated Aβ solutions would be allowed to interact with PC-12 cells while measuring metabolic activity.

AMY-1 has a protective mechanism reducing cytotoxicity in vitro >90% only in the presence of aggregated Aβ solutions. While equimolar solutions of aggregated Aβ/AMY-1 (10-50 μM) were nontoxic to PC-12 cells, AMY-2/Aβ solutions (1:1) reduced cell viability of PC-12 cells 85-90% at identical concentrations. AMY-1 and AMY-2 alone both reduced cell viability (~40% and 100% respectively) at a concentration of 50 μM as compared to an untreated cell control. This suggests that at high concentrations, AMY-1 inhibitory capacity is significantly reduced and AMY-2 is lethal. HC-K_6, *N*MHC, and HC-B_3 peptides did not significantly reduce the cellular viability of PC-12 cells. Similar nontoxic effects were observed in equimolar

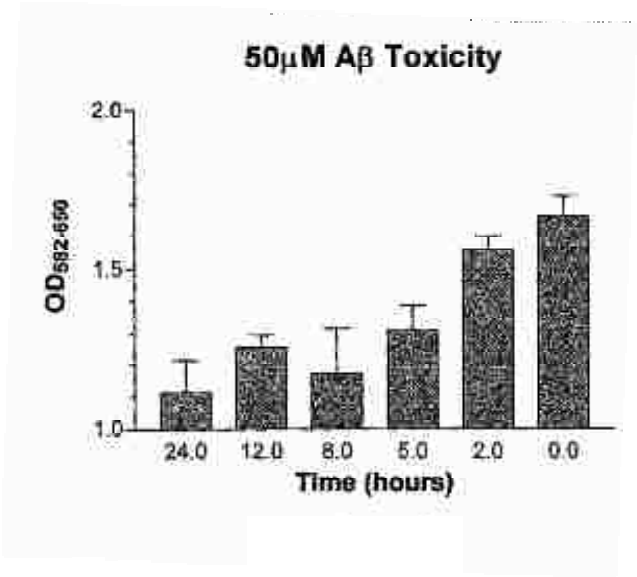

Figure 4.6. MTT viability assay of PC-12 cells co-incubated with aggregated Aβ solutions. Aβ was incubated at a monomer concentration of 50 μM for 7 days at 37 °C while agitated continuously.

in equimolar mixtures of each peptide mitigator with aggregated Aβ solutions at varying concentrations (10-50 μM).

The PC-12 metabolic reduction assay has a number of problems including high concentrations and volumes of Aβ required to achieve toxicity and the PC-12 cell-line is an undifferentitated cell-line. A common problem observed in control experiments was aggregated

Aβ solutions were capable of inducing a cytotoxic response. However, in toxicity experiments where AMY peptide mitigators were assayed, aggregated Aβ fibril solutions were unsuccessful at producing a cytotoxic response in cell cultures. PC-12 cells are fairly homogenous, yet they are disadvantageous when measuring cytotoxicity because they are a rapidly proliferating cell line that is more resistant to Aβ than primary neurons.

Primary cells, although they may have mixed populations of neurons, are more closely related to in vivo neurons and are differentiated where synaptic signals can be transmitted. More recently, primary cortical neurons purchased from Genlantis (N200200) have been utilized. Cortical neuronal cells were isolated from 18-day-old embryonic Spargue/Dawley or Fischer 344 rat brains and cultured in poly-D-lysine coated 96 well-plates. Many research groups employ the use of DMEM supplemented media.[46, 86] In contrast, our cells were differentiated in B27-supplemented Neurobasal (0.5 mM glutamine), which increases long-term cell viability.[22] Aggregated Aβ and Aβ/AMY-1 (1:1) solutions were allowed to incubate as described by Sato et al. [87] with final peptide concentrations of 5.5 μM and samples were exposed to neuronal cultures for 24 h. Preliminary neurotoxicity results suggest that Aβ alone reduced cell viability 43% (% of neuronal survival following treatment) as compared to the control (cells with no peptide treatment). Aβ/AMY-1 aggregated samples reduced cell viability 50 %. Fibrils were present in the Aβ sample while the Aβ/AMY-1 sample (1:1) had no signs of fibrils, only the presence of peptide aggregates (imaged by TEM). Ambiguity lies in the veracity of the cortical neuronal assays. Time and concentration-dependent exposure of aggregated Aβ samples to cells have yet to be determined for primary neuron cultures.

In vivo studies, collaboration with Dr. David Morgan from the University of South Flordia, of APP transgenic mice offer promising results towards the inhibitory affect of the

AMY-1 peptide mitigator. Figure 4.7 illustrates the increase in Aβ plaque deposition seven days after an intrahippocampus administration of peptide mitigator (1/3 nmole) on the contralateral hippocampus (panel A, C, E) and ipsilateral hippocampus (panels B, D, F) brain regions. The increase in plaque deposition was suggestive of *N*MHC inability to reduce Aβ plaque deposition thus inducing plaque deposition (Figure 4.5 panels C and D). In contrast, AMY-1 (Figure 4.7 panels E and F) was able to considerably reduce plaque deposition as compared to the Aβ control in PBS (Figure 4.7 panels A and B). A similar trend was seen in a Thioflavine-S (ThS) stain of identical hippocampal regions of the brain with identical incubation times (Figure 4.8). Amyloid deposits are large extracellular deposits that damage surrounding tissue, as a result, ThS stains amyloid apple green under a fluorescence microscope. Figure 4.8 panels A and B are Aβ control peptide in PBS, panels C and D are of *N*MHC, and panels E and F contain AMY-1. Panels C and D show increased levels of amyloid formation as seen with of the abundance of localized apple green fluorescence indicative of amyloid deposits. However, AMY-1 showed a reduction in Aβ amyloid formation as indicated by the absence of the apple green subsection. Unfortunately, preliminary in vivo results (data not shown) do agree with PC-12 cellular in vitro data suggesting that at high concentrations, AMY-1 induces microglial activity causing a decrease in cellular viability.

4.4 CONCLUSION

The design of peptide mitigators of Aβ fibrillogenesis builds on the premise that peptides containing the hydrophopic core of Aβ can interact with the corresponding residues of Aβ via self-recognition and disrupt the self-assembly of Aβ into protofibrils and fibrils.[4, 6, 88] In conclusion, a novel ααAA-containing peptide-based approach to mitigate the aggregation of the Aβ protein preventing the formation of mature fibrils has been developed. Studies show that

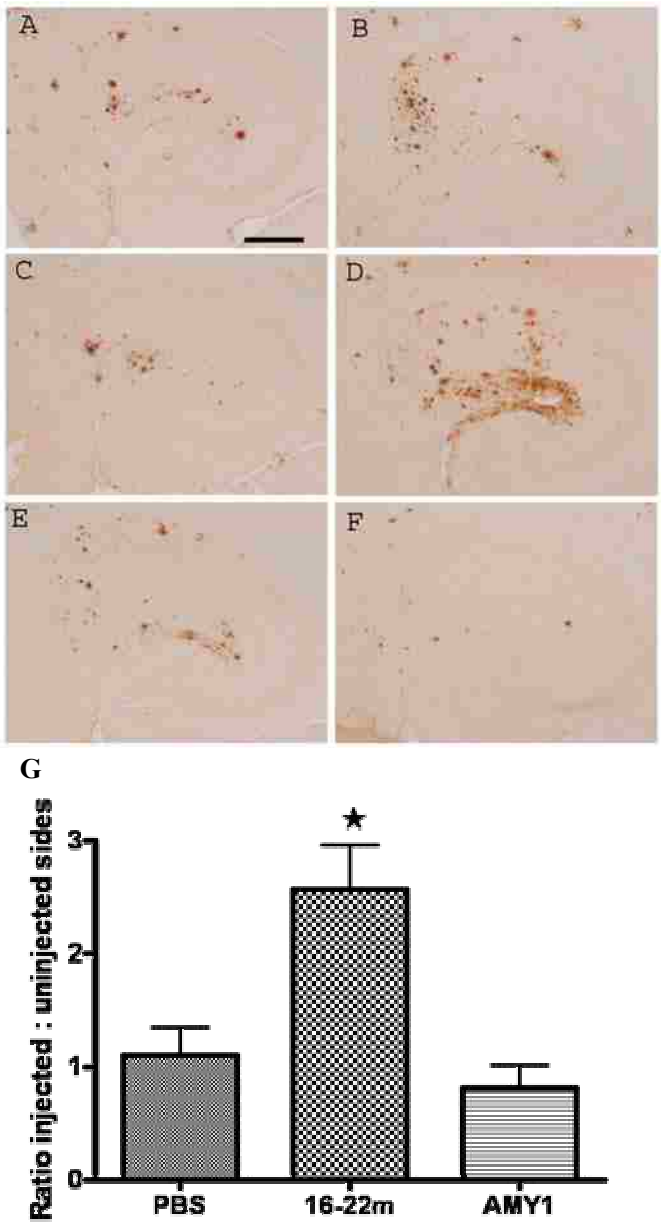

Figure 4.7. Total Aβ load following intrahippocampus administration of *N*MHC and AMY1. Panels A, C and E show total Aβ immunostaining in the contralateral hippocampal regions; Panels B, D and F show ipsilateral hippocampal regions. Panels A and B show PBS control group; Panels C and D show *N*MHC (1/3 nmole) and panels E and F show AMY1 group (1/3 nmole). Scale bar =120 μm. Panel G shows quantification of total Aβ immunohistochemistry in the hippocampus as the ratio of injected side (right) to uninjected side (left). Data are presented as mean±sem, ∗P< 0.05 compare to PBS control group. Sample size is 8-10 per group.

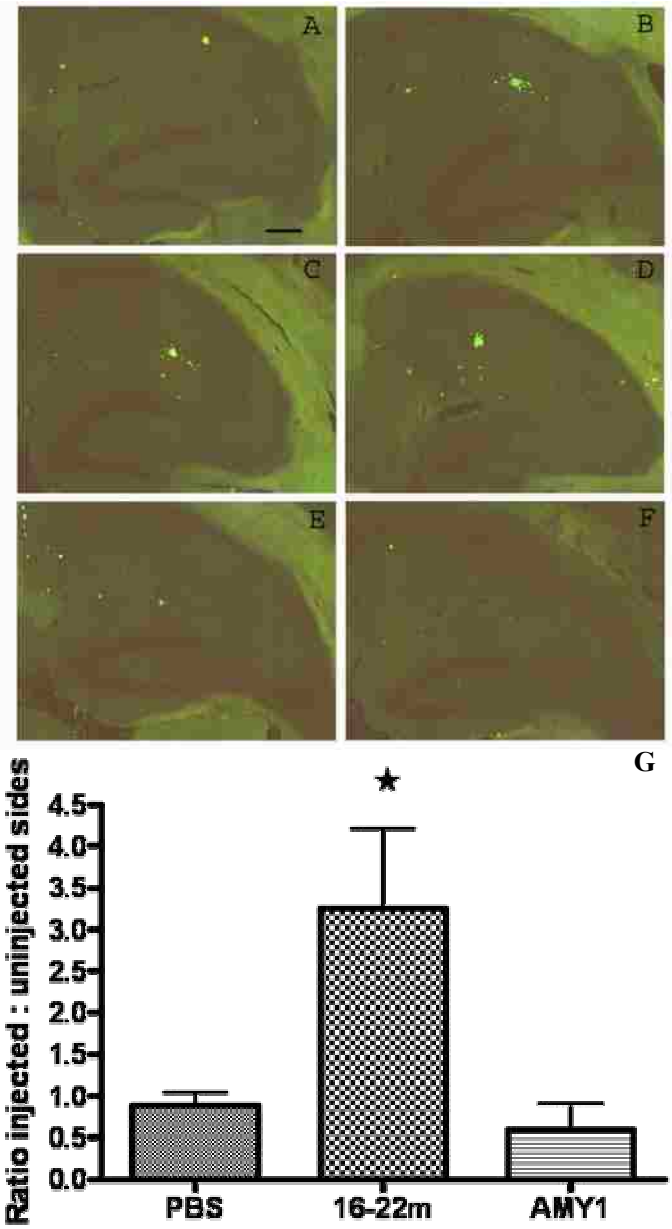

Figure 4.8. Thioflavine-S staining of *N*MHC and AMY-1 in APP transgenic mice. Panels A, C and E show total Aβ immunostaining in the contralateral hippocampal regions; Panels B, D and F show ipsilateral hippocampal regions. Panels A and B show PBS control group; Panels C and D show *N*MHC (1/3 nmole) and panels E and F show AMY1 group (1/3 nmole). Scale bar =120 μm. Panel G shows the ratio of thiosflavine-S staining of injected side (right) to uninjected side (left) in the hippocampus of APP transgenic mice. Data are presented as mean±sem, ∗P< 0.05 compare to PBS control group. Sample size is 8-10 per group.

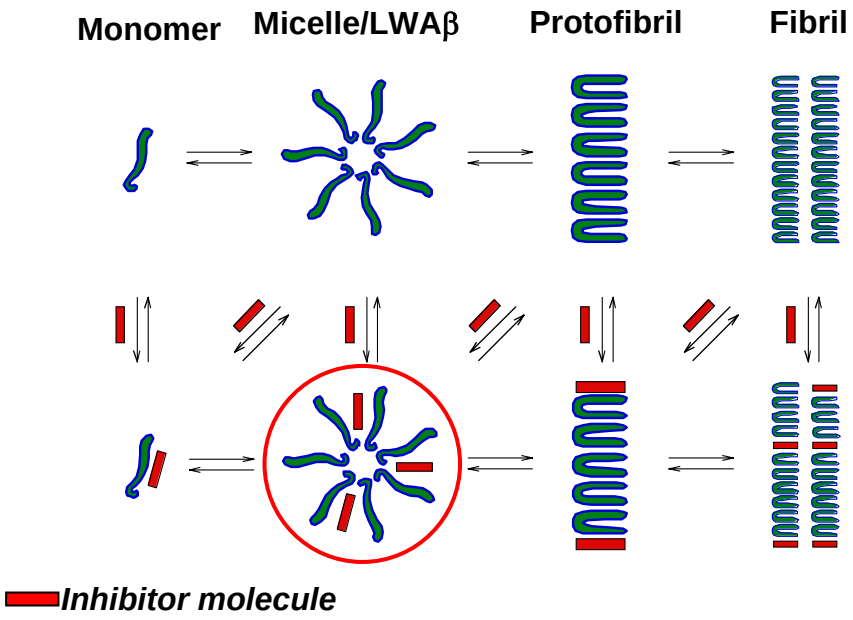

Figure 4.9. Alternate pathway to Aβ aggregation derived from ααAA based peptide mitigators.

peptides with alternating L-amino acids and ααAAs incorporated into the hydrophobic core of Aβ dramatically alters aggregation behavior. Spectroscopic studies suggest that these novel peptides interact through the formation of β-sheet assemblies, but the mechanism and duration of fibril inhibition is unique relative to other peptide and non-peptide based inhibitors. A plausible mechanistic pathway explaining fibril inhibition is that the peptide mitigators could interact at the aggregate state and intercalate the Aβ globular aggregate disrupting the formation of mature fibrils by encapsulating the aggregate precursors (Figure 4.9) and producing an off-pathway mechanism. Further characterization of the AMY/Aβ aggregate size, structure, and stability as well as in vitro and in vivo toxicity assays are underway.

4.5 REFERENCES

1. Adessi, C.; Soto, C. β-sheet breaker strategy for the treatment of Alzheimer's disease. *Drug Dev. Res.* **2002,** 56, 184-193.

2. Soto, C.; Kindy, M. S.; Baumann, M.; Frangione, B. Inhibition of Alzheimer's amyloidosis by peptides that prevent β-sheet conformation. *Biochem. Biophys. Res. Commun.* **1996,** 226, 672-680.

3. Soto, C.; Sigurdsson, E. M.; Morelli, L.; Kumar, R. A.; Castano, E. M.; Frangione, B. β-sheet breaker peptides inhibit fibrillogenesis in a rat brain model of amyloidosis: Implications for Alzheimer's therapy. *Nat. Med.* **1998,** 4, 822-826.

4. Ghanta, J.; Shen, C. L.; Kiessling, L. L.; Murphy, R. M. A strategy for designing inhibitors of β-amyloid toxicity. *J. Biol. Chem.* **1996,** 271, 29525-29528.

5. Lowe, T. L.; Strzelec, A.; Kiessling, L. L.; Murphy, R. M. Structure-function relationships for inhibitors of β-amyloid toxicity containing the recognition sequence KLVFF. *Biochemistry* **2001,** 40, 7882-7889.

6. Pallitto, M. M.; Ghanta, J.; Heinzelman, P.; Kiessling, L. L.; Murphy, R. M. Recognition sequence design for peptidyl modulators of β-amyloid aggregation and toxicity. *Biochemistry* **1999,** 38, 3570-3578.

7. Sciarretta, K. L.; Gordon, D. J.; Meredith, S. C., Peptide-based inhibitors of amyloid assembly. In *Amyloid, Prions, and Other Protein Aggregates, Pt C*, Elsevier Academic Press Inc: San Diego, 2006; Vol. 413, pp 273-312.

8. Gordon, D. J.; Sciarretta, K. L.; Meredith, S. C. Inhibition of β-amyloid(40) fibrillogenesis and disassembly of β-amyloid(40) fibrils by short β-amyloid congeners containing *N*-methyl amino acids at alternate residues. *Biochemistry* **2001,** 40, 8237-8245.

9. Gordon, D. J.; Tappe, R.; Meredith, S. C. Design and characterization of a membrane permeable *N*-methyl amino acid-containing peptide that inhibits Aβ(1-40) fibrillogenesis. *J. Peptide Res.* **2002,** 60, 37-55.

10. Chalifour, R. J.; McLaughlin, R. W.; Lavoie, L.; Morissette, C.; Tremblay, N.; Boule, M.; Sarazin, P.; Stea, D.; Lacombe, D.; Tremblay, P.; Gervais, F. Stereoselective interactions of peptide inhibitors with the β-amyloid peptide. *J. Biol. Chem.* **2003,** 278, 34874-34881.

11. Tjernberg, L. O.; Lilliehook, C.; Callaway, D. J. E.; Naslund, J.; Hahne, S.; Thyberg, J.; Terenius, L.; Nordstedt, C. Controlling amyloid β-peptide fibril formation with protease-stable ligands. *J. Biol. Chem.* **1997,** 272, 12601-12605.

12. Gilead, S.; Gazit, E. Inhibition of amyloid fibril formation by peptide analogues modified with α-aminoisobutyric acid. *Angew. Chem. Int. Edit.* **2004,** 43, 4041-4044.

13. Awasthi, S. K.; Shankaramma, S. C.; Raghothama, S.; Balaram, P. Solvent-induced β-hairpin to helix conformational transition in a designed peptide. *Biopolymers* **2001,** 58, 465-476.

14. Toniolo, C.; Crisma, M.; Formaggio, F.; Peggion, C. Control of peptide conformation by the Thorpe-Ingold effect (C^{α}-tetrasubstitution). *Biopolymers* **2001,** 60, 396-419.

15. Karle, I. L.; Kaul, R.; Rao, R. B.; Raghothama, S.; Balaram, P. Stereochemical analysis of higher α,α-dialkylglycine containing peptides. Characterization of local helical conformations at dipropylglycine residues and observation of a novel hydrated multiple β-turn structure in crystals of a glycine rich peptide. *J. Am. Chem. Soc.* **1997,** 119, 12048-12054.

16. Kaul, R.; Banumathi, S.; Velmurugan, D.; Balaji Rao, R.; Balaram, P. Conformational choice at α,α-di-*N*-propylglycine residues: Helical or fully extended structures? *Biopolymers* **2000,** 54, 159-167.

17. Kaul, R.; Banumathi, S.; Velmurugan, D.; Ravikumar, K.; Rao, R. B.; Balaram, P. Context-dependent conformation of diethylglycine residues in peptides. *J. Peptide Res.* **2000,** 55, 271-278.

18. Wysong, C. L.; Yokum, T. S.; McLaughlin, M. L.; Hammer, R. P. Controlling peptide structure. *Chem. Tech.* **1997,** 27, 26-33.

19. Wysong, C. L.; Yokum, T. S.; Morales, G. A.; Gundry, R. L.; McLaughlin, M. L.; Hammer, R. P. 4-Aminopiperidine-4-carboxylic acid: A cyclic α,α-disubstituted amino acid for preparation of water-soluble highly helical peptides. *J. Org. Chem.* **1996,** 61, 7650-7651.

20. Sole, N. A.; Barany, G. Optimization of solid-phase synthesis of [Ala8]-dynorphin A. *J. Org. Chem.* **1992,** 57, 5399-403.

21. Grant, G. A., *Synthetic Peptides: A User's Guide*. 2 ed.; Oxford University Pess: New York, 2002.

22. Brewer, G. J.; Torricelli, J. R.; Evege, E. K.; Price, P. J. Optimized survival of hippocampal-neurons in B27-supplemented neurobasal™, a new serum-free medium combination. *J. Neurosci. Res.* **1993,** 35, 567-576.

23. Shearman, M. S.; Hawtin, S. R.; Tailor, V. J. The intracellular component of cellular 3-(4,5-dimethylthiazol-2-yl)-2,5-diphenyltetrazolium bromide (MTT) reduction is specifically inhibited by β-amyloid peptides. *J. Neurochem.* **1995,** 65, 218-227.

24. Shearman, M. S.; Ragan, C. I.; Iversen, L. L. Inhibition of PC-12 cell redox activity is a specific, early indicator of the mechanism of β-amyloid-mediated cell-death. *Proc. Natl. Acad. Sci. U. S. A.* **1994,** 91, 1470-1474.

25. Hertel, C.; Hauser, N.; Schubenel, R.; Seilheimer, B.; Kemp, J. A. β-Amyloid-induced cell toxicity: Enhancement of 3-(4,5-dimethylthiazol-2-yl)-2,5-diphenyltetrazolium bromide-dependent cell death. *J. Neurochem.* **1996,** 67, 272-276.

26. Shearman, M. S., Toxicity of protein aggregates in PC 12 cells: 3-(4, 5-dimethylthiazol-2-yl)-2,5-diphenyltetrazolium bromide assay. In *Amyloid, Prions, and Other Protein Aggregates*, Academic Press Inc: San Diego, 1999; Vol. 309, pp 716-723.

27. Fu, Y.; Hammarstroem, L. G. J.; Miller, T. J.; Fronczek, F. R.; McLaughlin, M. L.; Hammer, R. P. Sterically hindered $C^{\alpha,\alpha}$-disubstituted α-amino acids: Synthesis from α-nitroacetate and incorporation into peptides. *J. Org. Chem.* **2001,** 66, 7118-7124.

28. Fu, Y.; Etienne, M. A.; Hammer, R. P. Facile synthesis of α,α-diisobutylglycine and anchoring its derivatives onto PAL-PEG-PS resin. *J. Org. Chem.* **2003,** 68, 9854-9857.

29. Fu, Y.; Hammer, R. P. Efficient acylation of the *N*-terminus of highly hindered $C^{\alpha,\alpha}$-disubstituted amino acids via amino acid symmetrical anhydrides. *Org. Lett.* **2002,** 4, 237-240.

30. Woody, R. W. Circular dichroism of peptides and proteins. *Circ. Dichroism* **1994**, 473-96.

31. Greenfield, N. J., Analysis of circular dichroism data. In *Numerical Computer Methods, Pt D*, Academic Press Inc: San Diego, 2004; Vol. 383, pp 282-317.

32. Woody, R. W., Circular dichroism of protein-folding intermediates. In *Energetics of Biological Macromolecules, Pt E*, Academic Press Inc: San Diego, 2004; Vol. 380, pp 242-285.

33. Sreerama, N.; Manning, M. C.; Powers, M. E.; Zhang, J. X.; Goldenberg, D. P.; Woody, R. W. Tyrosine, phenylalanine, and disulfide contributions to the circular dichroism of proteins: Circular dichroism spectra of wild-type and mutant bovine pancreatic trypsin inhibitor. *Biochemistry* **1999,** 38, 10814-10822.

34. Sreerama, N.; Woody, R. W. Computation and analysis of protein circular dichroism spectra. *Methods Enzymol.* **2004,** 383, 318-351.

35. Shao, H. Y.; Jao, S. C.; Ma, K.; Zagorski, M. G. Solution structures of micelle-bound amyloid β-(1-40) and β-(1-42) peptides of Alzheimer's disease. *J. Mol. Biol.* **1999,** 285, 755-773.

36. Petkova, A. T.; Leapman, R. D.; Guo, Z. H.; Yau, W. M.; Mattson, M. P.; Tycko, R. Self-propagating, molecular-level polymorphism in Alzheimer's β-amyloid fibrils. *Science* **2005,** 307, 262-265.

37. Fezoui, Y.; Hartley, D. M.; Harper, J. D.; Khurana, R.; Walsh, D. M.; Condron, M. M.; Selkoe, D. J.; Lansbury, P. T.; Fink, A. L.; Teplow, D. B. An improved method of preparing the amyloid β-protein for fibrillogenesis and neurotoxicity experiments. *Amyloid* **2000,** 7, 166-178.

38. Shen, C. L.; Murphy, R. M. Solvent effects on self-assembly of β-amyloid peptide. *Biophys. J.* **1995,** 69, 640-651.

39. O'Nuallain, B.; Thakur, A. K.; Williams, A. D.; Bhattacharyya, A. M.; Chen, S. M.; Thiagarajan, G.; Wetzel, R., Kinetics and thermodynamics of amyloid assembly using a high-performance liquid chromatography-based sedimentation assay. In *Amyloid, Prions, and Other Protein Aggregates, Pt C*, Elsevier Academic Press Inc: San Diego, 2006; Vol. 413, pp 34-74.

40. Fezoui, Y.; Teplow, D. B. Kinetic studies of amyloid β-protein fibril assembly: Differential effects of α-helix stabilization. *J. Biol. Chem.* **2002,** 277, 36948-36954.

41. Huang, T. H. J.; Fraser, P. E.; Chakrabartty, A. Fibrillogenesis of Alzheimer Aβ peptides studied by fluorescence energy transfer. *J. Mol. Biol.* **1997,** 269, 214-224.

42. Harper, J. D.; Lieber, C. M.; Lansbury, P. T. Atomic force microscopic imaging of seeded fibril formation and fibril branching by the Alzheimer's disease amyloid-β protein. *Chem. Biol.* **1997,** 4, 951-959.

43. Harper, J. D.; Wong, S. S.; Lieber, C. M.; Lansbury, P. T. Observation of metastable Aβ amyloid protofibrils by atomic force microscopy. *Chem. Biol.* **1997,** 4, 119-125.

44. Nichols, M. R.; Moss, M. A.; Reed, D. K.; Cratic-McDaniei, S.; Hoh, J. H.; Rosenberry, T. L. Amyloid-β protofibrils differ from Amyloid-β aggregates induced in dilute hexafluoroisopropanol in stability and morphology. *J. Biol. Chem.* **2005,** 280, 2471-2480.

45. Wood, S. J.; Maleeff, B.; Hart, T.; Wetzel, R. Physical, morphological and functional differences between pH 5.8 and 7.4 aggregates of the Alzheimer's amyloid peptide AP. *J. Mol. Biol.* **1996,** 256, 870-877.

46. Walsh, D. M.; Hartley, D. M.; Kusumoto, Y.; Fezoui, Y.; Condron, M. M.; Lomakin, A.; Benedek, G. B.; Selkoe, D. J.; Teplow, D. B. Amyloid β-protein fibrillogenesis: Structure and biological activity of protofibrillar intermediates. *J. Biol. Chem.* **1999,** 274, 25945-25952.

47. Walsh, D. M.; Lomakin, A.; Benedek, G. B.; Condron, M. M.; Teplow, D. B. Amyloid β-protein fibrillogenesis: Detection of a protofibrillar intermediate. *J. Biol. Chem.* **1997,** 272, 22364-22372.

48. Edwin, N. Characterization of β-amyloid peptide aggregation and acceleration with non-fibrillar forming peptide-based mediators. PhD Dissertation Louisiana State University, Baton Rouge, 2006.

49. Soto, C.; Branes, M. C.; Alvarez, J.; Inestrosa, N. C. Structural determinants of the Alzheimer's amyloid β-peptide. *J. Neurochem.* **1994,** 63, 1191-1198.

50. Gregersen, N.; Bross, P.; Vang, S.; Christensen, J. H. Protein misfolding and human disease. *Annu. Rev. Genomics Hum. Genet.* **2006,** 7, 103-124.

51. Chennamsetty, N.; Bock, H.; Scanu, L. F.; Siperstein, F. R.; Gubbins, K. E. Cosurfactant and cosolvent effects on surfactant self-assembly in supercritical carbon dioxide. *J. Chem. Phys.* **2005,** 122.

52. Aucoin, J. P. Protein aggregation studies: Inhibiting and encouraging β-amyloid aggregation. PhD Dissertation Louisiana State University, Baton Rouge, 2003.

53. Schmechel, A.; Zentgraf, H.; Scheuermann, S.; Fritz, G.; Pipkorn, R. D.; Reed, J.; Beyreuther, K.; Bayer, T. A.; Multhaup, G. Alzheimer β-amyloid homodimers facilitate β-fibrillization and the generation of conformational antibodies. *J. Biol. Chem.* **2003,** 278, 35317-35324.

54. Morimoto, A.; Irie, K.; Murakami, K.; Masuda, Y.; Ohigashi, H.; Nagao, M.; Fukuda, H.; Shimizu, T.; Shirasawa, T. Analysis of the secondary structure of β-amyloid (Aβ 42) fibrils by systematic proline replacement. *J. Biol. Chem.* **2004,** 279, 52781-52788.

55. Naiki, H.; Higuchi, K.; Hosokawa, M.; Takeda, T. Fluorometric-determination of amyloid fibrils in vitro using the fluorescent dye, thioflavine-T. *Anal. Biochem.* **1989,** 177, 244-249.

56. Naiki, H.; Higuchi, K.; Matsushima, K.; Shimada, A.; Chen, W. H.; Hosokawa, M.; Takeda, T. Methods in laboratory investigation. Fluorometric examination of tissue amyloid fibrils in murine senile amyloidosis: Use of the fluorescent indicator, thioflavine-T. *Lab. Invest.* **1990,** 62, 768-773.

57. Naiki, H.; Higuchi, K.; Nakakuki, K.; Takeda, T. Kinetic-analysis of amyloid fibril polymerization in vitro. *Lab. Invest.* **1991,** 65, 104-110.

58. Levine, H. Thioflavine-T interaction with synthetic Alzheimer's disease β-amyloid peptides: Detection of amyloid aggregation in solution. *Protein Sci.* **1993,** 2, 404-410.

59. LeVine, H., Quantification of β-sheet amyloid fibril structures with thioflavin T. In *Amyloid, Prions, and Other Protein Aggregates*, **1999**; Vol. 309, pp 274-284.

60. Khurana, R.; Coleman, C.; Ionescu-Zanetti, C.; Carter, S. A.; Krishna, V.; Grover, R. K.; Roy, R.; Singh, S. Mechanism of thioflavin T binding to amyloid fibrils. *J. Struct. Biol.* **2005,** 151, 229-238.

61. Kim, J. R.; Gibson, T. J.; Murphy, R. M. Predicting solvent and aggregation effects of peptides using group contribution calculations. *Biotechnol. Prog.* **2006,** 22, 605-608.

62. Fu, Y. W.; Bieschke, J.; Kelly, J. W. E-olefin dipeptide isostere incorporation into a polypeptide backbone enables hydrogen bond perturbation: Probing the requirements for Alzheimer's amyloidogenesis. *J. Am. Chem. Soc.* **2005,** 127, 15366-15367.

63. Kayed, R.; Head, E.; Thompson, J. L.; McIntire, T. M.; Milton, S. C.; Cotman, C. W.; Glabe, C. G. Common structure of soluble amyloid oligomers implies common mechanism of pathogenesis. *Science* **2003,** 300, 486-489.

64. Pike, C. J.; Burdick, D.; Walencewicz, A. J.; Glabe, C. G.; Cotman, C. W. Neurodegeneration induced by β-Amyloid peptides in vitro: The role of peptide assembly state. *J. Neurosci.* **1993,** 13, 1676-1687.

65. Chacon, M. A.; Barria, M. I.; Soto, C.; Inestrosa, N. C. β-sheet breaker peptide prevents Aβ-induced spatial memory impairments with partial reduction of amyloid deposits. *Mol.Psych.* **2004,** 9, 953-961.

66. Chong, Y. H.; Shin, Y. J.; Lee, E. O.; Kayed, R.; Glabe, C. G.; Tenner, A. J. ERK1/2 activation mediates Aβ oligomer-induced neurotoxicity via caspase-3 activation and tau cleavage in rat organotypic hippocampal slice cultures. *J. Biol. Chem.* **2006,** 281, 20315-20325.

67. Bitan, G.; Fradinger, E. A.; Spring, S. M.; Teplow, D. B. Neurotoxic protein oligomers - what you see is not always what you get. *Amyloid* **2005,** 12, 88-95.

68. Hartley, D. M.; Walsh, D. M.; Ye, C. P. P.; Diehl, T.; Vasquez, S.; Vassilev, P. M.; Teplow, D. B.; Selkoe, D. J. Protofibrillar intermediates of amyloid β-protein induce acute electrophysiological changes and progressive neurotoxicity in cortical neurons. *J. Neurosci.* **1999,** 19, 8876-8884.

69. Walsh, D. M.; Selkoe, D. J. Deciphering the molecular basis of memory failure in Alzheimer's disease. *Neuron* **2004,** 44, 181-193.

70. Selkoe, D. J. Amyloid protein and Alzheimer's disease. *Sci.Am.* **1991,** 265, 40-47.

71. Mattson, M. P.; Partin, J.; Begley, J. G. Amyloid β-peptide induces apoptosis-related events in synapses and dendrites. *Brain Res.* **1998,** 807, 167-176.

72. Iversen, L. L.; Mortishiresmith, R. J.; Pollack, S. J.; Shearman, M. S. The toxicity in vitro of β-amyloid protein. *Biochem. J* **1995,** 311, 1-16.

73. Cardoso, S. M.; Santana, I.; Swerdlow, R. H.; Oliveira, C. R. Mitochondria dysfunction of Alzheimer's disease cybrids enhances Aβ toxicity. *J. Neurochem.* **2004,** 89, 1417-1426.

74. Kienlen-Campard, P.; Miolet, S.; Tasiaux, B.; Octave, J. N. Intracellular amyloid-β 1-42, but not extracellular soluble amyloid-β peptides, induces neuronal apoptosis. *J. Biol. Chem.* **2002,** 277, 15666-15670.

75. Tamagno, E.; Parola, M.; Guglielmotto, M.; Santoro, G.; Bardini, P.; Marra, L.; Tabaton, M.; Danni, O. Multiple signaling events in amyloid β-induced, oxidative stress-dependent neuronal apoptosis. *Free Radical Biol. Med.* **2003,** 35, 45-58.

76. Sayre, L. M.; Zagorski, M. G.; Surewicz, W. K.; Krafft, G. A.; Perry, G. Mechanisms of neurotoxicity associated with amyloid-β deposition and the role of free radicals in the pathogenesis of Alzheimer's disease: A critical appraisal. *Chem. Res. Toxicol.* **1997,** 10, 518-526.

77. Eckert, A.; Keil, U.; Marques, C. A.; Bonert, A.; Frey, C.; Schussel, K.; Muller, W. E. Mitochondrial dysfunction, apoptotic cell death, and Alzheimer's disease. *Biochem. Pharmacol.* **2003,** 66, 1627-1634.

78. Irie, K.; Murakami, K.; Masuda, Y.; Morimoto, A.; Ohigashi, H.; Ohashi, R.; Takegoshi, K.; Nagao, M.; Shimizu, T.; Shirasawa, T. Structure of β-amyloid fibrils and its relevance to their neurotoxicity: Implications for the pathogenesis of Alzheimer's disease. *J. Biosci. Bioeng.* **2005,** 99, 437-447.

79. Schoneich, C.; Pogocki, D.; Hug, G. L.; Bobrowski, K. Free radical reactions of methionine in peptides: Mechanisms relevant to β-amyloid oxidation and Alzheimer's disease. *J. Am. Chem. Soc.* **2003,** 125, 13700-13713.

80. Bucciantini, M.; Calloni, G.; Chiti, F.; Formigli, L.; Nosi, D.; Dobson, C. M.; Stefani, M. Prefibrillar amyloid protein aggregates share common features of cytotoxicity. *J. Biol. Chem.* **2004,** 279, 31374-31382.

81. Defelice, F. G.; Ferreira, S. T. Physiopathological modulators of amyloid aggregation and novel pharmacological approaches in Alzheimer's disease. *Anais Da Academia Brasileira De Ciencias* **2002,** 74, 265-284.

82. Stefani, M.; Dobson, C. M. Protein aggregation and aggregate toxicity: new insights into protein folding, misfolding diseases and biological evolution. *J. Mol. Med.* **2003,** 81, 678-699.

83. Bucciantini, M.; Giannoni, E.; Chiti, F.; Baroni, F.; Formigli, L.; Zurdo, J. S.; Taddei, N.; Ramponi, G.; Dobson, C. M.; Stefani, M. Inherent toxicity of aggregates implies a common mechanism for protein misfolding diseases. *Nature* **2002,** 416, 507-511.

84. Calamai, M.; Canale, C.; Relini, A.; Stefani, M.; Chiti, F.; Dobson, C. M. Reversal of protein aggregation provides evidence for multiple aggregated states. *J. Mol. Biol.* **2005,** 346, 603-616.

85. Stefani, M.; Baglioni, S.; Bucciantini, M.; Chiti, F.; Dobson, C. M.; Taddei, N.; Casamenti, F. Neuronal cell death is triggered by prefibrillar protein aggregates. *Protein Sci.* **2004,** 13, 174-175.

86. Fifre, A.; Sponne, I.; Koziel, V.; Kriem, B.; Potin, F. T. Y.; Bihain, B. E.; Olivier, J. L.; Oster, T.; Pillot, T. Microtubule-associated protein MAP1A, MAP1B, and MAP2 proteolysis during soluble amyloid β-peptide-induced neuronal apoptosis - Synergistic involvement of calpain and caspase-3. *J. Biol. Chem.* **2006,** 281, 229-240.

87. Sato, T.; Kienlen-Campard, P.; Ahmed, M.; Liu, W.; Li, H. L.; Elliott, J. I.; Aimoto, S.; Constantinescu, S. N.; Octave, J. N.; Smith, S. O. Inhibitors of amyloid toxicity based on β-sheet packing of Aβ 40 and Aβ 42. *Biochemistry* **2006,** 45, 5503-5516.

88. Tjernberg, L. O.; Callaway, D. J. E.; Tjernberg, A.; Hahne, S.; Lilliehook, C.; Terenius, L.; Thyberg, J.; Nordstedt, C. A molecular model of Alzheimer amyloid β-peptide fibril formation. *J. Biol. Chem.* **1999,** 274, 12619-12625.

CHAPTER 5.

SUMMARY

5.1 DISCUSSION

Most protein conformational diseases occur as a result of protein misfolding, and a common pathological feature among these diseases is the formation of fibrillar deposits that contain β-sheet secondary structures.[1-4] Understanding specific interactions that stabilize β-sheet secondary structures is paramount for the development of medicinal strategies that could prevent the progression of these diseases. In this vein, the study of β-sheet structures serves as a basis for elucidating protein folding and misfolding mechanisms. Peptides with ordered conformations are good models to study secondary structure and folding propensities because they can provide fundamental characteristics of native proteins.[5] This dissertation has focused on the design, synthesis, and structural analysis of conformationally-constrained peptides containing $C^{\alpha,\alpha}$-disubstituted amino acids. ααAAs are excellent structural elements that are capable of stabilizing β-sheet motifs and mitigating protein aggregation.

Chapter 2 of the dissertation focuses on investigating the formation and stability of β-sheets using β-hairpin peptide models. Within chapter 2, the importance of ααAAs as design elements in both strand portions and the turn region of β-hairpin peptides was explored. Stable turn motifs are pre-requisites for the formation and stability of β-hairpins and are important well-defined linking segments that connect prefabricated secondary structure modules.[6] Also, nucleation of specific turn types gives detailed structural information about side-chain interactions between adjoining β-strands.[7-12] CD and NMR analysis revealed that incorporation of Aib-Gly and Aib-DAla turn sequences into the *i+1* and *i+2* positions of a β-turn resulted in the formation of β-hairpins that nucleate type-I' β-turns. Substitution of the Aib turn inducers

with more bulky and branched, Dpg-Gly and Dibg-Gly turn sequences, ultimately resulted in the formation of less ordered β-sheets (CD analysis). The difference in the CD spectra for the more bulky ααAAs is suggestive of the nucleation of a different type of β-turn.

Side-chain interactions, and electrostatic and hydrophobic interactions strongly regulate β-sheet stability. To access the effects of ααAAs on β-sheet or β-strand stability, Dpg and Dibg, were incorporated into position-3 of a model β-hairpin model first introduced by Gellman.[13] These particular amino acid residues are highly hydrophobic and were hypothesized to induce β-sheet formation. [U^3]-Ω^DPG formed a highly ordered β-sheet, while the Dpg-containing peptides (Dpg located in the β-strand region and in the *i+1* position of a β-turn) formed less ordered β-sheet structures. CD and NMR analysis have shown that although Dibg is an excellent inducer of sheet formation relative to its position in β-strands, this bulky ααAA has less of an impact on β-sheet formation when located in the *i+1* residue of β-hairpins. These results are in agreement with previous work performed in the Hammer laboratory that suggests ααAAs contribution to secondary structure is sequence-dependent (local primary structure). To date, this is one of the first studies that explains the context-dependent nature of ααAAs on conformational preferences in an aqueous buffer. Other studies have introduced this idea, but relied heavily on crystallographic data[14, 15] and organic solvents.[16, 17] Future conformational studies will explore the use of more bulky ααAAs, such as dibenzylglycine (Dbzg), incorporated into β-turns and their effects on β-sheet motifs. Also, the stereochemistry of the *i+2* amino acid residue will be investigated. Chiral ααAAs will be incorporated into specific regions of the β-strand portion and in the turn region of model β-hairpin peptides and evaluated to determine their contribution to β-sheet secondary structures. The use of bulky ααAAs are expected to promote

extended peptide conformations and could offer vital information in the design of *de novo* peptides for biologically active molecules.

Chapter 3 introduces Alzheimer's disease (AD).[18, 19] A hallmark feature of AD is the presence of senile plaques mostly consisting of the Aβ protein. Abnormal processing of APP leads to neurotoxic isoforms of Aβ. Initially, fibrils of Aβ were thought to be directly related to neurodegeneracy, but more recently, protofibrillar aggregates of $A\beta_{1\text{-}40}$ and $A\beta_{1\text{-}42}$ isoforms have been associated with cytotoxicity. The goal for this project was to mitigate protein aggregation of monomeric Aβ, thereby preventing the formation of mature fibrils. Peptide analogs aimed at mitigating Aβ aggregation and reducing cytotoxicity were developed. Chapter 4 describes the design, synthesis, physical characterization, and in vitro cell studies of peptide analogs and their interaction with Aβ.

The Aβ fibril structure is aligned in a parallel β-sheet orientation and is stabilized by intrastrand/interstrand hydrogen bonding and interstrand side-chain interactions (hydrophobic and electrostatic interactions). A common approach toward mitigating Aβ protein aggregation is through "β-sheet" breaker peptides. The AMY peptide mitigators have been designed based on a specific hydrophobic region of Aβ primary sequence (region 16-22, the hydrophobic core, KLFVVAE), and their design incorporates ααAAs at alternating positions within this sequence. AMY/Aβ solutions prevent fibril formation for both short- and long-term incubation periods and globular assemblies are produced as observed through microscopy studies. CD studies indicated that the AMY peptides interact with Aβ by forming β-sheet secondary structures that further assemble to form the globular aggregates observed. The formation of the globular aggregates occur because the AMY peptides block one face of LWAβ from hydrogen-bonding to another moiety of Aβ, thus preventing the formation of higher order aggregate material. Although the

AMY peptides are excellent candidates for peptide-based in vitro therapeutics agents, they must be modified if they are to be used as pharmacological agents. Currently, the focus of this project is to improve the bioavailability of the AMY peptide mitigators. The AMY-mitigators are largely hydrophobic and have a large molecular weight. Molecules that are largely lipophilic, uncharged, and have low molecular weights are easily transported across the blood brain barrier (BBB).[20] Variants of the AMY-1 peptide mitigator are being developed with reduced hydrophobicity, molecular weight, and charge (Table 5.1). The β-sheet blocker mechanism is being maintained while accessing the requirement of each ααAA in the peptide modifications. Once the peptide modifications are optimized, the newly synthesized AMY peptide variants will be further altered to increase proteolytic stability.

Table 5.1. Primary sequence of AMY-peptide mitigators under investigation.

PEPTIDE	**PEPTIDE SEQUENCE (N→C)**						
	1	**2**	**3**	**4**	**5**	**6**	**7**
AMY-1	***Lys_1***	***Dibg***	***Val***	***Dbzg***	***Phe***	***Dpg***	***Lys_6***
AMY-5	Lys_1	Leu	Val	Dbzg	Phe	Dpg	Lys_6
AMY-6	Lys_1	Dibg	Val	Phe	Phe	Dpg	Lys_6
AMY-7	Lys_1	Dibg	Val	Dbzg	Phe	Ala	Lys_6
AMY-8	Lys_1	Dibg	Val	Dbzg	Phe	---	Lys_6
AMY-9	Lys_1	Dibg	Val	Dbzg	Phe	---	Lys_4
AMY-10	Lys_1	Dibg	Val	Dbzg	Phe	---	Lys_2

*The proposed peptide mitigator design is devised based on the AMY-1 peptide. AMY-1 was effective at preventing fibril formation in vitro and reducing plaque deposition in vivo at stoichiometric and substiochiometric concentrations thus taking the fibrillogenesis process off-pathway producing globular aggregates.

Additionally, the biological activity of peptide mitigators and AMY-X/Aβ will be evaluated. AMY- peptide mitigators that exhibit similar inhibitory properties as AMY-1 will be used to measure their affect on the metabolic activity of differentiated SH-SY5Y neuroblastoma cells. Currently AMY-1 reduces cytotoxicity in vitro and decreases plaque deposition in vivo. A more detailed in vivo investigation into to efficacy of the peptide mitigator on both the hippocampal and cortical regions of the brain are underway.

5.2 REFERENCES

1. Carrell Robin, W. Cell toxicity and conformational disease. *Trends Cell Biol.* **2005,** 15, 574-80.

2. Howlett, D. R. Protein misfolding in disease: Cause or response? *Curr. Med. Chem.* **2003,** 3, 371-383.

3. Thompson, A. J.; Barrow, C. J. Protein conformational misfolding and amyloid formation: characteristics of a new class of disorders that include Alzheimer's and Prion diseases. *Curr. Med. Chem.* **2002,** 9, 1751-1762.

4. Lin, J. C.; Liu, H. L. Protein conformational diseases: from mechanisms to drug designs. *Curr. Drug Discov. Technol.* **2006,** 3, 145-53.

5. Gunasekaran, K.; Ramakrishnan, C.; Balaram, P. β-Hairpins in proteins revisited: lessons for de novo design. *Protein Eng.* **1997,** 10, 1131-1141.

6. Venkatraman, J.; Shankaramma, S. C.; Balaram, P. Design of folded peptides. *Chem. Rev.* **2001,** 101, 3131-3152.

7. Huang, R.; Setnicka, V.; Etienne, M. A.; Kim, J.; Kubelka, J.; Hammer, R. P.; Keiderling, T. A. Cross-strand coupling of a β-hairpin peptide stabilized with an Aib-Gly turn studied using isotope-edited IR spectroscopy. *J. Am. Chem. Soc.* **2007,** 129, 13592-13603.

8. Kiehna, S. E.; Waters, M. L. Sequence dependence of β-hairpin structure: Comparison of a salt bridge and an aromatic interaction. *Protein Sci.* **2003,** 12, 2657-2667.

9. Tatko, C. D.; Waters, M. L. Selective aromatic interactions in β-hairpin peptides. *J. Am. Chem. Soc.* **2002,** 124, 9372-9373.

10. Tatko, C. D.; Waters, M. L. The geometry and efficacy of cation-π interactions in a diagonal position of a designed β-hairpin. *Protein Sci.* **2003,** 12, 2443-2452.

11. Haque, T. S.; Gellman, S. H. Insights on β-hairpin stability in aqueous solution from peptides with enforced type-I' and type-II' β-turns. *J. Am. Chem. Soc.* **1997,** 119, 2303-2304.

12. Syud, F. A.; Stanger, H. E.; Gellman, S. H. Interstrand sidechain-sidechain interactions in a designed β-hairpin: Significance of both lateral and diagonal pairings. *J. Am. Chem. Soc.* **2001,** 123, 8667-8677.

13. Stanger, H. E.; Gellman, S. H. Rules for antiparallel β-sheet design: D-Pro-Gly is superior to L-Asn-Gly for β-hairpin nucleation. *J. Am. Chem. Soc.* **1998,** 120, 4236-4237.

14. Aravinda, S.; Shamala, N.; Rajkishore, R.; Gopi, H. N.; Balaram, P. A crystalline β-hairpin peptide nucleated by a type-I' Aib-D-Ala β-turn: Evidence for cross-strand aromatic interactions. *Angew. Chem. Int. Edit.* **2002,** 41, 3863-3865.

15. Toniolo, C.; Crisma, M.; Formaggio, F.; Peggion, C. Control of peptide conformation by the Thorpe-Ingold effect (C^{α}-tetrasubstitution). *Biopolymers* **2001,** 60, 396-419.

16. Karle, I. L.; Kaul, R.; Rao, R. B.; Raghothama, S.; Balaram, P. Stereochemical analysis of higher α,α-dialkylglycine containing peptides. Characterization of local helical conformations at dipropylglycine residues and observation of a novel hydrated multiple β-turn structure in crystals of a glycine rich peptide. *J. Am. Chem. Soc.* **1997,** 119, 12048-12054.

17. Kaul, R.; Banumathi, S.; Velmurugan, D.; Ravikumar, K.; Rao, R. B.; Balaram, P. Context-dependent conformation of diethylglycine residues in peptides. *J. Peptide Res.* **2000,** 55, 271-278.

18. In *National Center for Health Statistics of the Centers for Disease Control*, http://www.eniorjournal.com/NEWS/Health/6-04-20 AlzheimersClimbs.html: 2004.

19. http://www.alz.org/alzheimers_disease_alzheimer_statistics.asp, Alzheimer's Facts and Figures. In 2007.

20. Bryan, J. Crossing the blood brain barrier: Drug delivery to the brain is still elusive. *Pharm. J.* **2004,** 273, 475-476.

APPENDIX A
NMR SPECTRA

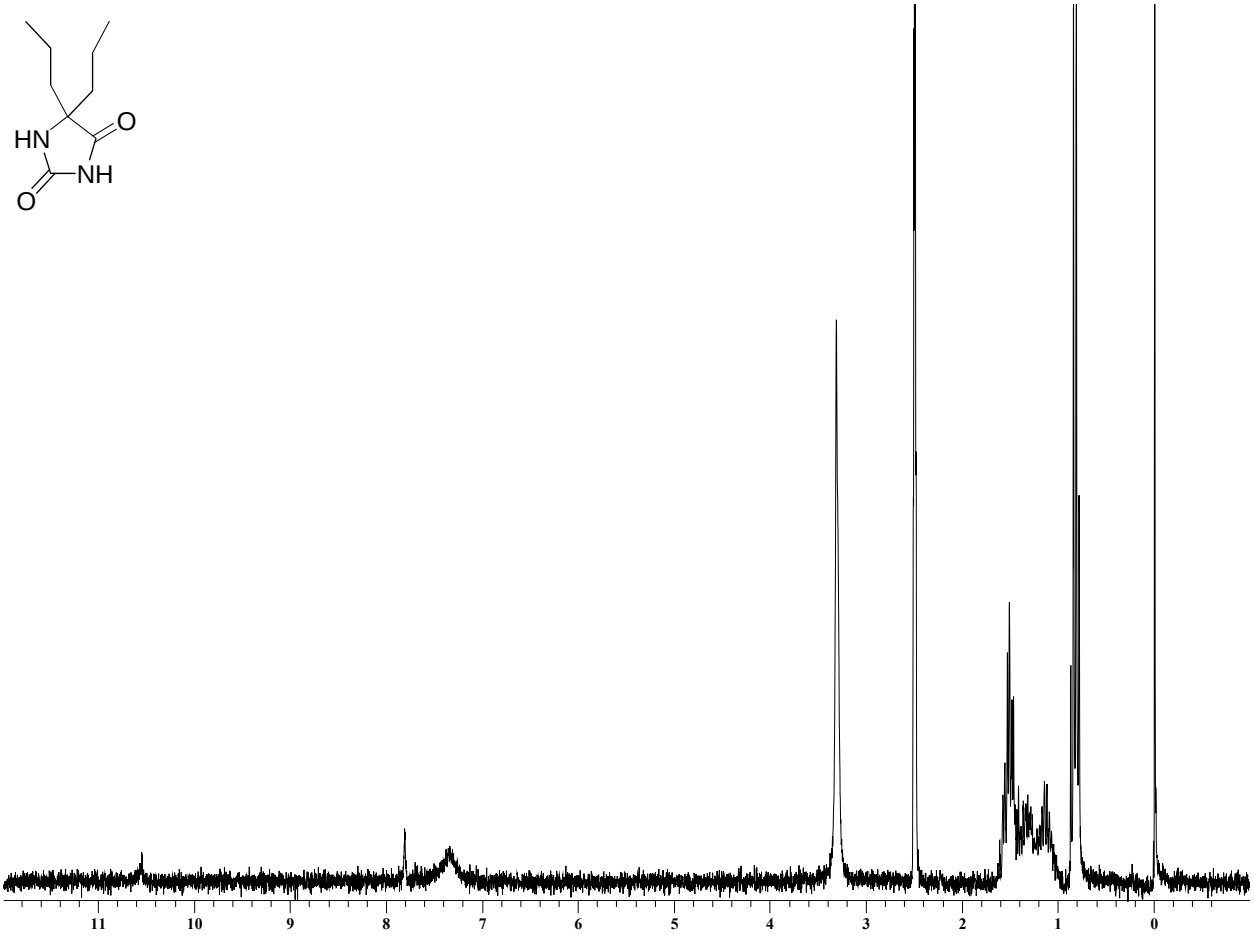

A-1. ^{1}H NMR of 5,5-Dipropylhydantion (1) in DMSO

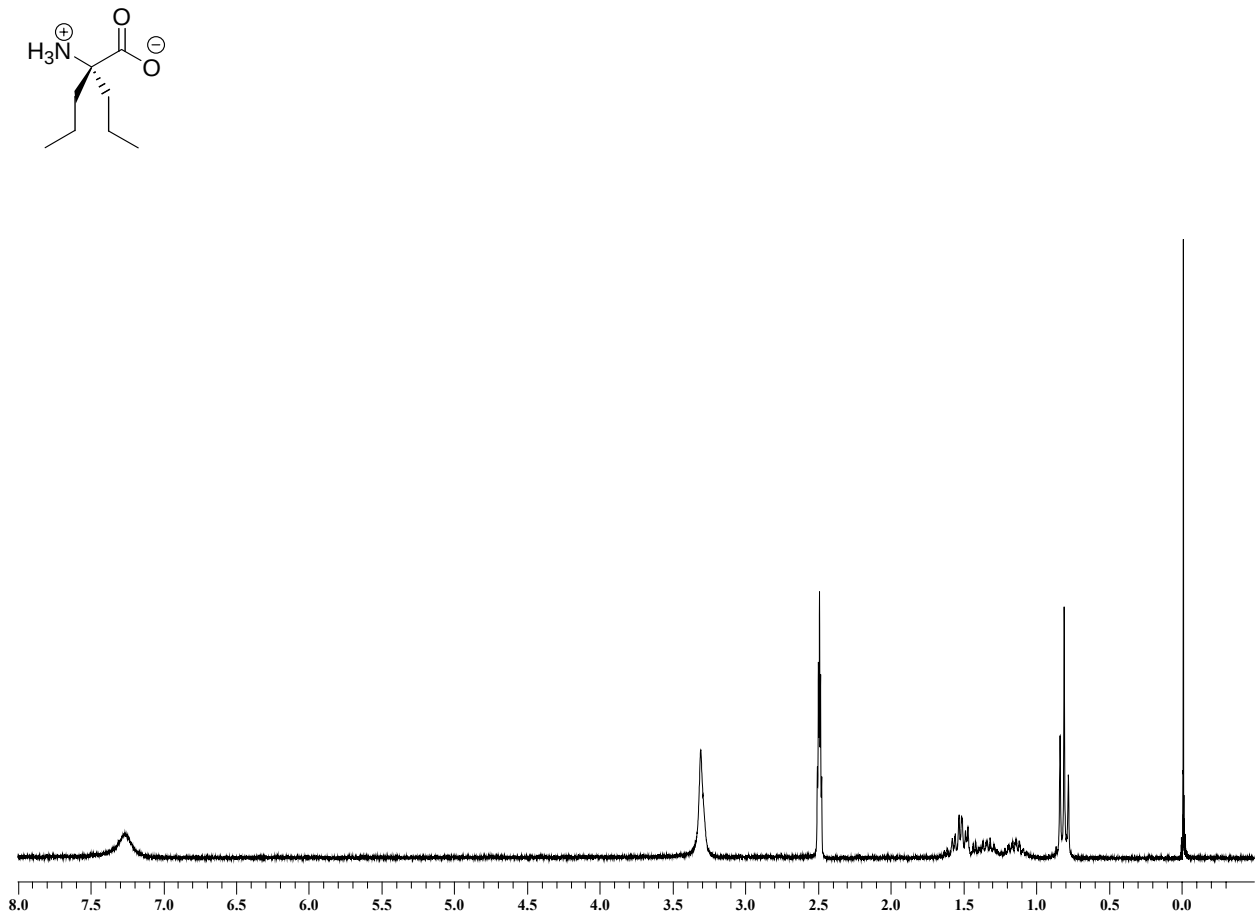

A-2. ^{1}H NMR of 2,2-Dipropylgylcine (2) in DMSO

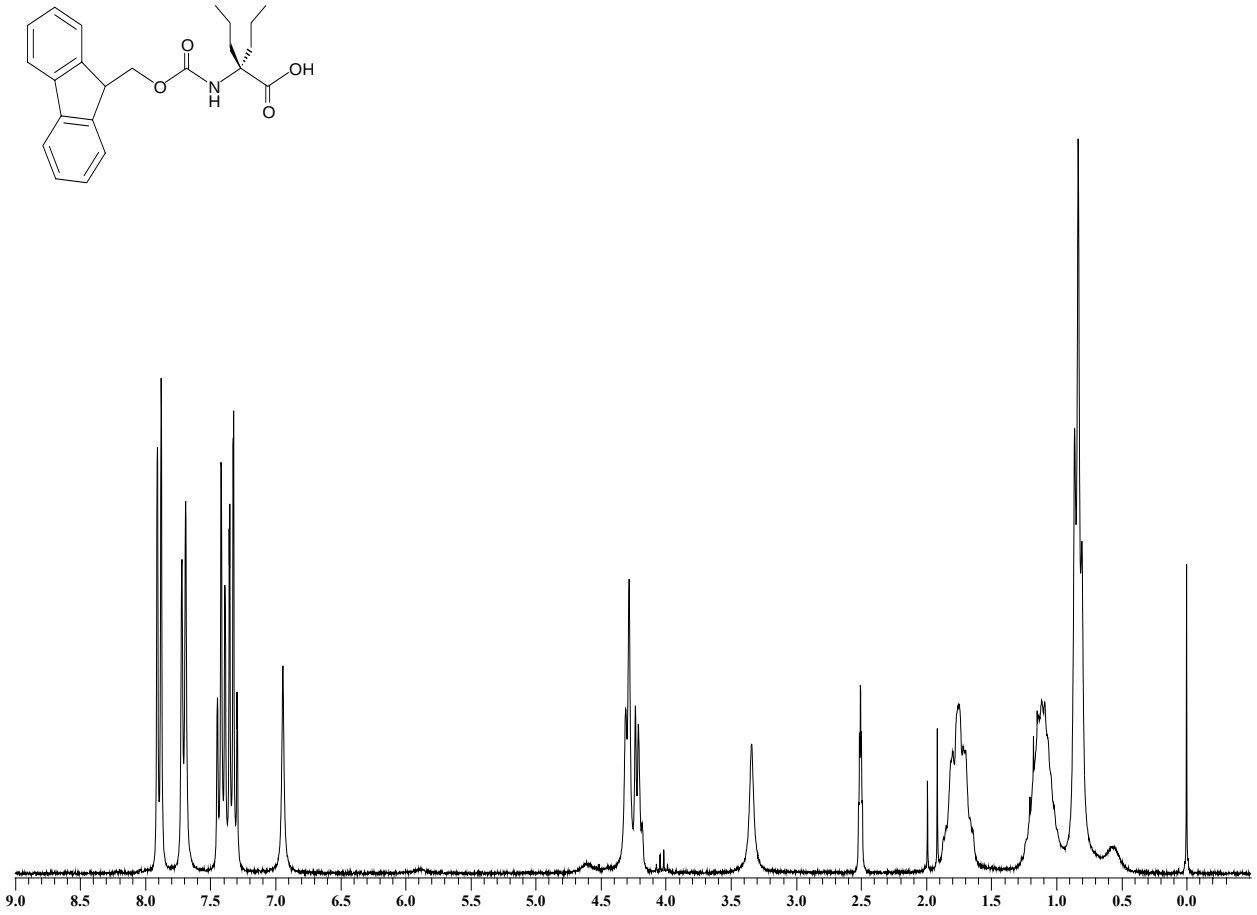

A-3. ^{1}H NMR of N^{α}(9-Fluorenlymethoxycarbonyl)-2-,2-Dipropylglycine (3) in DMSO

APPENDIX B
HPLC AND MALDI-MS DATA

Linear gradients of 0.1% aqueous TFA in H_2O (v/v) (Buffer A) and 0.1% TFA in CH_3CN (v/v) (Buffer B) were utilized in all HPLC. MALDI-MS peptide samples were crystallized using CCA matrix.

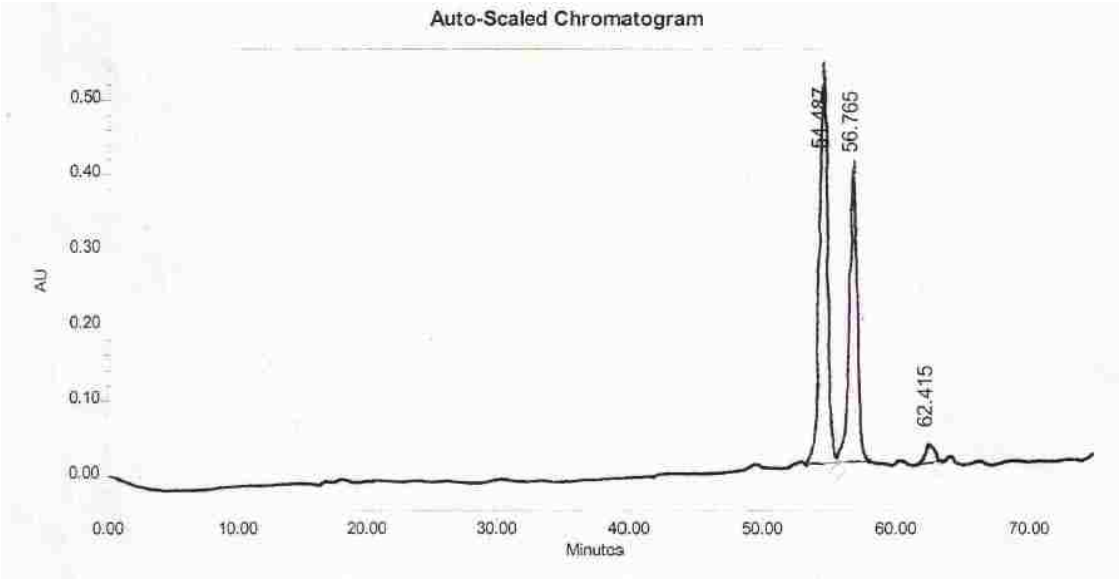

B-1. HPLC chromatogram of crude $[J^3]$-Ω^DPG

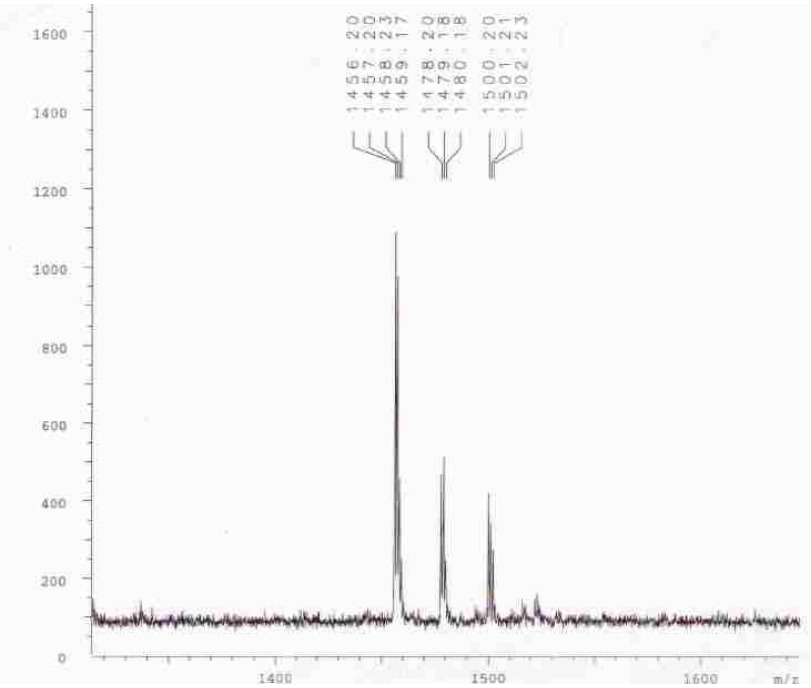

B-2. MALDI-MS of $[J^3]$-Ω^DPG

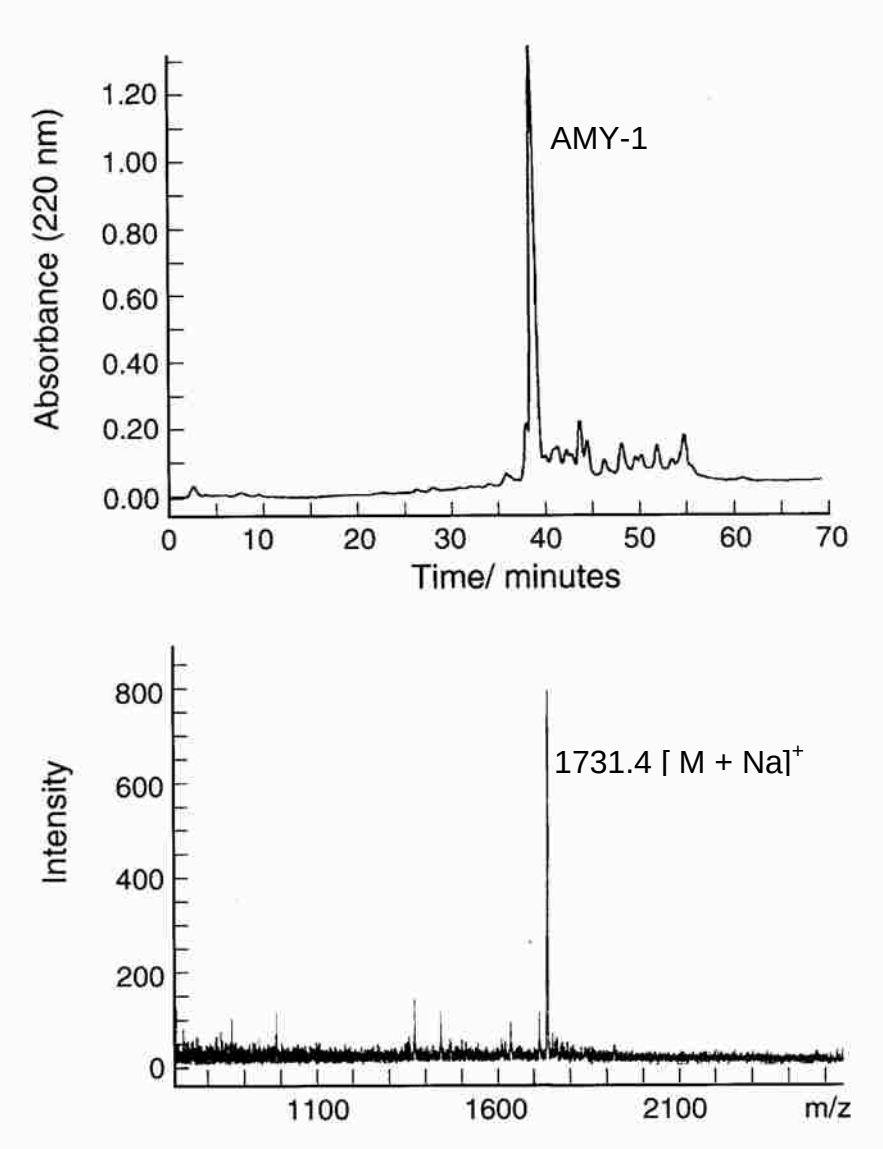

B-3. HPLC chromatogram of crude AMY-1 and MALDI-MS data

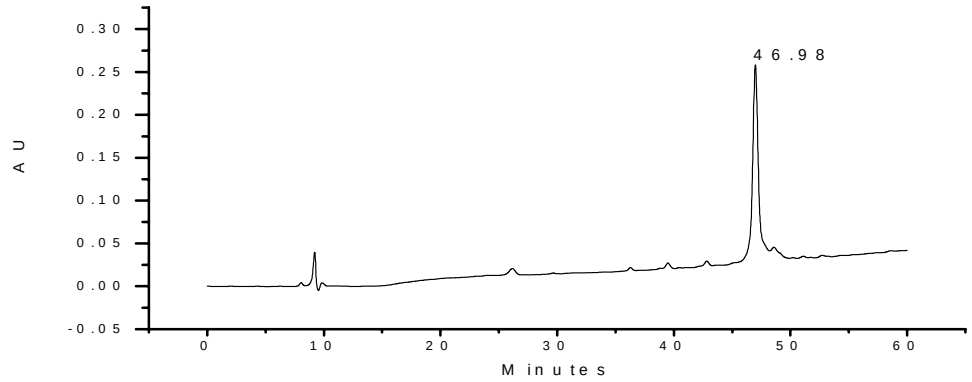

B-4. HPLC chromatogram of crude AMY-2

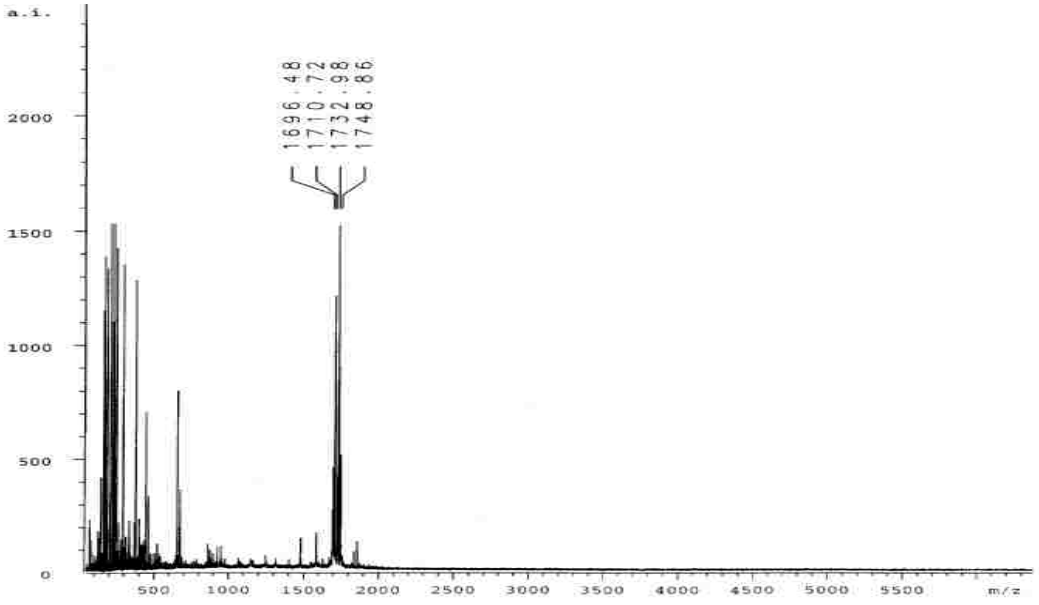

B-5. MALDI-MS of AMY-2

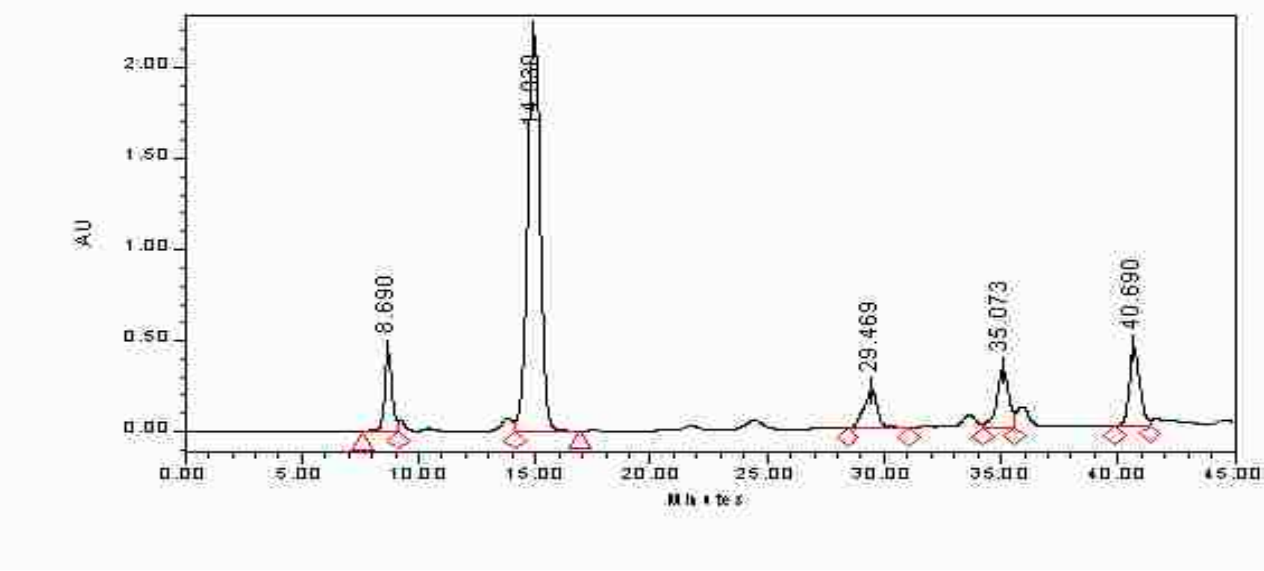

B-6. HPLC chromatogram of crude AMY-3

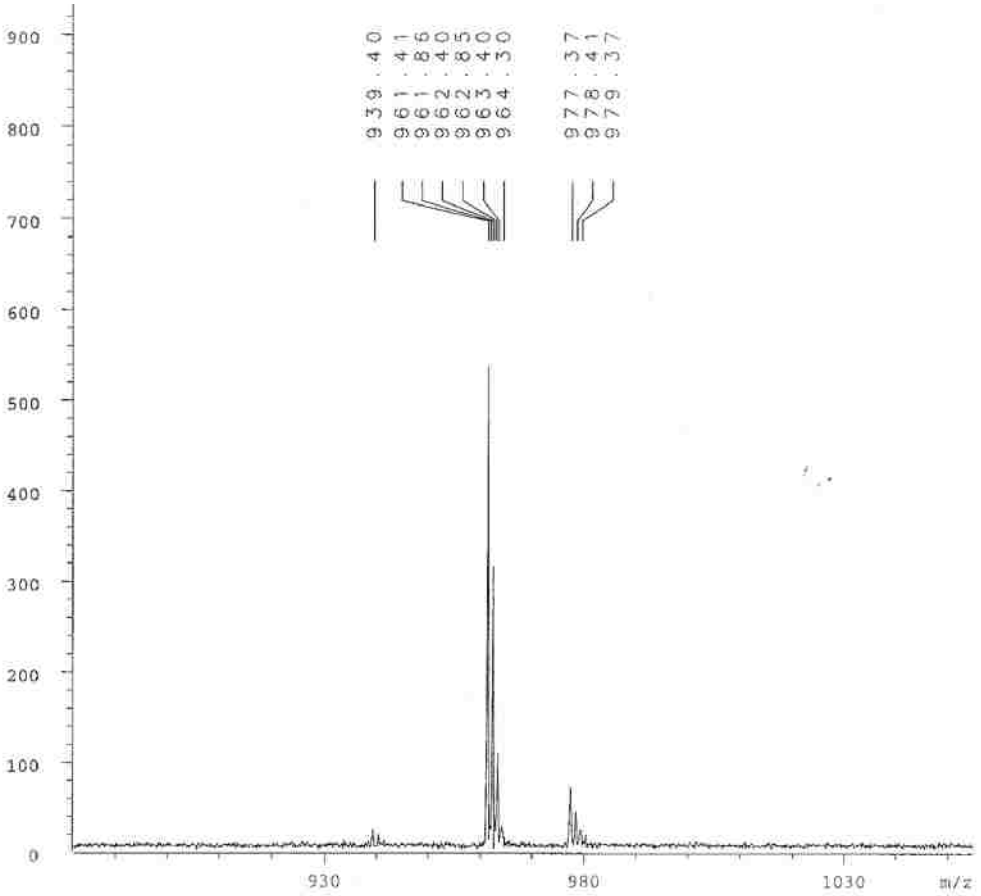

B-7. MALDI-MS of AMY-3

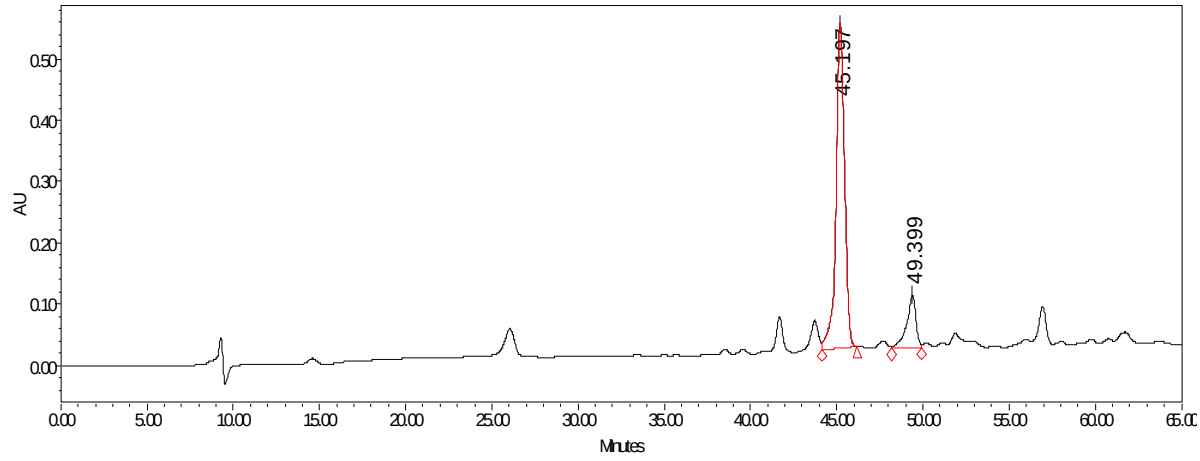

B-8. HPLC chromatogram of crude AMY-4

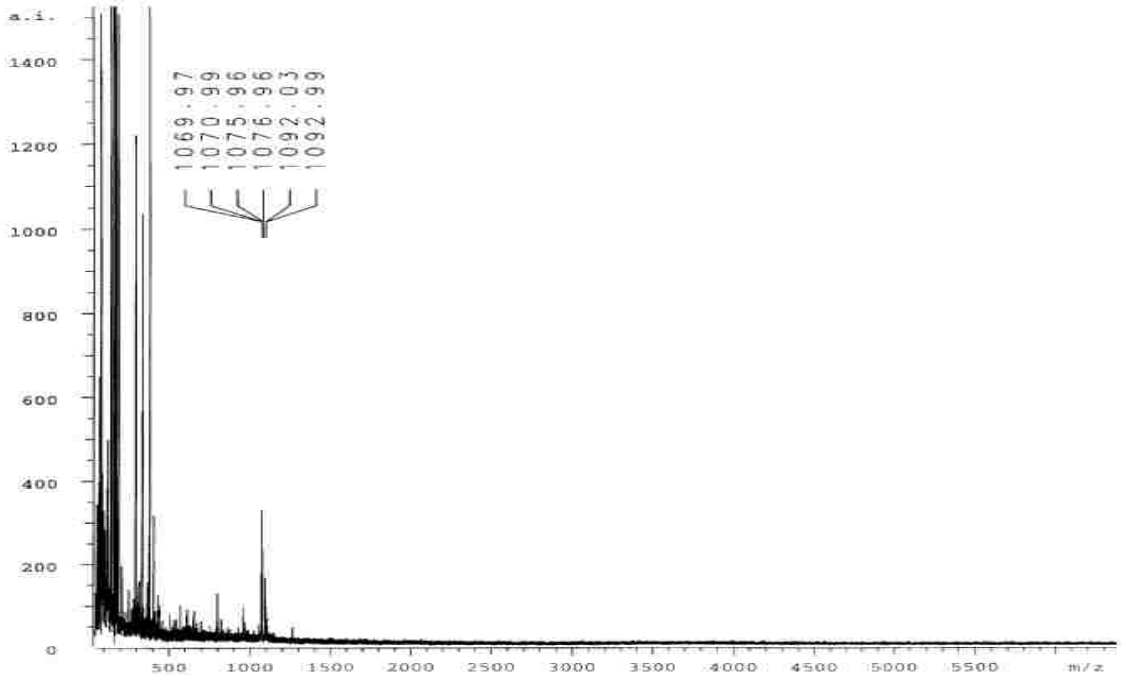

B-9. MALDI-MS of AMY-4

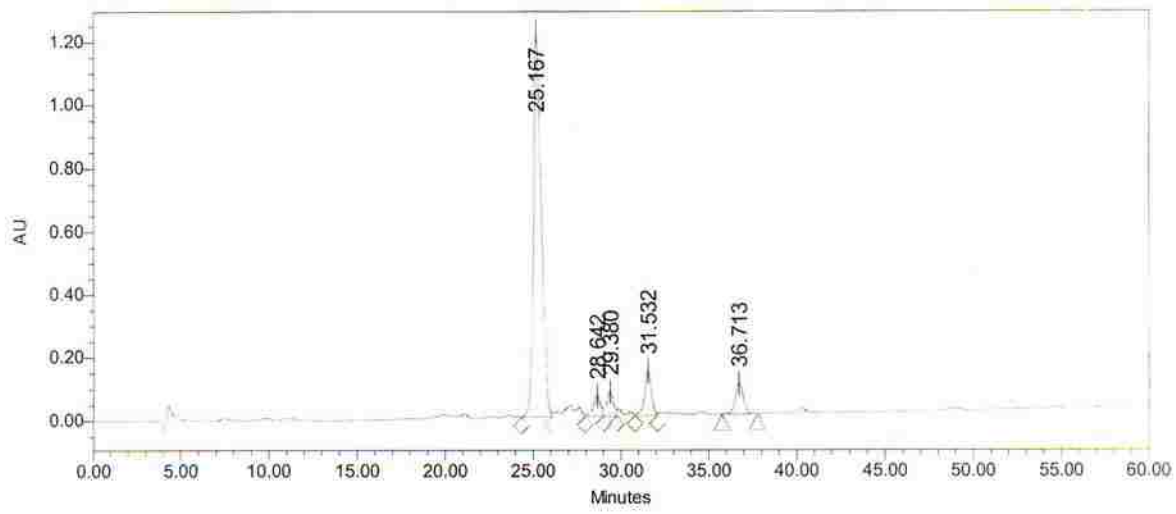

B-10. HPLC chromatogram of crude HC-K_6

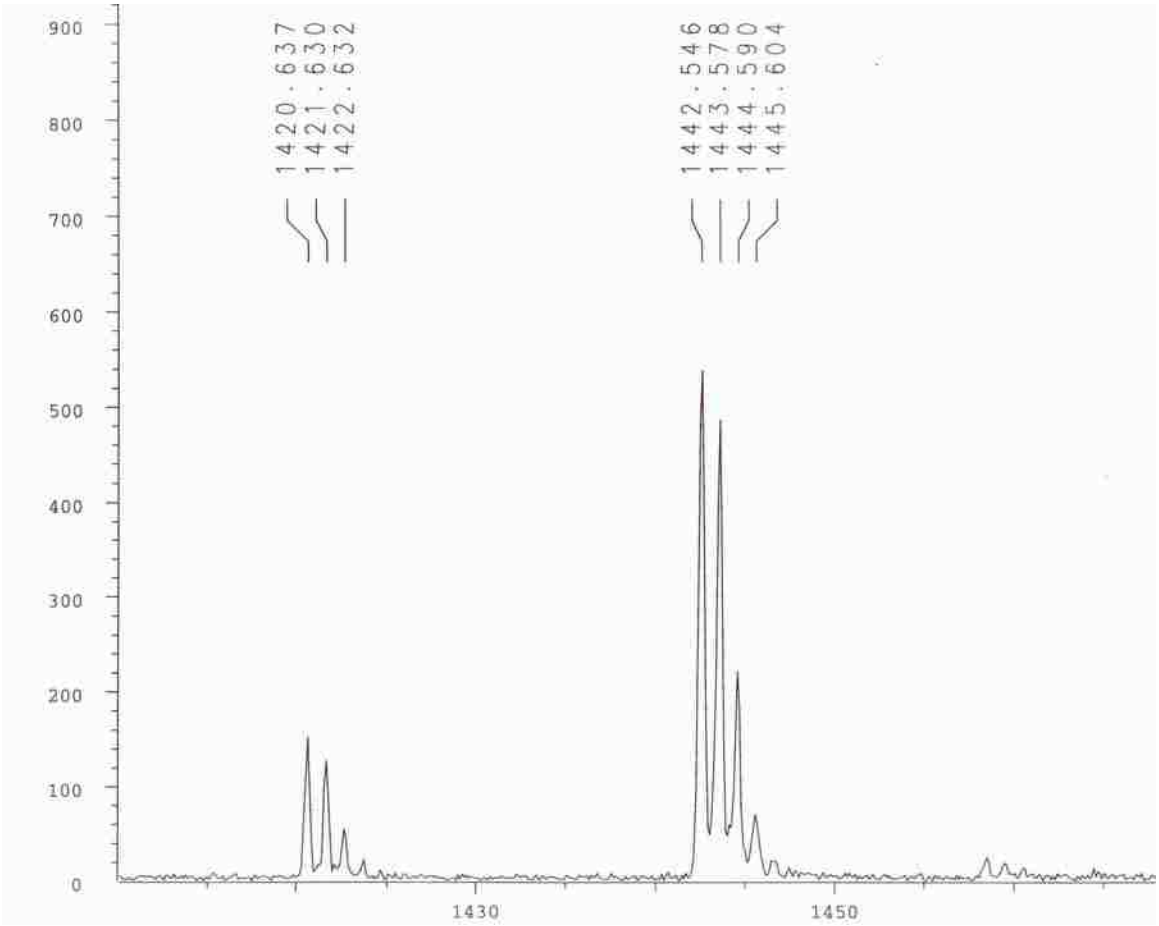

B-11. MALDI-MS of HC-K_6

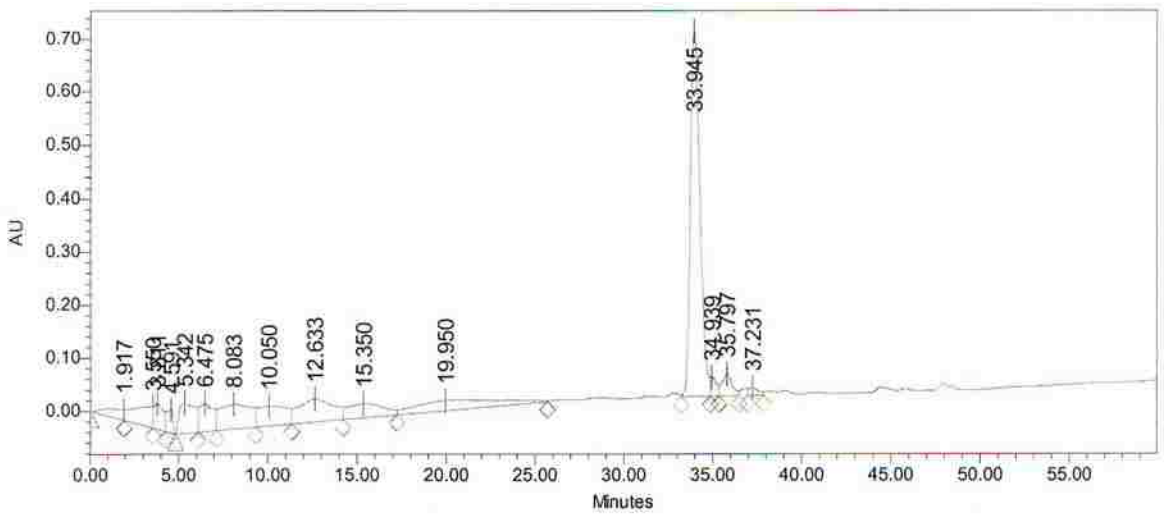

B-12. HPLC chromatogram of crude HC-B_3

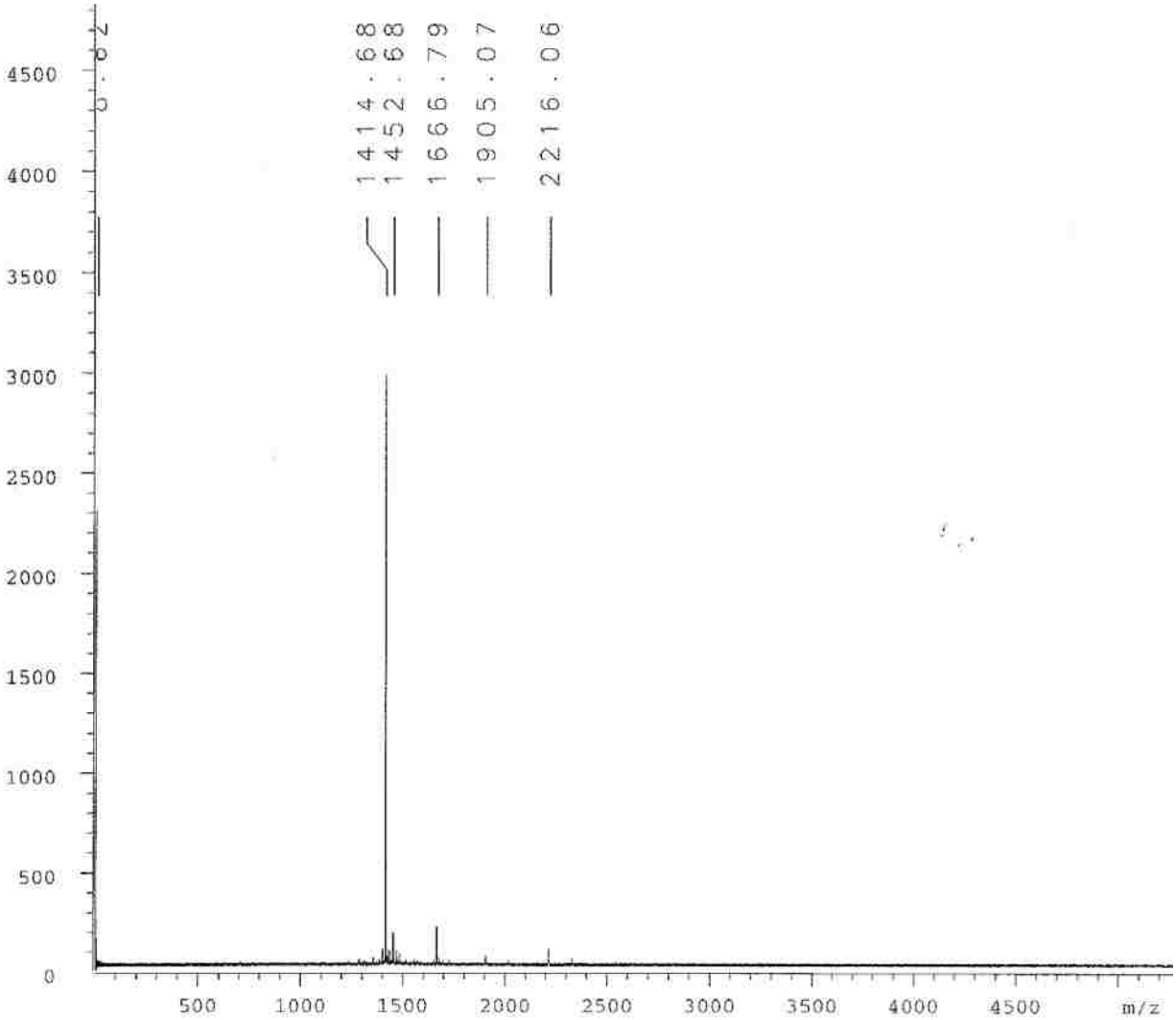

B-13. MALDI-MS of HC-B_3

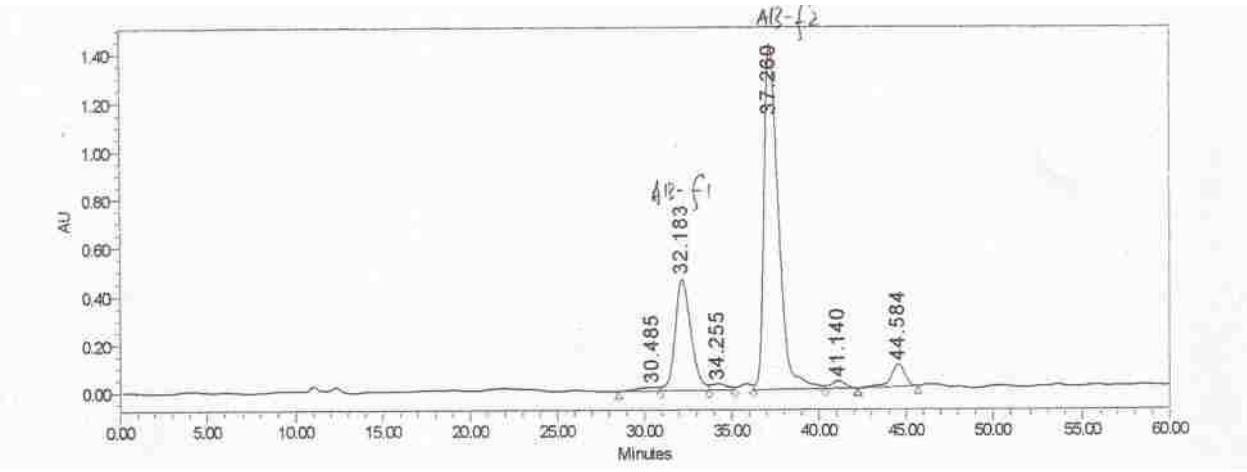

B-14. HPLC chromatogram of crude *N*MHC

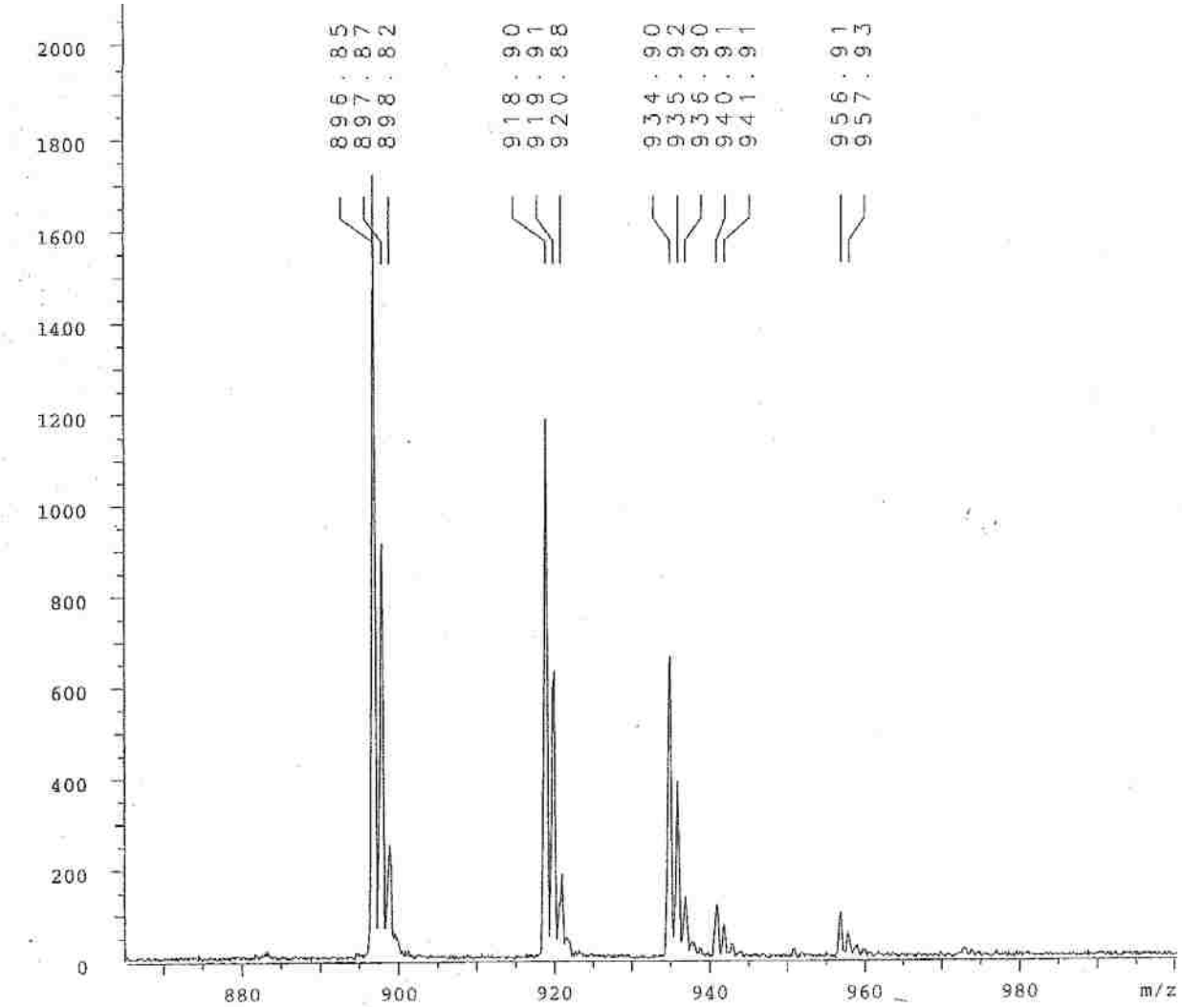

B-15. MALDI-MS of *N*MHC

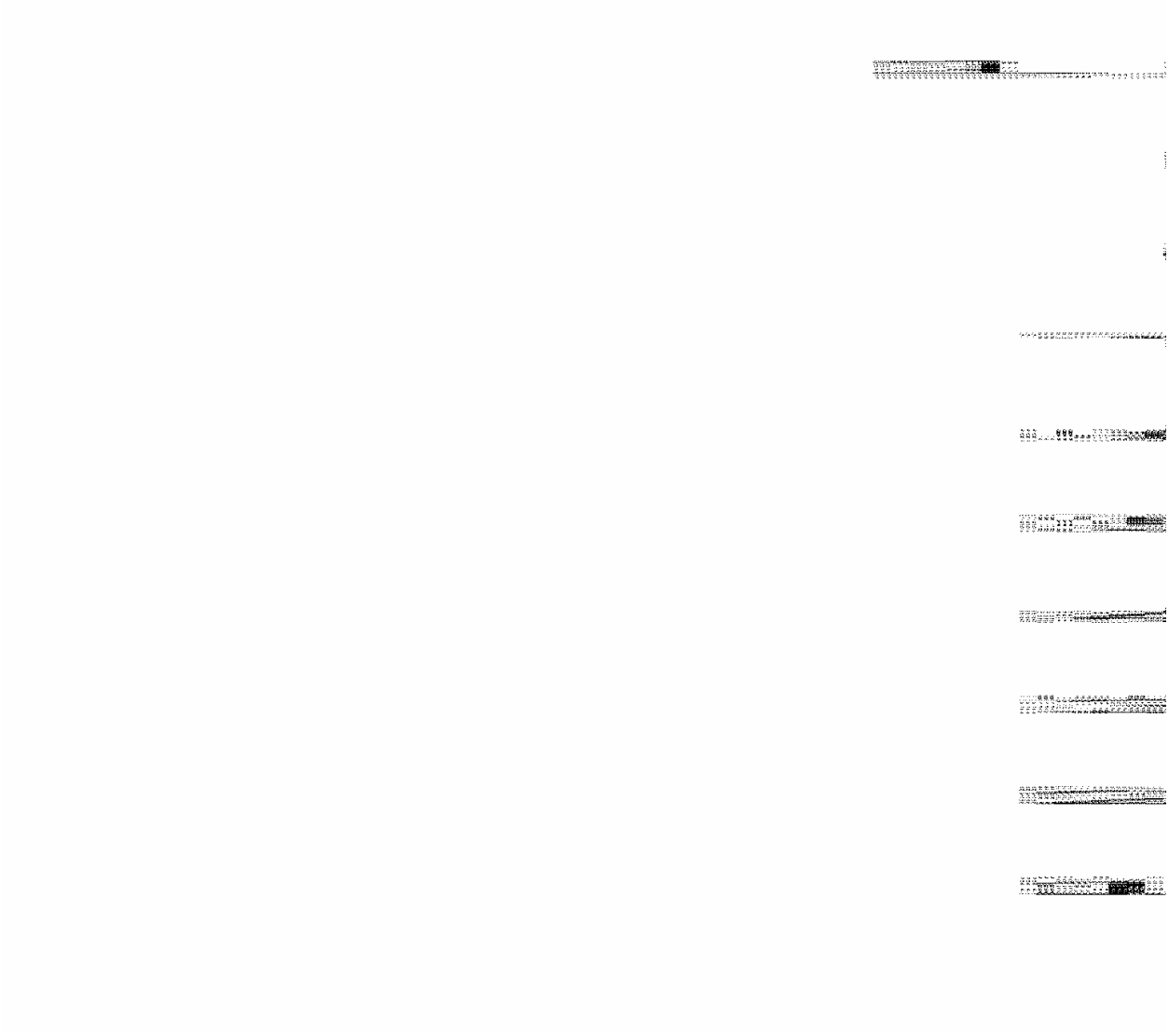

B-16. MALDI-MS of Ω^{D}PG

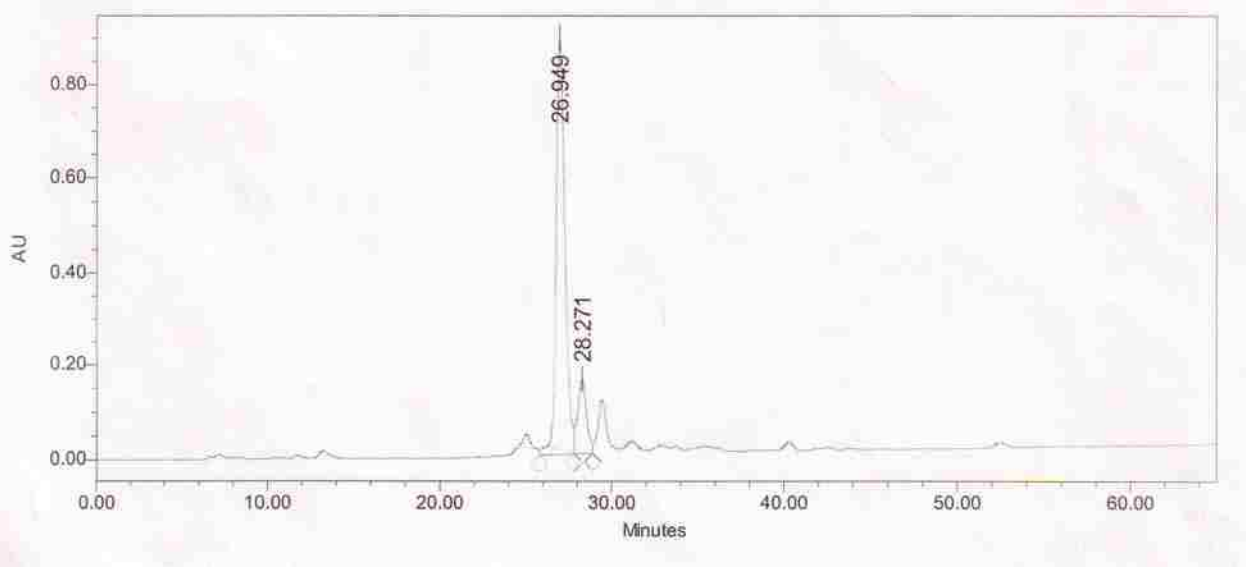

B-17. HPLC chromatogram of crude ΩAG

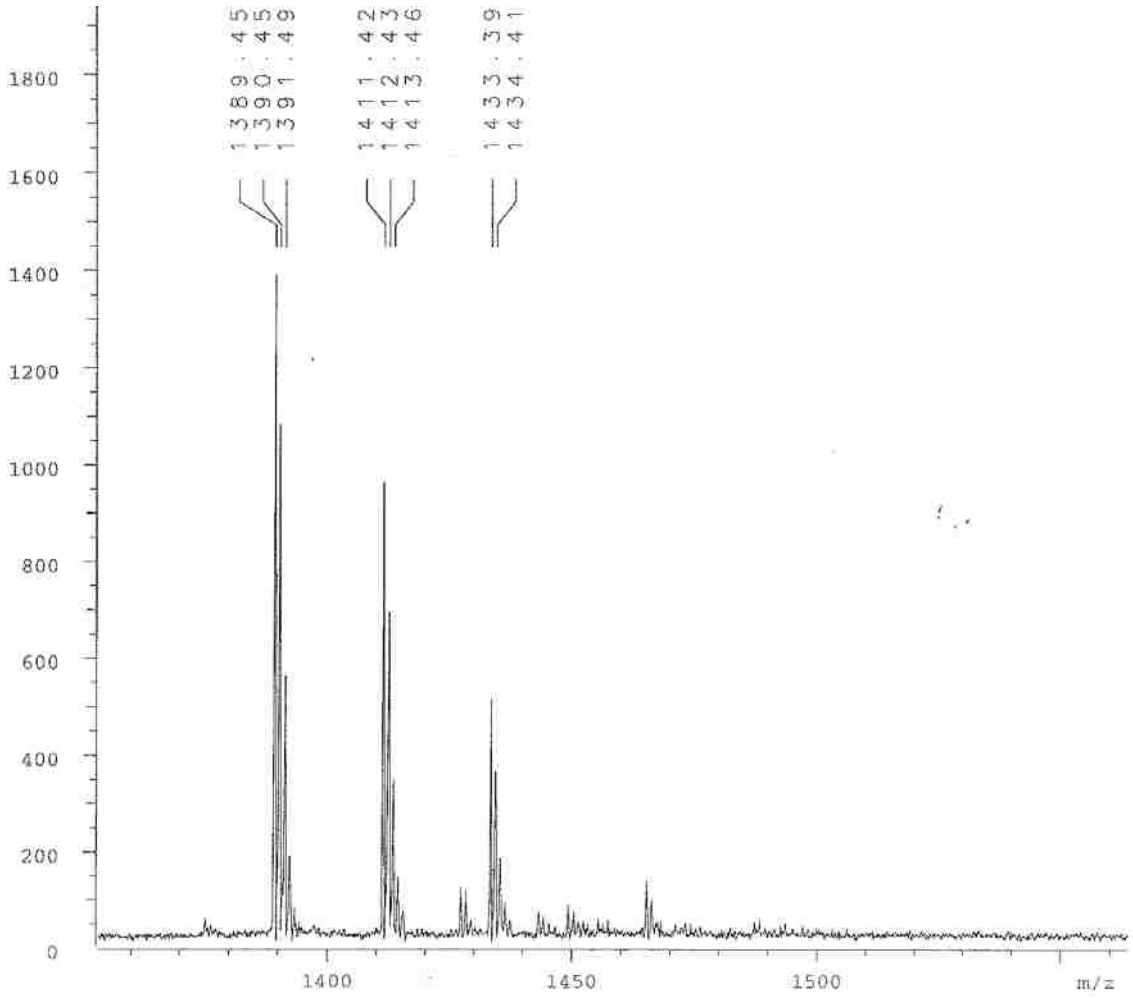

B-18. MALDI-MS of ΩAG

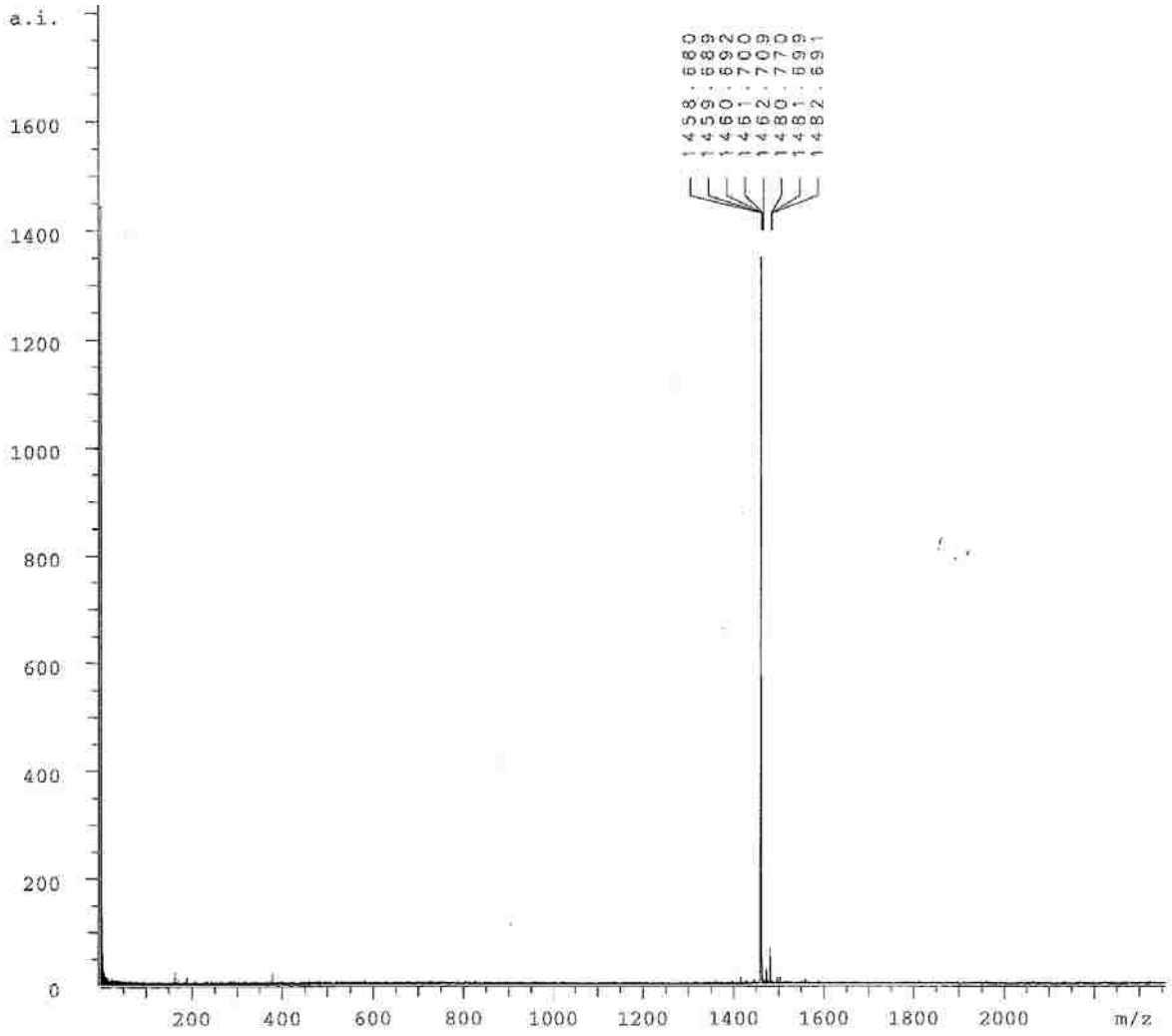

B-19. MALDI-MS of ΩJG

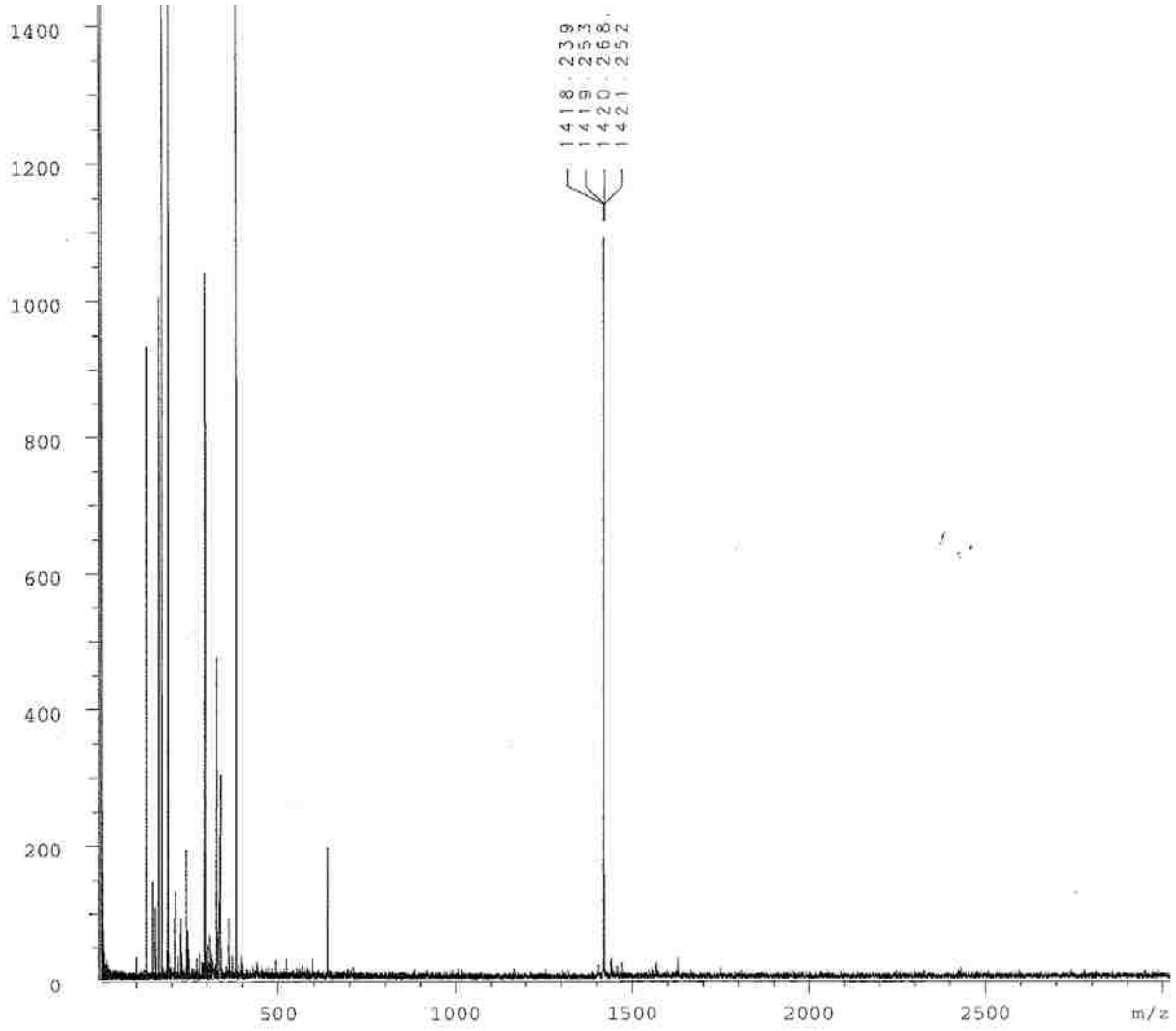

B-20. MALDI-MS of $\Omega B^{D}A$

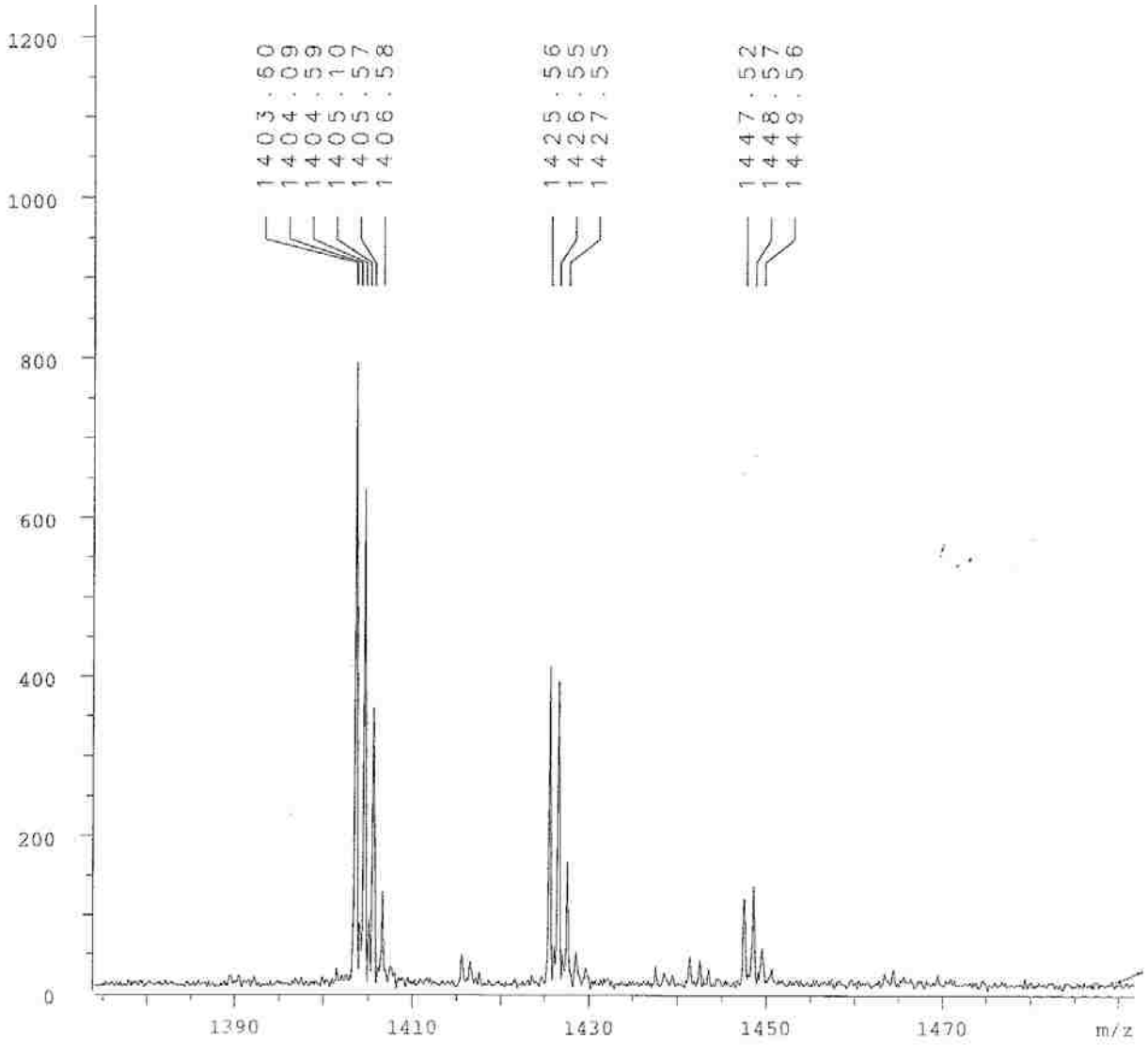

B-21. MALDI-MS of ΩBG

APPENDIX C
CIRCULAR DICHROISM DATA

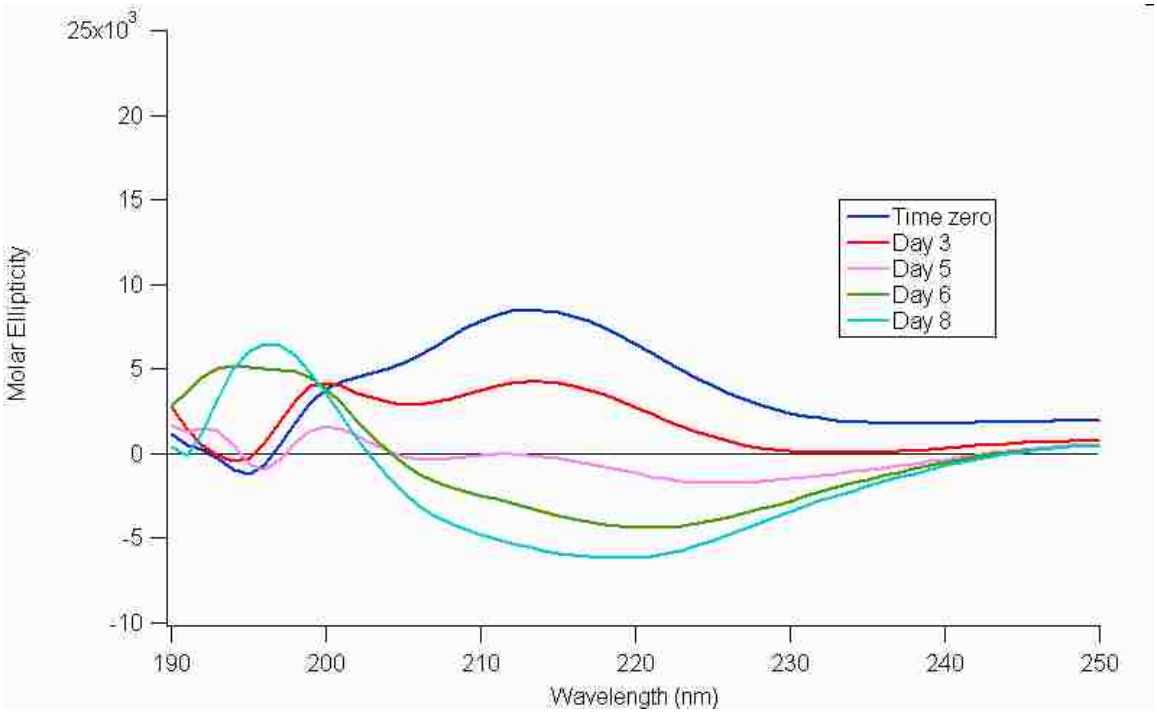

C-1. CD spectrum of equimolar mixture of Aβ/AMY-2 for t=0-8 days; taken in 50 mM PBS (150 mM NaCl); pH 7.4. Molar Ellipticity- [θ] units: deg cm^2 dmol^{-1}.

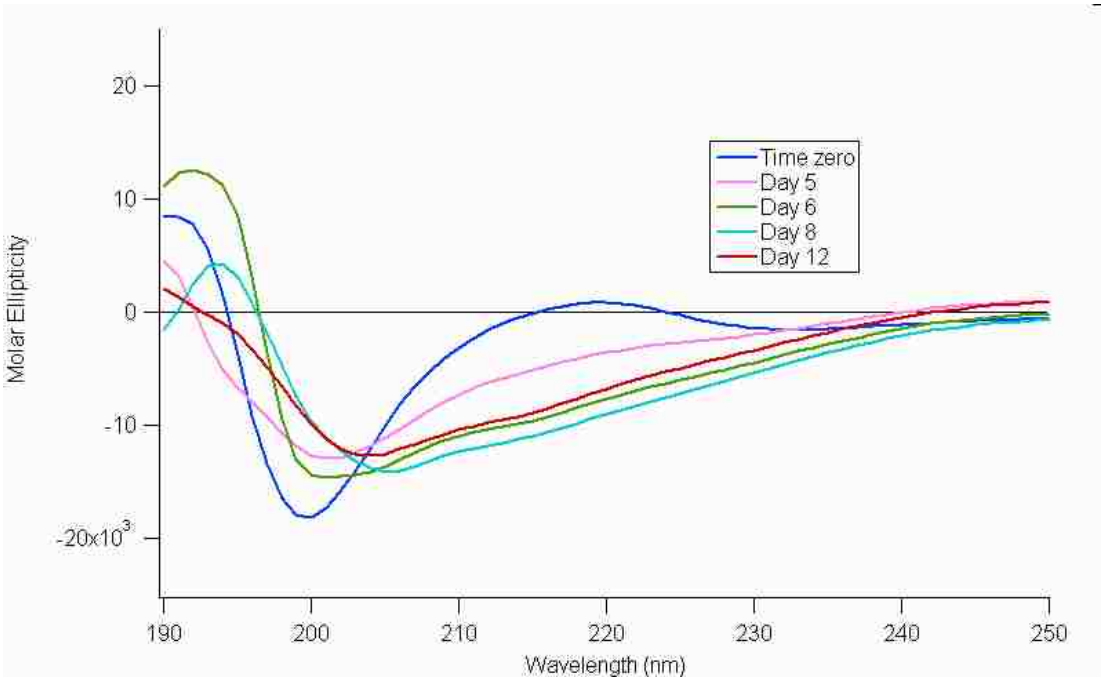

C-2. CD spectrum of equimolar mixture of Aβ/HC-K_6 for t=0-12 days; taken in 50 mM PBS (150 mM NaCl); pH 7.4. Molar Ellipticity- [θ] units: deg cm^2 $dmol^{-1}$.

APPENDIX D
MICROSCOPY

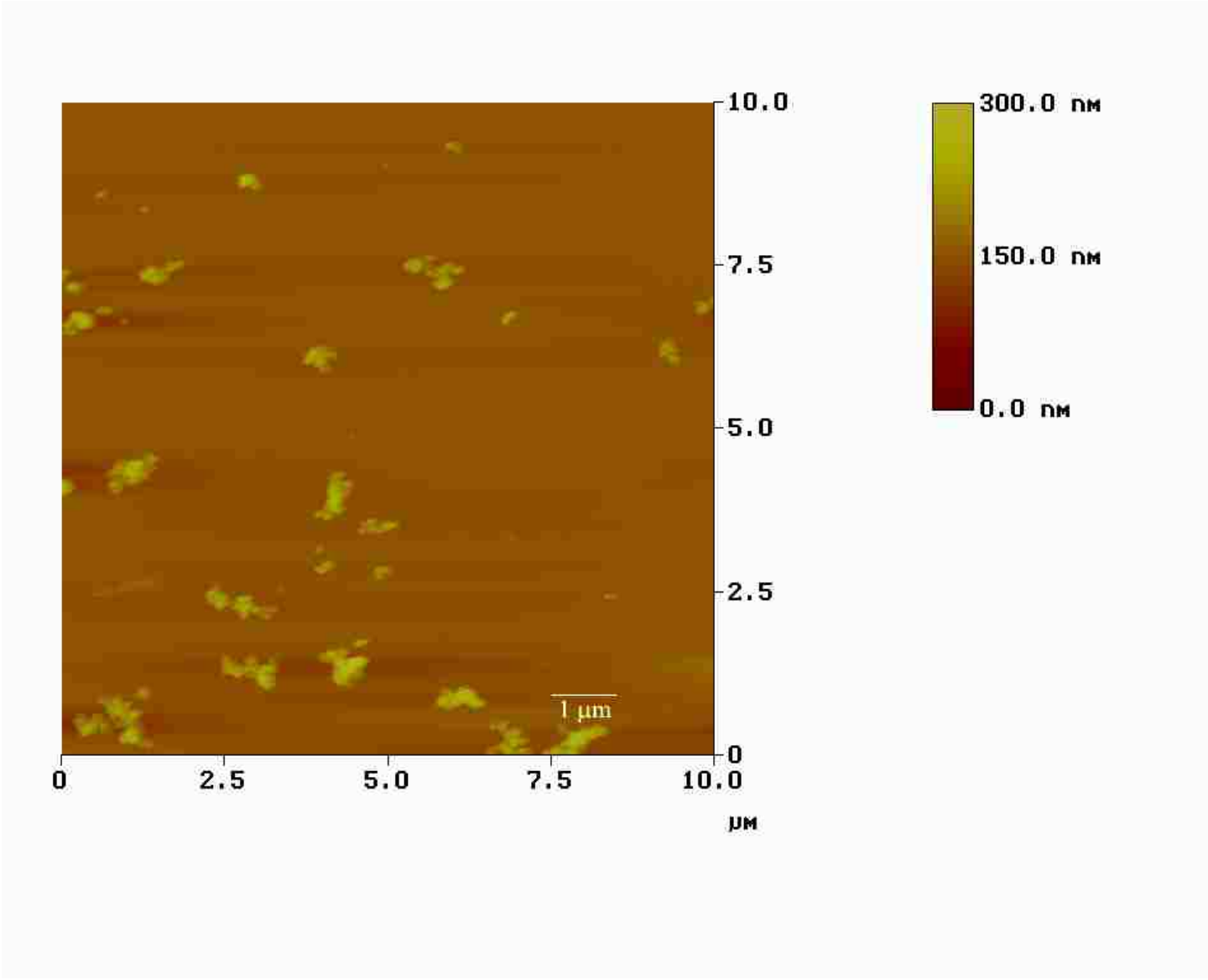

D-1. SFM image of AMY-2/Aβ (1:1; 50 μM). Samples were incubated in PBS (50 mM 150 mM NaCl, pH 7.4) at 37 °C for 1.5 hours then remained at room temperature under N_2 atmosphere for 1 week. Sample imaged by Dr. Jed P. Aucoin.

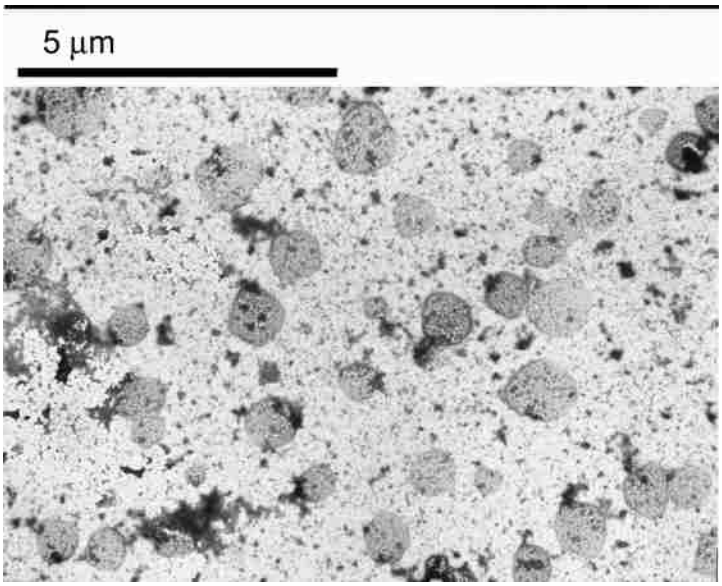

D-2. TEM image of AMY-2/Aβ (1:1; 50 μM). Sample was incubated in PBS (50 mM 150 mM NaCl, pH 7.4) at 37 °C for 48 hours.

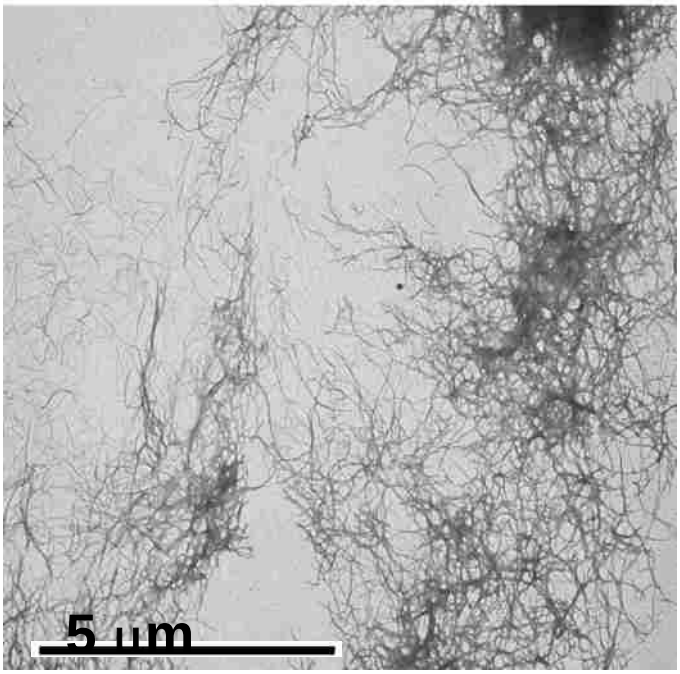

D-3. TEM image of HC-K_6/Aβ (1:1; 50 μM). Sample was incubated in PBS (50 mM 150 mM NaCl, pH 7.4) at 37 °C for 72 hours while agitating continuously.

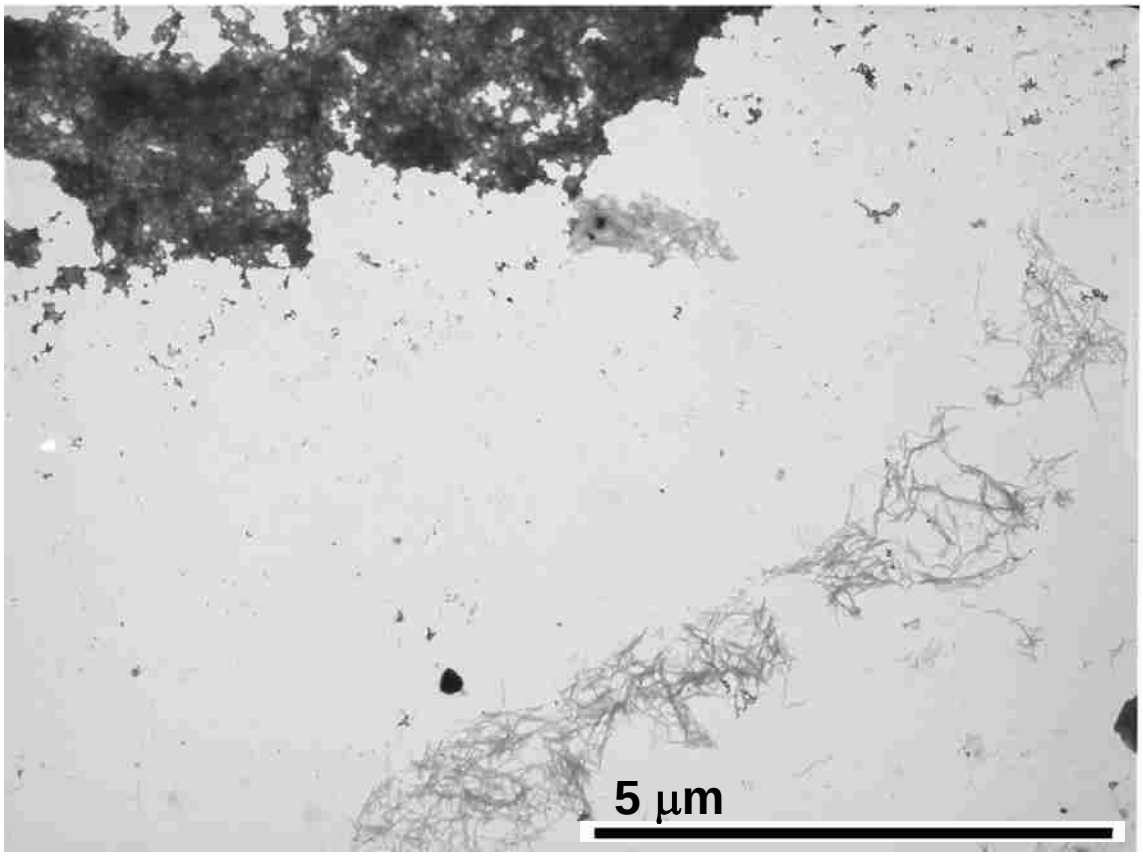

D-4. TEM image of *N*MHC/Aβ (1:1; 50 μM). Sample was incubated in PBS (50 mM 150 mM NaCl, pH 7.4) at 37 °C for 72 hours while agitated continuously.

APPENDIX E
LETTERS OF PERMISSION

August 27, 2007

John Wiley & Sons, Inc.
Permissions Department
111 River Street
Hoboken, NJ 07030-5774

To Whom It May Concern:

Wiley ~~&~~ Inc.

I am writing to request permission for the use of two figures and portions of the text from Peptide Science. I am currently a graduate student in the Department of Chemistry at Louisiana State University and in the process of writing my doctoral dissertation. I am the second author on the article would like to include the Figure 4 and Figure 5 in my doctoral dissertation. The article is "Nonstereogenic α-Aminoisobutyryl-Glycyl Dipeptidyl Unit Nucleates Type I' β-Turn In Linear Peptides In Aqueous Solution", Masterson, L. R.; Etienne, M. A.; Porcelli, F.; Barany, G.; Hammer, R. P.; Veglia, G., and was published online April 10, 2007.

Vol. 89, Issue 5, p. 746-753.

Thank you for your consideration of this request.

Sincerely,

Marcus Etienne
Louisiana State University
Department of Chemistry
Choppin Hall, Room 232
Baton Rouge, LA 70803
Tel: (225) 578-3369; Fax: (225) 578-3458
Email: metien2@lsu.edu

PERMISSION GRANTED
BY: _____ 9/12/07
Global Rights Dept., John Wiley & Sons, Inc.

NOTE: No rights are granted to use content that appears in the work with credit to another source

American Chemical Society

Publications Division
Copyright Office

1155 Sixteenth Street, NW
Washington, DC 20036
Phone: (1) 202-872-4368 or -4367
Fax: (1) 202-776-8112 E-mail: copyright@acs.org

VIA FAX: 225-578-3458 DATE: September 6, 2007

TO: Marcus Etienne, Department of Chemistry, Louisiana State University, Choppin Hall, Room 232, Baton Rouge, LA 70803

FROM: C. Arleen Courtney, Copyright Associate C. Arleen Courtney

Thank you for your request for permission to include **your** paper(s) or portions of text from **your** paper(s) in your thesis. Permission is now automatically granted; please pay special attention to the implications paragraph below. The Copyright Subcommittee of the Joint Board/Council Committees on Publications approved the following:

> Copyright permission for published and submitted material from theses and dissertations
> ACS extends blanket permission to students to include in their theses and dissertations their own articles, or portions thereof, that have been published in ACS journals or submitted to ACS journals for publication, provided that the ACS copyright credit line is noted on the appropriate page(s).
>
> Publishing implications of electronic publication of theses and dissertation material
> Students and their mentors should be aware that posting of theses and dissertation material on the Web prior to submission of material from that thesis or dissertation to an ACS journal may affect publication in that journal. Whether Web posting is considered prior publication may be evaluated on a case-by-case basis by the journal's editor. If an ACS journal editor considers Web posting to be "prior publication", the paper will not be accepted for publication in that journal. If you intend to submit your unpublished paper to ACS for publication, check with the appropriate editor prior to posting your manuscript electronically.

If your paper has **not** yet been published by ACS, we have no objection to your including the text or portions of the text in your thesis/dissertation in **print and microfilm formats**; please note, however, that electronic distribution or Web posting of the unpublished paper as part of your thesis in electronic formats might jeopardize publication of your paper by ACS. Please print the following credit line on the first page of your article: "Reproduced (or 'Reproduced in part') with permission from [JOURNAL NAME], in press (or 'submitted for publication'). Unpublished work copyright [CURRENT YEAR] American Chemical Society." Include appropriate information.

If your paper has already been published by ACS and you want to include the text or portions of the text in your thesis/dissertation in **print or microfilm formats**, please print the ACS copyright credit line on the first page of your article: "Reproduced (or 'Reproduced in part') with permission from [FULL REFERENCE CITATION.] Copyright [YEAR] American Chemical Society." Include appropriate information.

Submission to a Dissertation Distributor: If you plan to submit your thesis to UMI or to another dissertation distributor, you should not include the unpublished ACS paper in your thesis if the thesis will be disseminated electronically, until ACS has published your paper. After publication of the paper by ACS, you may release the entire thesis **(not the individual ACS article by itself)** for electronic dissemination through the distributor; ACS's copyright credit line should be printed on the first page of the ACS paper.

Use on an Intranet: The inclusion of your ACS unpublished or published manuscript is permitted in your thesis in print and microfilm formats. If ACS has published your paper you may include the manuscript in your thesis on an intranet that is not publicly available. Your ACS article cannot be posted electronically on a publicly available medium (i.e. one that is not password protected), such as but not limited to, electronic archives, Internet, library server, etc. The only material from your paper that can be posted on a public electronic medium is the article abstract, figures, and tables, and you may link to the article's DOI or post the article's author-directed URL link provided by ACS. This paragraph does not pertain to the dissertation distributor paragraph above. 06/07/05

PERMISSION REQUEST FORM

Date: 08-27-07

To: Copyright Office
Publications Division
American Chemical Society
1155 Sixteenth Street, N.W.
Washington, DC 20036

FAX: 202-776-8112

From: Marcus Etienne
Louisiana State University
Department of Chemistry
Choppin Hall Rm 231
Baton Rouge, LA 70803

Your Phone No. 225-979-5372
Your Fax No. 225-578-3458

I am preparing a paper entitled:

C^α-Dimethylated Amino Acid Incorporation into Beta Sheet Peptides

to appear in a (**circle one**) book, magazine, journal, proceedings, (other) doctoral dissertation entitled:

to be published by: Louisiana State University

I would appreciate your permission to use the following ACS material in print and other formats with the understanding that the required ACS copyright credit line will appear with each item and that this permission is for only the requested work listed above:

From ACS journals or magazines (for ACS magazines, also include issue no.):

ACS Publication Title	Issue Date	Vol.	No.	Page(s)	Material to be used*
"Insights into the Amyloid Folding Problem from Solid-State work", Tycko, R. Biochemistry		Vol. 42	No. 11	pp 3151-3159.	Requesting the use of Figure 1. and Figure 6.

From ACS books: include ACS book title, series name and number, year, page(s), book editor=s name(s), chapter author's name(s), and material to be used, such as Figs. 2 & 3, full text, etc.*

* If you use more than three figures/ta... will also be required.

Questions? Please call Arleen Courtn...

PERMISSION TO REPRINT IS GRANTED BY THE AMERICAN CHEMICAL SOCIETY

ACS CREDIT LINE REQUIRED. Please follow this sample: Reprinted with permission from (reference citation). Copyright (year) American Chemical Society.

APPROVED BY: C. Arleen Courtney 9/06/07
ACS Copyright Office

☐ **If box is checked, author permission is also required. See original article for address.**

This space is reserved for ACS Copyright Office Use

12/3/99

From: "Essenpreis, Alice, Springer DE" <Alice.Essenpreis@springer.com>
To: metien2@lsu.edu
CC:
Subject: WG: Permissions Request
Date: Tuesday, September 11, 2007 2:19:55 AM

Dear Mr. Etienne,

Thank you for your e-mail.

With reference to your request (copy herewith) to re-use material on which Springer controls the copyright, our permission is granted free of charge, on the following condition:

* full credit (book title, volume, year of publication, page, chapter/article title, name(s) of author(s), figure number(s), original copyright notice) is given to the publication in which the material was originally published by adding: With kind permission of Springer Science and Business Media.

With best regards,

—

Alice Essenpreis
Springer
Rights and Permissions

—

Tiergartenstrasse 17 | 69121 Heidelberg GERMANY
FAX: +49 6221 487 8223
permissions.Heidelberg@springer.com
WWW.springer.com/rights

—

From: Marcus Etienne [mailto:metien2@lsu.edu]
Sent: Wednesday, September 05, 2007 8:37 PM
To: Permissions Heidelberg, Springer DE
Subject: Permissions Request

To Whom It May Concern:

I am writing to request permission for the use of an article published in Peptide Characterization and Application Protocols. I am a graduate student in the Department of Chemistry at Louisiana State University. I am the first author on the article and would like to include the article in my doctoral dissertation. The article is "Amyloid β- Protein Aggregation", Etienne, Marcus A.; Edwin, Nadia J.; Aucoin, Jed P.; Russo, Paul S.; McCarley, Robin L.; Hammer, Robert P. *Peptide Characterization and Application Protocols*, (Gregg B. Fields, Ed.) Humana Press, Clifton, NJ (2006)

Thank you for your consideration of this request.

Sincerely,

Marcus Etienne
Louisiana State University
Department of Chemistry
Choppin Hall, Room 232
Baton Rouge, LA 70803
Tel: (225) 578-3369; Fax: (225) 578-3458
Email: metien2@lsu.edu

VITA

Marcus Etienne was born July 1979, in Lake Charles, Louisiana, to Gwen Hanchett and Marvin Etienne. He graduated Lake Charles-Boston High School as class salutatorian in 1997. After graduating high school, Marcus began his undergraduate career at Southern University seeking a bachelor's degree in chemistry. During his tenure at Southern University, Marcus participated in many undergraduate research opportunities. In the summer of 1999, he worked with Dr. Maria Ngu synthesizing cyclic octapeptides as a part of the LSU/SU REU summer program. He later worked with Dr. Robert Gooden in the Department of Chemistry at Southern University investigating the thermal and photochemical properties of poly(ethylene-co-carbon monoxide) polymers. In 2000, Marcus was selected as a participant in the University of Alabama's SURP Program where he worked with Dr. Robert Metzger synthesizing carbon nanotubes that were to be used as electron emitting devices. In the fall of 2000, Marcus joined the research group of Dr. Edwin Walker in the Department of Chemistry at Southern University where he performed research on the synthesis and characterization of spinel compounds and in the spring of 2001, he successfully completed his undergraduate thesis. Mr. Etienne graduated from Southern University's Honors College in May 2001. Following graduation from Southern University, Marcus pursed a post-baccalaureate degree at Louisiana State University in the Department of Chemistry where he joined Dr. Robert Hammer's research group. During his tenure at Louisiana State University, Marcus has authored several peer review research publications and received numerous departmental, university, and community honors. He will receive the degree of Doctor of Philosophy in chemistry at the spring 2008 commencement ceremony.